Maria de Fátima de Jesus Leal Júlio

Licenciatura em Ciências da Engenharia Química e Bioquímica

Carbon key-properties for microcystin adsorption in drinking water treatment: Structure or surface chemistry?

Dissertação para obtenção do Grau de Mestre em Engenharia Química e Bioquímica

Orientador: Rui Viegas, Doutor, LNEC

Co-orientadora: Isabel Fonseca, Professora Doutora, FCT-UNL

Júri:

Presidente: Professora Doutora Maria Madalena Alves Campos de Sousa Dionísio Andrade, FCT-UNL

Arguente: Doutora Maria João Filipe Rosa, LNEC

FACULDADE DE CIÊNCIAS E TECNOLOGIA
UNIVERSIDADE NOVA DE LISBOA

Setembro 2011

UNIVERSIDADE NOVA DE LISBOA

FACULDADE DE CIÊNCIAS E TECNOLOGIA

CARBON KEY-PROPERTIES FOR MICROCYSTIN ADSORPTION IN DRINKING WATER TREATMENT: STRUCTURE OR SURFACE CHEMISTRY?

MARIA DE FÁTIMA DE JESUS LEAL JÚLIO

Dissertação para Obtenção de Grau de Mestre em Engenharia Química e Bioquímica

Orientador: Rui Viegas, Doutor, LNEC

Co-orientadora: Isabel Fonseca, Professora Doutora, FCT-UNL

Júri:

Presidente: Professora Doutora Maria Madalena Alves Campos de Sousa Dionísio Andrade, FCT-UNL

Arguente: Doutora Maria João Filipe Rosa, LNEC

SETEMBRO
2011

CARBON KEY-PROPERTIES FOR MICROCYSTIN ADSORPTION IN DRINKING WATER TREATMENT: STRUCTURE OR SURFACE CHEMISTRY?

ACKNOWLEDGEMENTS

I would like to express my sincere appreciation to everyone who contributed to the development of this thesis.

First, I would like to express my gratitude to my supervisor Dr. Rui Viegas for promoted truly stimulating discussions and gave me valuable suggestions which have helped steering this work. A special thanks to Dr. Maria João Rosa for his insightful suggestions and discussions. Their support was determinant to improve the quality of the thesis.

My gratitude also goes to Eng. Sérgio Teixeira for receiving me at the National Laboratory for Civil Engineering and to Dr. José Menaia for receiving me at the LABES.

I am also very grateful to Professor Isabel Fonseca for all affection and availability suggestions. Thanks to Nuno and Carla for the analytical determination of the activated carbon surface functional groups and elemental analysis and to Inês for help me in activated carbon preparation.

I would like to thank to my colleagues at the LABES, Ana, Laura, Rosário and Cristina. But a special thanks to Vítor Napier because will not be possible the entire laboratory work without him.

A loving thanks to Elsa Mesquita for the constant support, for her suggestions that helped me so much in the conclusion of this work.

Rita, thank you for you friendship and support, without you this was not possible, you know it!

Last but not least, I would like to thank to my family and my friends, especially to Alexandra, Joana, Jo, Teresa, Pinto and Rodolfo for their unconditional support. In particular Tiago to be always present.

ABSTRACT

The carbon key-properties (structure and surface chemistry) for microcystin-LR (MC-LR) adsorption onto activated carbon were investigated. Waters with an inorganic background matrix approaching that of the soft natural water (2.5 mM ionic strength) were used. Also, model waters with controlled ionic make-up and NOM surrogate with similar size of MC-LR (tannic acid - TA) with MC-LR extracts were tested with activated carbon NORIT 0.8 SUPRA. For this AC, two particle sizes, 125-180 μm and 63-90 μm were tested. The surface chemistry of NOR 125-180 μm was modified by thermal treatment and was also preloaded with TA. The integrated analysis of carbon's chemical and textural characterization and of kinetic and isotherm modeling using non-linear models allowed concluding that: i) the heating method is an efficient and simple process for reducing a relatively hydrophilic activated carbon and thereby enhancing its MC-LR adsorption capacity; ii) from a combination of the modification of the carbon surface chemistry and the carbon structure, it is demonstrates that both properties play an important role in the adsorption process, although carbon surface chemistry seems to be more important than its porous structure – MC-LR adsorption correlated with meso and macroporous volume and particularly well with carbon hydrophobicity (inverse of oxygen content); iii) the smaller the particle size, the more important is external mass transfer over intraparticle diffusion; iv) similar sized NOM strongly competes with MC-LR for the same AC sites; v) direct competition governs the simultaneous MC-LR and NOM adsorption; vi) the preloading phenomena reduces significantly the performance of activated carbon adsorption.

Key-words: Activated carbon adsorption, drinking water treatment, microcystin-LR, natural organic matter competition, activated carbon structure, activated carbon surface chemistry

RESUMO

As propriedades-chave (estrutura e química de superfície) para a adsorção em carvão activado de microcistina-LR (MC-LR) foram investigadas. Foram usadas águas com uma matriz inorgânica que se aproxima da água natural macia (2.5 mM de força iónica). Além disso, águas modelo em condições controladas de pH e força iónica, mas com NOM com tamanho similar ao de MC-LR (ácido tânico) e com extractos de MC-LR foram testadas com o carvão activado NORIT 0.8 SUPRA. Para este carvão, duas granulometrias foram usadas: 125-180 µm e 63-90 µm. A química de superfície do carvão NOR 125-180 µm foi modificada por tratamento térmico e foi também carregado (preloaded) com ácido tânico. A análise integrada da caracterização química e textural do carvão, assim como a modelação de cinéticas e isotérmicas de equilíbrio utilizando modelos não-lineares permitiu concluir que: i) o método de tratamento térmico é um processo simples e eficiente para modificar a superfície do carvão tornando-o mais básico e reforçando assim a adsorção de MC-LR; ii) a partir da combinação da modificação química da superfície do carvão e da sua estrutura, demonstrou-se que ambas as propriedades têm um papel importante na adsorção, embora a química de superfície do carvão pareça ser mais importante do que a sua estrutura porosa – a adsorção de MC-LR correlacionada com o volume de meso e macroporos é particularmente bem relacionada com a hidrofobicidade do carvão (inverso do teor de oxigénio); iii) quanto mais pequena a granulometria, mais importante se torna a transferência de massa externa ao longo da difusão dentro da partícula; iv) NOM de tamanho similar ao da MC-LR compete fortemente com MC-LR pelos mesmos locais de adsorção; v) a competição directa governa a adsorção simultânea de MC-LR e NOM; vi) o fenómeno de *preloading* reduz significativamente o desempenho da adsorção em carvão activado.

Palavras-chave: Adsorção, Carvão activado, Tratamento de água, Microcistina-LR, Competição com matéria orgânica natural, Estrutura do carvão, Química de superfície

TABLE OF CONTENTS

INDEX OF FIGURES

INDEX OF TABLES

ABBREVIATIONS

AC	Activated Carbon
AOM	Algogenic organic matter
BET	Brunauer, Emmet and Teller
C/F/S	Coagulation/flocculation/sedimentation
C_0	Initial concentration
DOC	Dissolved organic carbon
DPB	Disinfection byproducts
EC	Electrical conductivity at 25ºC
EOM	Extracellular organic matter
GAC	Granular activated carbon
HPLC	High performance liquid chromatography
IOM	Intracellular organic matter
IR	Infrared spectroscopy
IS	Ionic strength
LD_{50}	Lethal dose (50%)
MC	Microcystins
MC-LA	Microcystin-LA
MC-LF	Microcystin-LF
MC-LR	Microcystin-LR
MC-LW	Microcystin-LW
MC-LY	Microcystin-LY
MIB	Methylisoborneol
MW	Molecular weight
NF	Nanofiltration
NOM	Natural organic matter
PAC	Powdered activated carbon

PAC/UF	Powdered activated carbon adsorption/ultrafiltration
PDA	Photo diode array
pH_{pzc}	pH at the point of zero charge
PSD	Pore size distribution
TA	Tannic acid
TCE	Trichloroethylene
TFA	Trifluoracetic acid
TPD	Temperature programmed desorption
UF	Ultrafiltration
UPW	Ultrapure water
WHO	World Health Organization
WTP	Water treatment plant
XPS	X-ray photoelectron spectroscopy

1. INTRODUCTION

1.1. BACKGROUND

Eutrophication of freshwater resources has been studied worldwide and its consequences are of concern especially in waters used for recreation or human consumption (Vasconcelos, 2006). The occurrence of cyanobacteria blooms in surface water used for water catchment for human consumption is now the most important problem associated to the growing attendance conditions od eutrophication in surface waters (Menaia and Rosa, 2006). Cyanobacterial blooms seasonally challenge drinking water treatment due to the massive input of cells and also the release of algogenic organic matter (AOM) into the water, causing poor settling, filter clogging, tastes and odors, disinfectant consumption and production of disinfection by – products (Campinas, 2009). But the greatest concern is the ability of several cyanobacteria strains to produce and release (during "cell death" – lysis) potent toxins as secondary metabolites, cyanotoxins, including cyclic peptide hepatotoxins (e.g. Microcystins).

Microcystins-LR are the most frequently occurring cyanotoxins and may cause both severe and chronic effects (liver damage and tumor promoting). Furthermore, microcystins (MCs) are the only ones for which the World Health Organization (WHO) derived a drinking water provisional guideline value (1 μg/L for daily exposure to the microcystin-LR (MC-LR)), adopted as a national standard for drinking water quality (DL 306/2007). Additionally, these toxins where found in water reservoirs in Portugal (Vasconcelos, 2006; Osswald, 2007) which increases the importance of developing knowledge related to their removal (and to promote its dissemination) at national level.

For cyanotoxins, the removal in treatment processes is difficult by the fact that the toxins may be contained inside the intact cell (intracellular), and may be dissolved (extracellular). The microcystins are formed inside cyanobacterial cells. Cyanobacteria lysis releases the microcystins into the water. Once released from the cell, the toxins, being highly soluble, will exist in dissolved form (Drikas et al., 2001). An optimal water treatment requires the removal of intact cyanobacterial cells.

Conventional treatment (coagulation, flocculation, sedimentation and filtration) is considered ineffective (Drikas et al., 2001) for the removal of dissolved toxins, so advanced treatment processes must be implemented. The development of technologies that may adequately remove

these toxins from water is presently a major challenge and concern for the water management authorities and the water industry.

Activated carbon has been widely used for many years as an adsorbent in the drinking water and wastewater treatment, in the food, beverage, pharmaceutical and chemical industries and is the adsorbent of choice in most commercial adsorption separation processes due to its performance relative to its cost (Pendleton et al., 2001). It is also proven to be particularly effective on the removal of cyanotoxins from water, either in powdered (PAC) or granular (GAC) form (Lambert et al., 1996; Pendleton et al., 2001). The use of PAC has been mostly limited to a seasonal period when episodes of high levels of cyanotoxins occur. On the other hand, GAC is generally applied in water treatment plants when a permanent and safe barrier is required, not just for cyanotoxins (and other micropollutants) control, but also for the removal of the cyanobacterial cells (Hrudey et al., 1999). Also, several studies have been published showing the removal potential of MC-LR by activated carbon treatment (Falconer et al., 1989; Donati et al., 1994; Lambert et al., 1996; Drikas et al., 2001; Campinas, 2009; Costa, 2010).

However, AC performance depends on the type of water, carbon properties and raw water characteristics (inorganic and organic background matrices). Regarding the carbon properties most affecting the adsorption of microcystins, a broad consensus has not been obtained. Some authors' show that the removal efficiency depends upon the physical properties of activated carbon and the water background matrix, while surface chemistry characteristics do not affect the adsorption of microcystin-LR (Donati et al., 1994). However Huang and Cheng (2007) showed that both physical and chemical properties simultaneously affect the adsorption process. This thesis search for answers about these properties, looking for "key properties" of AC that lead to a better adsorption rate and capacity.

All drinking water treatment processes involve competitive adsorption between the adsorbate of interest and many other dissolved species, e.g. humic substances and dissolved organic matter (Pendleton et al., 2001). Several studies have demonstrated the impact of natural organic matter (NOM) on the adsorption kinetics and/or adsorption capacity for micropollutants, which adsorb in pores that NOM cannot access. However, microcystin-LR is hydrophobic and carries a negative net charge at pH 5-9 (Antoniou et al., 2005). Its molar mass (994 g/mol) is close to the NOM fraction of intermediate molar mass, which may change the competition mechanisms and the overall impact of NOM. The organic constituents compete with the target toxins for the AC adsorption sites and the inorganic compounds alter the electrostatic interactions between the adsorbate and the activated carbon. The presence of NOM has a harmful effect on activated

carbon adsorption because is usually present in much higher concentrations (mg/L levels) than toxins (μg/L levels) and compete directly for adsorption sites or by blocking pores.

The focus of this thesis was on MC-LR removal by AC adsorption. The impact of several carbon properties was evaluated and, with the aim of being able to understand and predict the process efficiency in real waters, an inorganic matrix was used and the competing mechanisms with NOM was studied. The NOM surrogate used for this study is tannic acid (TA). Tannic acid was selected as a representative of hydrophobic organics with a molecular weight of approximately 1700 g/mol. It contains phenolic groups and is expected to have a high competitive adsorption with MC-LR due to their similar molecular weight and charge (Campinas and Rosa, 2006).

It is within this context that arises the development of this thesis, focusing on the main questions involving the adsorption and the properties of the activated carbon for the adsorption of MC-LR, TA and for the competitive adsorption between MC-LR and TA.

1.2. OBJECTIVES

The present work attempts to contribute to the knowledge of MC-LR adsorption by AC's by investigating the effects of adsorbent surface chemistry and structure as well as the water background matrix, making the main objective to study the key properties of activated carbons, trying to reveal which has more importance: the structure of AC or its surface chemistry on the adsorption of microcystins in drinking water treatment. Recent studies indicate that not only the mesoporosity of an AC is important, but also its surface chemistry (Costa, 2010). This question and consequently, this thesis arise with the problematic suggested by Costa, 2010.
For this purpose, this general objective comprehends:

- Modify activated carbon (NOR 0.8 SUPRA) in order to modify its surface chemistry: reducing the oxygen content making it more basic;
- Studying mechanisms of competitive adsorption with natural organic matter with similar characteristics to those of MC-LR (tannic acid) in waters with similar characteristics of those of "blooms" occur, soft natural water (2.5 mM IS electrolyte: 1 mM KCl + 1.5 mM $CaCl_2$);
- Tests with TA-preloaded activated carbon, as well as its textural characterization, in order to study the predominant effects of competition (pore blocking or direct competition);

- Non-linear modeling of kinetic and isotherm adsorption models.

1.3. STRUCTURE OF THESIS

The thesis is divided in six chapters: (1) Introduction; (2) Literature review; (3) Materials and methods; (4) Results and discussion; (5) Conclusions and future work and (6) References.

The first chapter is introductory. This first chapter is also a brief presentation of the problem and "how to deal with the problem", the relevance of this study and the objectives of the thesis.

Chapter 2 includes a literature review to introduce the fundamentals and principles, and to characterize the state of the art of the main themes of this thesis. Chapter 2 presents a review regarding the main aspects of cyanobacteria and cyanotoxins, mainly the microcystin-LR, and a review of relevant legislation and guidelines for their presence in drinking water. The different treatment options for the removal of cyanobacteria and cyanotoxins (including MC-LR) are described. In particular, the activated carbon adsorption and the methodologies for the evaluation of the activated carbon performance are detailed (including the activated carbon properties, water matrix and the competitive mechanisms).

Chapter 3 includes the research strategy and describes the materials, methods and procedures used in the experiments to achieve the results presented in chapter 4, along with discussion.

Chapter 4 is divided in four sections. The first one describes the carbons used and their characterization. The second section presents and discusses the kinetic and isotherm studies with MC-LR and different activated carbons, discussing the effects of the surface chemistry and structure of activated carbon, and the models applied. The subchapter 4.3 presents and discusses the kinetic and isotherm studies with tannic acid onto different activated carbons, discussing also the effects of the surface chemistry and structure of activated carbons. The competitive adsorption between MC-LR and TA with different activated carbons is addressed in section 4.4. The MC-LR adsorption onto preloaded carbon is discussed on section 4.5. An integrated analysis of the results is made and the performances of the different types of activated carbon in similar conditions are compared.

Chapter 5 presents the main achievements of the work and suggestions for future research.

2. LITERATURE REVIEW

2.1. CYANOBACTERIA

Cyanobacteria, more commonly known as blue-green algae, are found worldwide in various aquatic environments as well as in water distribution systems (Antoniou et al., 2005). They are known as blue-green algae because these organisms have characteristics of both algae and bacteria. This is the only prokaryote group of algae and they have the distinction of being the oldest known fossils, more than 3500 million years old.
Cyanobacteria occur in a wide variety of habitats and partly because of their ability to fix atmospheric nitrogen, act as "primary colonizers" of terrestrial habitats in which few other organisms can multiply. They are able to carry out photosynthesis with the production of oxygen and their presence in large numbers in surface waters may reduce the potability of the water and may pose a risk to the health of those ingesting or having skin contact with the water (Mara and Horan 2003).

These bacteria are omnipresent in soil and surface waters, where, in the absence of eutrophication, are imperceptible to the naked eye. However, in the presence of conditions that promote eutrophication of water, lush blooms are formed and are predominantly composed of cyanobacteria. Sunlight is the energy source that cyanobacteria use to multiply, hence its importance for the formation of blooms (Menaia and Rosa, 2006).

Freshwater cyanobacteria may accumulate in surface waters as "blooms" and may concentrate on the surface as blue-green scum (Guidelines of Canadian Drinking Water, 2002).

The growth of cyanobacteria and the formation of blooms are influenced by a variety of physical, chemical and biological factors. Cyanobacteria blooms persist in water supplies when adequate levels of nutrients, especially phosphorus and nitrogen, are coupled with favorable environmental conditions: water temperatures generally between 15 and 30°C and a pH between 6 and 9 (Lambert et al., 1994). Timing and duration of the cyanobacterial bloom season depend largely on the climatic conditions of the region. In temperate zones, cyanobacterial blooms are most prominent during the late summer and early autumn and may last for 2-4 months. In warmer climates, like the ones of Portugal and Spain, blooms may occur for up to 6 months or longer (Sivonen and Jones, 1999).

These blooms report color, odor, and taste problems in water. More importantly, such blooms produce and release toxic compounds (during "cell death" - lysis) that intensely prejudice the quality of water bodies (Antoniou et al., 2005). Up to 50% of the recorded blooms can be expected to contain toxins (Carmichael, 1992). These compounds have severe and sometimes

irreversible effects on mammalian health. Exposure to cyanobacterial toxins can affect the number and diversity of wild animal populations, cause bioaccumulation of toxins in the tissues of fish and shellfish, and indirectly affect other organisms through the food chain. Moreover, the presence of cyanobacterial toxins in sources of drinking water supply has raised major concerns (Antoniou et al., 2005). *Microcystis* species are the most common toxic bloom-forming cyanobacteria in Europe, with *M. aeruginosa*, *M. viridis* and *M. weisenbergii* (Premazzi and Volterra, 1993).

Figure 2.1. Some countries (●) where cyanobacteria water blooms producing cyanotoxins have been documented (adapted from Carmichael, 2007).

2.2. CYANOBACTERIAL TOXINS

2.2.1. General

A toxin is a substance which has specific functional groups arranged on the molecule resulting in a strong physiological toxicity. When compared against other biological toxins, algal toxins rank more toxic than plant, fungal and somewhat less toxic than most bacterial toxins (Premazzi and Volterra, 1993).

As previously stated, cyanobacterial toxins are toxins produced by cyanobacteria. They include neurotoxins which affect the nervous system (e.g. anatoxins), hepatotoxins (e.g. microcystins), dermatotoxins, which cause irritations of the skin and other organs. About 50 species of cyanobacteria are known to produce toxins, but not all compounds produced during cyanobacterial blooms are toxic to humans and animals (Antoniou et al., 2005). Cyanobacterial toxins can also be grouped based on structure: cyclic peptides (hepatotoxins), alkaloids (neurotoxins) and lipopolysaccharides (LPSs). The hepatotoxins and neurotoxins are produced by cyanobacteria commonly found in surface water supplies and therefore appear to be of most relevance to water supplies at present (Guidelines for Canadian Drinking Water, 2002).

Microcystins (MC) have a molecular weight of 900-1100 Da (Vesterkvist e Meriluoto, 2003). Structurally, they are monocyclic heptapeptides that contain two variable L-amino acids and two novel D-amino acids. The two novel D-amino acids in microcystins are *N*-methyl dehydroalanine (Mdha), which hydrolyses to methylamine, and a unique non-polar-linked amino acid 3-amino-9-methoxy-2, 6, 8-trimethyl-10-phenyldeca-4, 6-dienoic acid, also known as Adda. The key component for biological activity appears to be linked with the Adda side chain, as cleavage of the Adda side chain from the cyclic peptide renders both components non-toxic (Dawson, 1998; Guidelines for Canadian Drinking Water, 2002).

Microcystins are amphiphatic molecules containing some hydrophilic functions such as the carboxyl groups and the guanidine group in the frequently present arginine residue, and some hydrophobic parts such as the Adda residue (which contains two conjugated double bonds).

Microcystin-LR, produced as a secondary metabolite by *Microcystis aeruginosa* and other blue-green algal species, appears to be the most commonly occurring microcystin (Carmichael, 1992) and has been the focus of most researchers dealing with such problems around the world.

2.2.2. Microcystin-LR

Microcystins are named according to their variable L-amino acids, so microcystin-LR (MC-LR) contains leucine (L) and arginine (R) (Dawson, 1998). MC-LR is a hydrophobic compound with a molecular mass of 994 g/mol. MC-LR was found to have a half-life of three to four days in aquatic systems under laboratory conditions. Even so, some studies have reported persistence of MC-LR for up to nine days in concentrations as high as 1300-1800 µg/L before any significant degradation occurred (Antoniou et al., 2005).

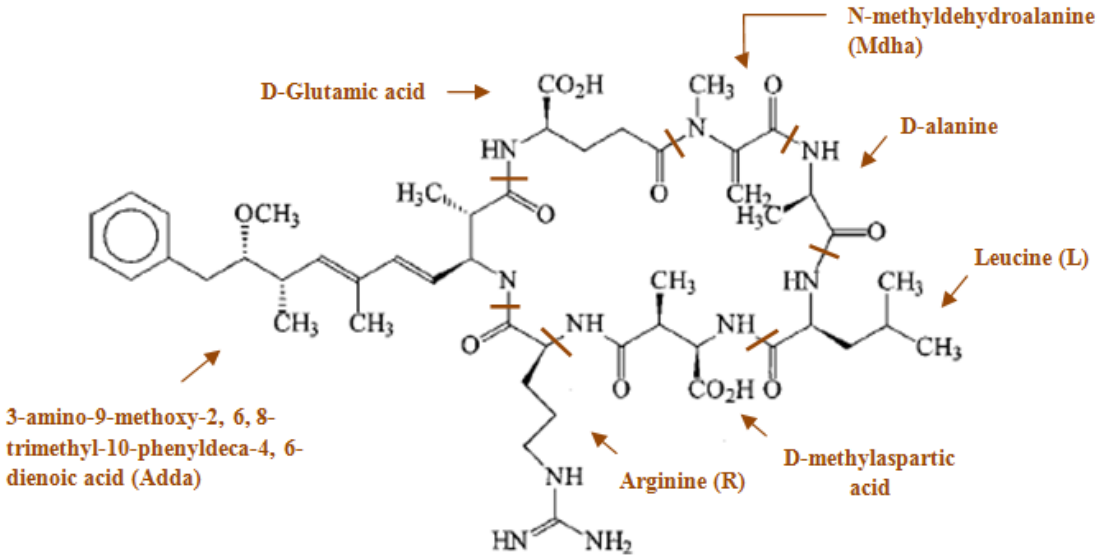

Figure 2.2. Structural formula ($C_{49}H_{74}N_{10}O_{12}$) of microcystin-LR (adapted from Antoniou, Cruz and Dionysiou, 2005).

Health related episodes in humans and animals caused by MC-LR contamination have been reported in several countries, including the United States, Australia, China, Great Britain and Brazil (Carmichael, 2005). After the first human fatal incident ocurred in Brazil in 1996, the World Health Organization (WHO) set the provisional concentration limit of MC-LR in potable water to 1µg/L (WHO, 2008). The guideline value is the concentration at which, over a lifetime of exposure, a "tolerable risk to the health of the consumer" is not exceeded (WHO, 2008). Although toxicological evidence is missing to support regulation of many cyanotoxin compounds, several countries have or are in the process of considering the establishment of guidelines and/or regulations for the limitation of cyanobacterial toxins in drinking water supplies. At least 14 countries have set standards to limit toxin concentrations in drinking water (Burch, 2007). Many of the countries have followed the legislation of the WHO (Table 2.1). The guideline value is calculated assuming a body weight, fraction of the intake allotted to

water consumption, and the amount of water ingested (based on 60 kg, 80%, and 2L/day, respectively).

Table 2.1. Guidelines or legislation for MC-LR in drinking waters (adapted from Antoniou et al., 2005, Burch 2007 and WHO 2008).

COUNTRY	GUIDELINE VALUE/STANDARD
Argentina	1.3 µg/L total Microcystins, expressed as toxicity equivalents of MC-LR
Brazil	1.0 µg/L for microcystins
Canada	1.5 µg/L cyanobacterial toxins as MC-LR
Czech Republic	1 µg/L for MC-LR
China	1 µg/L for MC-LR
France	1 µg/L for MC-LR
Italy	0.85 µg/L for total microcystins
Japan	1 µg/L for MC-LR
Korea	1 µg/L for MC-LR
New Zealand	1.0 µg/L for MC-LR
Norway	1 µg/L for MC-LR
Poland	1 µg/L for MC-LR
Portugal	**1 µg/L for MC-LR**
South Africa	0-0.8 µg/L for MC-LR
Spain	1 µg/L for total microcystins
Thailand	No guideline currently
United States of America	No guideline currently
Uruguay	Under review

In Portugal, the Decree-Law Nº306/2007 establishes the value of 1µg/L for total (extra and intracellular) MC-LR in drinking water analyzed at the water treatment plant exit whenever the raw surface water is suspected of eutrophication.

MC-LR exerts their toxic effect by interfering with a major cellular signal transduction mechanism, i.e., reversible phosphorylation. Reversible phosphorylation is like a switch that turns biological processes on and off. This is used to control a wide variety of cellular processes as diverse as muscle contraction, cell division, metabolism, and memory. MC-LR inhibits reversible phosphorylation by inhibiting the function of protein phosphatases and has been shown to significantly inhibit the catalytic subunits of only two specific types of protein phosphatases, protein phosphatase 1 (PP-1c) and protein phosphatase 2A, which leads to contraction of hepatocytes (liver cells) (Lambert et al., 1994). The cells start to separate, and the blood retained between them leads to local hepatocellular damage and shock (Falconer, 1996). Lethal doses lead to death within a few hours; however the intake of small doses leads to chronic disorder of the digestive system and liver. The lethal dose resulting in 50 per cent deaths (LD_{50}) is in range 25-150 µg/kg body weight in mice (intra-peritoneal) (a value of 50 or 60 µg/kg body is commonly accepted (Kuiper-Goodman and Fitzgerald, 1999).

Human intoxications can occur when cyanobacteria toxin enter human organism orally, by inhalation or through the skin. Depending on the way of entrance and the dominant species in the bloom, intoxications can be divided into gastrointestinal, respiratory and dermatological (Premazzi and Volterra, 1993). Genera *Microcystis* is responsible practically for gastrointestinal intoxications.

MC-LR is believed to absorb into the intestinal cells and parenchymal cells via bile acid transporters. MC-LR may be excreted into the bile duct and excreted back into the intestine. The kidney removes MC-LR from blood by filtration in the glomerulus or possibly by active transport in the proximal tubules, as we can see in Figure 2.4 (Lambert et al., 1994).

When MC-LR is solvated in water, the solvated volume is 2.63 nm^3 and the solvated area is 1.8 nm^2. The longest molecular length in MC-LR, shown in Figure 2.3, is approximately 1.9 nm (Pendleton et al., 2001). MC-LR has an estimated diameter between 1.2 – 2.6 nm (Antoniou et al., 2005).

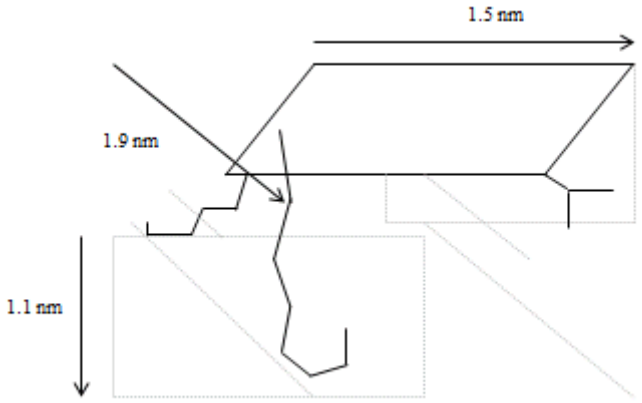

Figure 2.3. Typical structural dimensions of microcystin-LR (adapted from Pendleton et al., 2001).

The acid-base chemistry of MC-LR is controlled by three amino acids (Antoniou et al., 2005). D-methylaspartic acid and the D-glutamic acid have free carboxylic groups. The pKa for both is around 3.0 (2.09 and 2.19). L-arginine has two quanidino groups (basic group, pKa=12.48). With increasing pH, MC-LR loses two protons from the carboxylic groups, making the overall charge -1. This applies for most of the pH range ($3 < pH < 12$). At extremely basic pH, MC-LR loses the proton from the protonated basic group and the overall charge is -2. Thus, the overall charge transition (dissociation) of MC-LR in an aqueous medium can be summarized as (Antoniou et al., 2005):

$$MLRH_3^+ \leftrightarrow MLRH_2^0 \leftrightarrow MLRH^- \leftrightarrow MLR^{2-}$$

$$(+) \quad pk_1 = 2.09 \quad (0) \quad pk_2 = 2,19 \quad (-1) \quad pk_3 = 12.48 \quad (-2)$$

pH

The graphical representation of the fractional concentration of the species in solution and the overall charge is presented below (Figure 2.4). MC-LR carryies a -1 net charge at pH 6-9, which is the common pH range in water treatment.

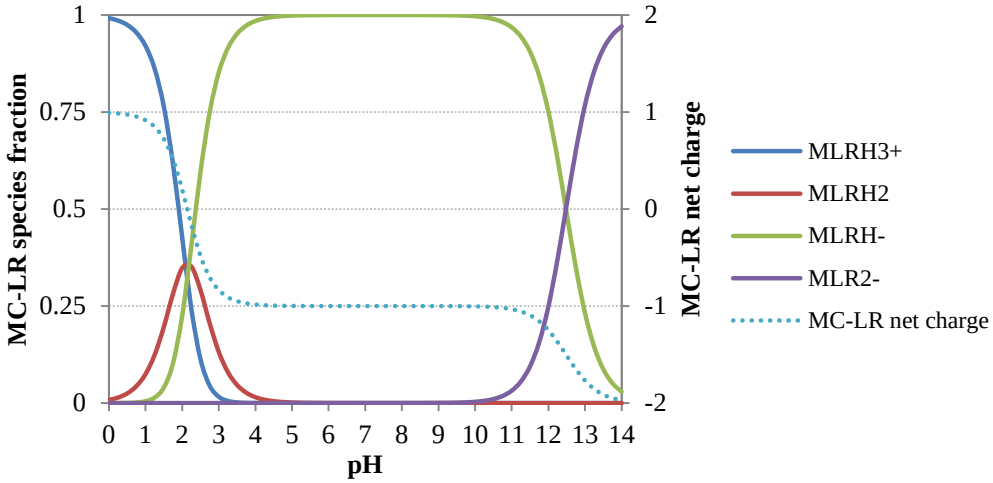

Figure 2.4. MC-LR species fraction and MC-LR net charge graph.

2.3. WATER TREATMENT OPTIONS FOR CYANOTOXINS

Soluble and particulate contaminant removal used in the by drinking water treatment: physical operations, chemical processes and biological processes (Table 2.2).

These operations may work singularly or in combination with each other to succeed contaminant reduction, which could be done through the ways of removal, degradation, and/or a reduction or inactivation of toxicity of the target compound. For cyanotoxins, the efficiency of removal in treatment processes is complicated by the fact that the toxins exist in two main forms: contained inside the intact cell (intracellular), and dissolved (extracellular). The microcystins are formed inside cyanobacterial cells. Dying and lysis of cyanobacteria release the microcystins into the water. Once released from the cell, the toxins, being highly soluble, will exist in dissolved form. The removal of intact cells is an effective way to prevent high

microcystin concentration in the treated water. Physical removal processes would therefore likely be the best form of treatment, although a toxin residual will be always released to water and dissolved toxins may require some additional treatment (Drikas et al., 2001).

Processes are considered with respect to their ability to remove both cyanobacterial cells and dissolved cyanotoxins, consequently evaluating total toxin removal capability. Physical and biological processes are often evaluated together.

Table 2.2. Cyanotoxin removal in drinking water treatment processes.

<table>
<tr><th colspan="2">CHEMICAL</th><th colspan="2">PHYSICAL/BIOLOGICAL</th></tr>
<tr><td rowspan="2">Oxidation</td><td rowspan="2">Chlorine
Chloramines
Chlorine dioxide
Potassium Permanganate
Ozone</td><td colspan="2">Coagulation
Sedimentation
Flotation</td></tr>
<tr><td>Filtration</td><td>Rapid rate
Slow sand
Membrane</td></tr>
<tr><td colspan="2">Advanced oxidation</td><td>Adsorption</td><td>Activated carbon</td></tr>
</table>

In addition to the form of cyanotoxin in water, the types of toxin and water matrix composition are important for consideration in treatment process evaluation. The chemical composition, structure, and molecular weight and charge vary between toxin types. Water quality parameters, such as pH and temperature, will impact chemical and biological reaction rates and the performance of physical treatment. Background contaminants, such as natural organic matter (NOM), may also impact the efficiency of some processes.

Chemical processes for cyanotoxins removal mainly involve the use of oxidants to break the organic molecules which cause toxicity. Oxidants may also cause damage to cyanobacterial cell membranes, which may result in cell lysis and subsequent toxin release. Thus the application of chemical processes for cyanotoxin removal must therefore be approached with caution, especially when used during the first stages of treatment.

Conventional water treatment processes by coagulation/flocculation/sedimentation/filtration can remove cyanobacterial cells, but not the dissolved toxins (Falconer et al., 1989). These processes have generally proven ineffective at removing microcystin toxins in drinking water (Himberg et al., 1989 and Lambert et al., 1994).

Ribau Teixeira and Rosa (2006) showed no significant removal of several dissolved microcystin variants in air flotation experiments. Therefore, flotation may be a good choice for toxin

removal if the toxins are still contained within the cell, but should most likely be used in combination with another process (es) if dissolved toxin removal is required.

Some treatment technologies have been developed to effectively remove the dissolved cyanotoxins. These technologies include oxidation and biological processes, membrane filtration and activated carbon adsorption. With respect to chemical removal, further studies are still needed for different cyanotoxins since they would respond differently to oxidation. For instance, permanganate, chlorine and ozone can effectively oxidize MC-LR (Arnette, 2009).

Micro-filtration (MF) and Ultra-filtration (UF) are used for particulate (i.e. cyanobacterial cell) removal and nanofiltration (NF) and reverse osmosis (RO) would be applicable for dissolved toxin removal, based on size exclusion. Nanofiltration has proved to be effective in the removal of cyanotoxins and cyanobacteria cells (Ribau Teixeira and Rosa, 2006).

Adsorption onto activated carbon (AC) is another technology that has proven to be mostly effective on the removal of cyanotoxins from water, although the efficiency of the removal depends on the type of water, carbon and type of toxin (Falconer et al., 1989 and Lambert et al., 1996; Campinas, 2009; Costa, 2010).

A summary of techniques described above can be seen in Table 2.3.

Table 2.3. Summary of techniques for treatment of cyanobacterial toxins (adapted from Newcombe and Nicholson, 2004).

Treatment Process	Cyanobacteria/Toxin	Treatment Efficiency
Intact cells		
Coagulation Sedimentation	Cyanobacterial cells	Very effective for the removal of intracellular toxins
Rapid filtration	Cyanobacterial cells	Very effective for the removal of intracellular toxins
Slow sand filtration	Cyanobacterial cells	As for rapid sand filtration, with additional possibility of biological degradation of dissolved toxins
Combined coagulation/ sedimentation/filtration	Cyanobacterial cells	Extremely effective for the removal of intracellular toxins
Membrane processes	Cyanobacterial cells	Very effective for the removal of intracellular toxins
Dissolved Air Flotation (DAF)	Cyanobacterial cells	Very effective for the removal of intracellular toxins
Oxidation processes	Cyanobacterial cells	Not recommended as a treatment for cyanobacterial cells as this process can lead to cell damage and lysis and consequent increase in dissolved toxin levels
Dissolved Toxins		
ADSORPTION		
Adsorption-powdered activated carbon (PAC)	Microcystins	Very effective. Doses required vary with water quality.
Adsorption-granular activated carbon (GAC)	All dissolved toxins	Very effective Depending on the type of toxin and the water quality
Biological filtration	All dissolved toxins	When functioning at the optimum this process can be very effective for the removal of most toxins. However, factors affecting the removal such as biofilm mass and composition, acclimation periods, temperature and water quality cannot be easily controlled

Treatment Process	Cyanobacteria/Toxin	Treatment Efficiency
Dissolved toxins		
OXIDATION		
Ozonation	All dissolved toxins	Ozonation is effective for all dissolved toxins except the saxitoxins. Doses will depend on water quality
Chlorination	All dissolved toxins	Most microcystins and cylindrospemopsin should be destroyed.
Chloramination	All dissolved toxins	Ineffective
Chlorine dioxide	All dissolved toxins	Not effective with doses used in drinking water treatment
Potassium permanganate	All dissolved toxins	Effective for microcystin, limited or no data for other toxins
Hydrogen peroxide	All dissolved toxins	Not effective on its own
UV radiation	All dissolved toxins	Capable of degrading microcystin-LR and cylindrospermopsin, but only at impractically high doses or in the presence of a catalyst
EXCLUSION		
Membrane processes	All dissolved toxins	Depends on membrane pore size distribution

2.4. FUNDAMENTALS OF ADSORPTION

2.4.1. General

Adsorption is the phenomenon of accumulating substances that are in solution on a suitable interface. Adsorption is a mass transfer operation in that a constituent in the liquid phase is transferred to the solid phase. The **adsorbate** is the substance that is being removed from the liquid phase at the interface (e.g. pollutant). The **adsorbent** (e.g. activated carbon) is the solid, liquid, or gas phase onto which the adsorbate accumulates (Metcalf and Eddy, 2003).

Adsorbates are held on the surface by various types of chemical forces such as hydrogen bonds, dipole-dipole interactions, and van der Walls forces. If the reaction is reversible, as it is for many compounds adsorbed to activated carbon, molecules continue to accumulate on the surface until the rate of the forward reaction (adsorption) equals the rate of the reverse reaction (desorption). When this condition exists, equilibrium has been reached and no further accumulation will occur (Snoeyink and Summers, 1999).

When the process involves only van der Walls forces and there is no chemical change of adsorbed molecules, this is called **physical adsorption** (Figueiredo and Ribeiro, 2007).

The adsorption is **chemical** when established chemical bonds may be with the surface active centers, leading to the formation of a chemical surface compound or a complex of adsorption (Figueiredo and Ribeiro, 2007).

Adsorbents of interest in water treatment include activated carbon, ion exchange resins; adsorbent resins; metal oxides, hydroxides, and carbonates; activated alumina; clays; and other solids that are suspended in or in contact with water (Snoeyink and Summers,1999).

Activated carbon (AC) adsorption is considered one of the best available technologies for advanced drinking water treatment, including for controlling dissolved microcystins.

2.4.2. Production, physical and chemical characteristics of activated carbon

Activated carbon can be used to adsorb specific organic molecules that cause taste and odor, mutagenicity, and toxicity, as well as natural organic matter (NOM) that causes color and that can react with chlorine to form disinfection byproducts (DPBs) (Snoeyink and Summers, 1999). Activated carbon is prepared by first making a char from organic materials such as almond, coconut, walnut hulls and other materials including woods, bone, and coal (Metcalf and Eddy, 2003). Wood, peat, lignite, subbituminous coal, and bituminous coal are the substances predominately used for drinking water treatment carbons (Snoeyink and Summers, 1999).

Both the physical and chemical manufacturing processes involve carbonization. The char is produced by heating the base material to a red heat (less than about 700°C) in a retort to drive off the hydrocarbons, but with an insufficient supply of oxygen to sustain combustion. The carbonization or char-producing process is essentially a pyrolysis process. The char particle is then *activated* by exposure to oxidizing gases such as steam and CO_2 at high temperatures, in the range from 800 to 900°C. These gases develop a porous structure in the carbon (Figure 2.5), and thus create a large internal surface area (Metcalf and Eddy, 2003). The resulting pore sizes are defined as **macropores** (> 500Å), **mesopores** (20Å - 500Å) and **micropores,** these can be divided into **primary micropores** (< 8Å) and **secondary micropores** (8Å - 20Å) (IUPAC, 2001).

The surface properties that result are a function of both the initial material used and the preparation procedure, so that many variations are possible. The type of base material from which the activated carbon is derived may also affect the pore-size distribution and the regeneration characteristics (Metcalf and Eddy, 2003).

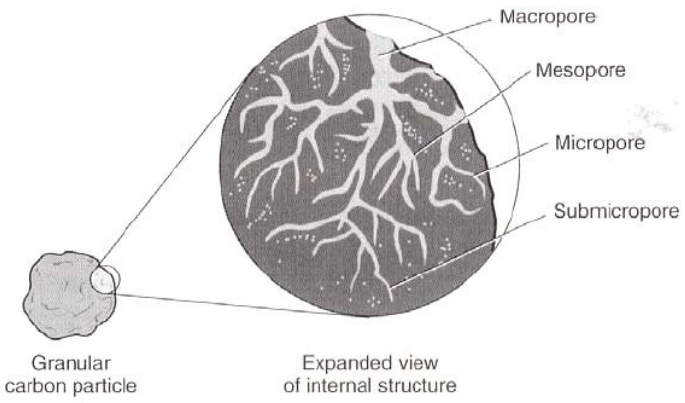

Figure 2.5. Macropore, mesopore, micropore and submicropore adsorption sites on activated carbon (adapted from Metcalf and Eddy, 2003).

After activation, the carbon can be separated into, or prepared in, different particle sizes with different adsorption capacities. The Figure 2.6 shows the two particle size classifications: **powdered activated carbon (PAC)**, which typically has a diameter of less than 0.074 nm (200 sieve), and **granular activated carbon (GAC)**, which has a diameter greater than 0.1 nm (~140 sieve) (Metcalf and Eddy, 2003). The correct selection of AC (PAC or GAC) is crucial for determining the efficiency and cost of the process (Table 2.4).

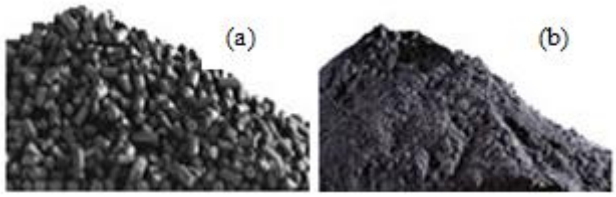

Figure 2.6. Granular (a) and powdered (b) activated carbon (adapted from Xinhui Carbon Co., 2010).

The common methods for the selection of AC are the molass test, the methylene blue number, the phenol test, the alkylbenzene sulphonate test, the iodine number and the dechlorination column test (Summers and Cummings, 1992). The values of these numbers give useful information about the abilities of various activated carbons to adsorb different types of organics. However, even though these tests can give some information of the behaviour of AC, they do not evaluate the kinetics and the capacity to adsorb a specific micropollutant (Snoeyink and Summers, 1999).

Table 2.4. Comparison of granular and powdered activated carbon (adapted from Metcalf and Eddy, 2003).

Parameter	Unit	Type of Activated Carbon [(a)]	
		GAC	PAC
Total surface area (BET)	m^2/g	700-1300	800-1800
Bulk density	kg/m^3	400-500	360-740
Particle density, wetted in water [(b)]	kg/L	1.0-1.5	1.3-1.4
Particle size range	mm (µm)	0.1-2.36	(5-50)
Effective size	mm	0.6-0.9	-
Iodine number		600-1100	800-1200
Ash	%	≤ 8	≤ 6
Moisture as packed	%	2-8	3-10

(a) Specific values will depend on the source material used for the production of the activated carbon

(b) The particle density wetted in water is the mass of solid activated carbon plus the mass of water required to fill the internal pores per unit volume of particle (Metcalf and Eddy, 2003).

The particle size is the main characteristic of PAC that differentiates it from GAC. The main advantages of using PAC are the low capital investment costs and the ability to change the PAC

dose as the water quality changes (Table 2.5). This advantage is especially important for systems that do not require an adsorbent for much of the year (Snoeyink and Summers, 1999).

The disadvantages (Table 2.5), according to Snoeyink and Summers (1999), are the high operating costs if high PAC doses are required for long periods of time, the inability to regenerate, the low TOC removal, the increased difficulty of sludge disposal, and the difficulty of completely removing the PAC particles from the water. GAC therefore becomes a more economical choice in larger systems or where taste and odor must be controlled continuously.

Table 2.5. Advantages (+) and disadvantages (-) of the PAC and GAC systems **(Cecílio et al., 2007)**.

CHARACTERISTIC	**PAC**	**GAC**
Easy adaptation to existing water treatment plants	+	-
Variation of dosage with the water quality	+	-
Removal capacity of AC on the downstream treatment	-	+
Larger volume of sludge and holding costs	-	+
Lower initial costs of investment	+	-
Higher adsorption capacity and better process control	-	+
Lifetime of AC (increased by biodegradation)	-	+

The point of PAC addition in the water treatment plant can occur in the rapid mix, in the flocculation stepor at the filter influent, not requiring any additional investment or special equipment, and being possible to use at any time. This is one of the major advantages of PAC. The major cost is related to the amount of PAC required, as it depends, not only on the micropollutant concentration, but also on the characteristics of the raw water. If the removal of microcystins from water is considered, doses above 20 mg/L of PAC are often required (Hrudey et al., 1999). Moreover, since PAC is not reutilized the amount of sludge produced is very high, and the cost of the treatment can be very high, especially if PAC is needed on a continuous basis.

When a micropollutant becomes a frequent and long-term problem, GAC adsorbers can be an efficient and a more sustainable alternative to PAC. GAC is used in columns or beds that allow higher adsorptive capacities to be achieved and easier process control than is possible with PAC, and it can be removed from the columns for reactivation when necessary (Snoeyink and Summers, 1999). These advantages normally tend to justify the high cost of the GAC system relatively to PAC. Furthermore, GAC removes both the cyanobacteria and the extracelular toxins (Hrudey et al., 1999).

Although the elemental composition of activated carbons can vary substantially, typical average elemental composition of activated carbon is approximately 88% C, 6-7% O, 1% S, 0.5% N, and 0.5% H, with the remainder being mineral matter (i.e., ash) (Edzwald, 1999).

Because of its abundance and significant effects on activated carbon hydrophilicity and surface charge, oxygen is generally the most important heteroatom of activated carbon surface chemistry. Oxygen commonly occurs in the form of carboxylic acid groups (–COOH), phenolic hydroxyl groups (–OH), and quinone carbonyl groups (>C=O). The activated carbon acidity is explained primarily by the formation of carboxylic acid and phenolic hydroxyl groups. The heteroatoms are important in determining the acidity/basicity of the AC surfaces in aqueous dispersion. Oxidation of activated carbon surfaces also occurs during the exposure of activated carbon to common oxidants used in water treatment, such as chlorine, permanganate, and ozone (Edzwald, 1999). Activated carbon can acquire an acidic character when exposed to oxygen between 473K and 973K or to oxidants such as air, water vapor, nitric acid, a mixture of nitric and sulfuric acids, and hydrogen peroxide, and acquire a basic character upon high-temperature (> 973K) treatment (Campinas, 2009).

2.4.3. Adsorption properties

Both physical and chemical characteristics of activated carbon affect its performance. Important adsorbent characteristics that affect adsorption include **surface area**, **pore size distribution**, and **surface chemistry** (Snoeyink and Summers, 1999).

The manufacturer provides typical data that usually include the **BET surface area**. This parameter is determined by measuring the adsorption isotherm for nitrogen gas molecules and then analyzing the data using the Brunauer-Emmett-Teller (BET) isotherm equation to determine the amount of nitrogen required to form a complete monolayer of nitrogen molecules on the carbon surface (Edzwald, 1999).

As one of the most important properties which influence the adsorption process, the **pore size distribution (PSD)** determines the fraction of the total pore volume that can be accessed by an adsorbate of a given size (Snoeyink and Summers, 1999). This influence occurs in two ways: (i) the adsorption strength increases with decreasing pore size because contact points between the adsorbate and the adsorbent surface increase (Newcombe et al., 1997) and (ii) adsorption potentials between opposing pore walls begin to overlap once the micropore width is less than about twice the adsorbate diameter (Sing, 1995). If pores are too small, size exclusion limits the

adsorption of contaminants. In aqueous systems, size exclusion is observed when the pore width is smaller than about 1.7 times the second largest dimension of the adsorbate (Li et al., 2002).

Hereupon, compounds are preferentially adsorbed in a pore of approximately its size, where there will be greater number of contact points and more promising adsorption energy (Newcombe et al., 1997) and they are size excluded if pores are too small compared to their size and shape. Consequently a correct pore size distribution provides not only the adsorption sites, but also the appropriate channels to transport, as a high volume of large transport pores (macro and mesopores), favors rapid diffusion to adsorption sites.

The **chemical surface** of the AC is heterogeneous due to the presence of atoms such as oxygen, nitrogen, hydrogen, sulphur and phosphorus. The acidic character of an AC is related to the oxygen contents. Functional groups such as carboxyl, phenol, lactones, lactol and quinones have been described as sources of surface acidity (Boehm, 1994). Hydrophobic adsorbents (i.e. activated carbons with low oxygen content) exhibit larger adsorption capacities for organic micropollutants than hydrophilic adsorbents (i.e. activated carbons with high oxygen content) with similar physical characteristics (Edzwald, 1999).

The carbon **surface charge** will change from positive to negative by increasing the pH of the wetting solution. This feature makes the **point of zero charge** (**pH_{pzc}**) a very common and important property of activated carbons. The point of zero charge (pzc) represents a pH condition where the surface ionic groups are neutralized to give an effectively uncharged surface (Pendleton et al., 2001). Below the pH_{pzc} carbons will carry a net positive charge, whereas they will be negatively charged above this point.

The **electrostatic interactions** between the carbon surface and the adsorbate molecules play an important part in the adsorption process. This means that a positive surface will attract a negatively charged molecule (Figure 2.7a) while a negatively charged surface will repel a negatively charged molecule (Figure 2.7b) (Newcombe et al., 1997).

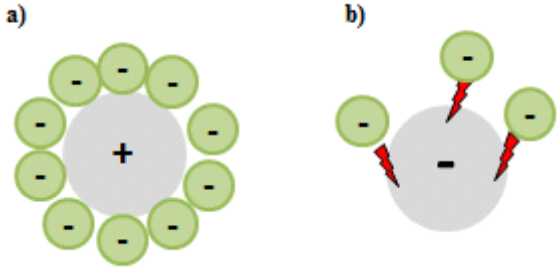

Figure 2.7. Electroestatic interactions between the carbon surface and the adsorbate molecules.

The mechanism and extent of adsorption have been shown to depend on: i) adsorbate structure (section 2.2.2); ii) AC characteristics (above mentioned); iii) solution chemistry and presence of competing compounds (section 2.4.4).

Both surface chemistry and pore volume distribution of AC play an important part in the adsorption, however, its relative importance will vary depending on the adsorbates and carbons. For example, for NOM, at pH 7, there is a strong evidence that electroestatic effects are determinant for adsorption (Newcombe and Drikas, 1997; Bjelopavlic et al., 1999). On the other hand, for microcystins, Pendleton et al., (2001) concluded about the major influence of the pore volume distribution (with a positive correlation with the volume of secondary micropores and mesopores) while Donati et al., (1994) showed no significant effect of the carbon surface chemistry.

The experimental techniques used to evaluate the AC properties include:

- **Elemental analysis**, employed in most studies as a quantitative and qualitative measurement for changes in carbon chemistry as a result of chemical modifications;
- **Surface titration**, which include *Boehm titration* (Boehm, 1994) and *mass titration*, to determine the pH_{pzc} (Bjelopavlic et al., 1999 and Moreno-Castilla et al., 2000);
- **Temperature-programmed desorption (TPD)**, for the characterization of the solid surfaces, namely surface oxygen groups on carbon materials decompose upon heating by releasing CO and CO_2 at different temperatures, producing distinct peaks (Figueiredo and Ribeiro, 2007);
- **Infrared spectroscopy (IR)**, for the determination of surface groups, namely by Fourier Transform IR (FTIR) (Moreno-Castilla et al., 2000);
- **X-ray photoelectron spectroscopy (XPS)**, based on the photoelectric effect, where the concept of photons impinging a surface is used to describe the resulting ejection of electrons from that surface. It is highly surface-specific due to the short range of the photoelectrons that are excited from the solid. The peak areas can be used to determine the chemical composition of the surface (Figueiredo and Ribeiro, 2007).

2.4.4. Solution chemistry

Besides the characteristics of the target adsorbate (e.g. molecular size, hydrophobicity, functional groups) and the adsorbent (e.g. AC surface area, pore size distribution, functional groups) which determine the adsorbent - adsorbate interactions and the adsorbate access to the adsorbent pores, the characteristics of the solution (e.g. temperature, pH, ionic strength, NOM) also influence the adsorption.

Although the greatest concern is the ability for several strains of cyanobacteria to produce potent toxins as secondary metabolites, the cyanotoxins, cyanobacterial blooms seasonally challenge drinking water treatment due to the massive input of cells and also the release of **algogenic organic matter** (AOM) into the water, causing poor settling, filter blockage, tastes and odors, disinfectant consumption and production of disinfection by-products. These organic substances include a wide range of compounds, such as oligo and polyssaccharides, proteins, peptides, amino acids and also traces of other organic acids (Pivokonsky et al., 2006).

2.4.4.1. Natural Organic Matter (NOM)

Natural organic matter (NOM) is present in all drinking water sources and is a complex mixture of compounds formed from the breakdown of plant and animal material in the environment (Bjelopavlic et al., 1999). Although strongly dependent on the nature of the local environment, NOM includes a wide range of compounds, from small, low molecular weight species (such as carboxylic and amino acids), to larger, high molecular weight (from 500 to 30000 Da) humic and fulvic acids and proteins.

Most of the compounds present in NOM carry a negative charge, generally attributed to carboxylic acid and phenolic groups, meaning that the larger compounds behave as polyelectrolytes in aqueous solution (Newcombe and Drikas, 1997).

The presence of NOM has been shown to impact upon all drinking water treatment processes, from alum coagulation (the removal of particulate and colloidal matter using aluminium sulphate) to chlorine disinfection. It has also a harmful effect on activated carbon adsorption as NOM is usually present in much higher concentrations (mg/L levels) than the target microcontaminants (μg/L levels) pesticides and algal toxins, and nanocontaminants (ng/L levels) taste and odor compounds, and competes directly for the adsorption sites or by blocking pores. When using activated carbon to remove microcontaminants, such as cyanotoxins, it is therefore essential to consider the NOM competition. (Bjelopavlic et al., 1999). Besides, NOM may change the surface properties of a carbon filter, resulting in reduced adsorption capacity.

This process is known as “carbon fouling” and is of special concern in water treatment plants (Newcombe and Drikas, 1997).

Carbon-adsorbate interactions are mainly of hydrophobic or electrostatic nature. In case of electrostatic interactions, the water ionic matrix plays an important role. Ionic strength may reduce or enhance AC adsorption of NOM (Newcombe and Drikas, 1997) and microcystins (Campinas and Rosa, 2006). Whenever the electrostatic interactions between the carbon surface and the adsorbate are attractive and the adsorbate’s concentration on the carbon surface (surface concentration) is low, an ionic strength increase will lessen adsorption (Newcombe and Drikas, 1997). Converse, if electrostatic interactions are repulsive or high concentrations occurs (which lead to lateral repulsion between adsorbed molecules), non-electrostatic forces govern adsorption and an ionic strength increase will enhance adsorption (Newcombe and Drikas, 1997; Campinas and Rosa, 2006) due to electrostatic shielding effects.

For both NOM (Newcombe and Drikas, 1997) and microcystins (Campinas and Rosa, 2006), such different ionic strength effects may be due to the prevailing type of adsorbate-adsorbent interactions (which depend upon the carbon and the adsorbent net charges and hydrophobicity), the cation charge (mono or divalent), and the adsorbate’s surface concentration and molecular size.

2.4.5. Adsorption mechanisms and models

The adsorption capacity of adsorbents is one of the most important criterions to assess the performance of the adsorbents. The most convenient and direct way to investigate the adsorption capacity for an adsorbent to an adsorbate is to conduct an equilibrium isotherm study (Ip et al., 2010). When the amount of solute being adsorbed onto the adsorbent is equal to the amount being desorbed, equilibrium is achieved and the capacity of the carbon has been reached (Metcalf and Eddy, 2003).

Adsorption, as illustrated on Figure 2.8, takes place in four (more or less defined) steps, being the slowest step called the rate-limiting step, which will control the rate of removal (Metcalf and Eddy, 2003).

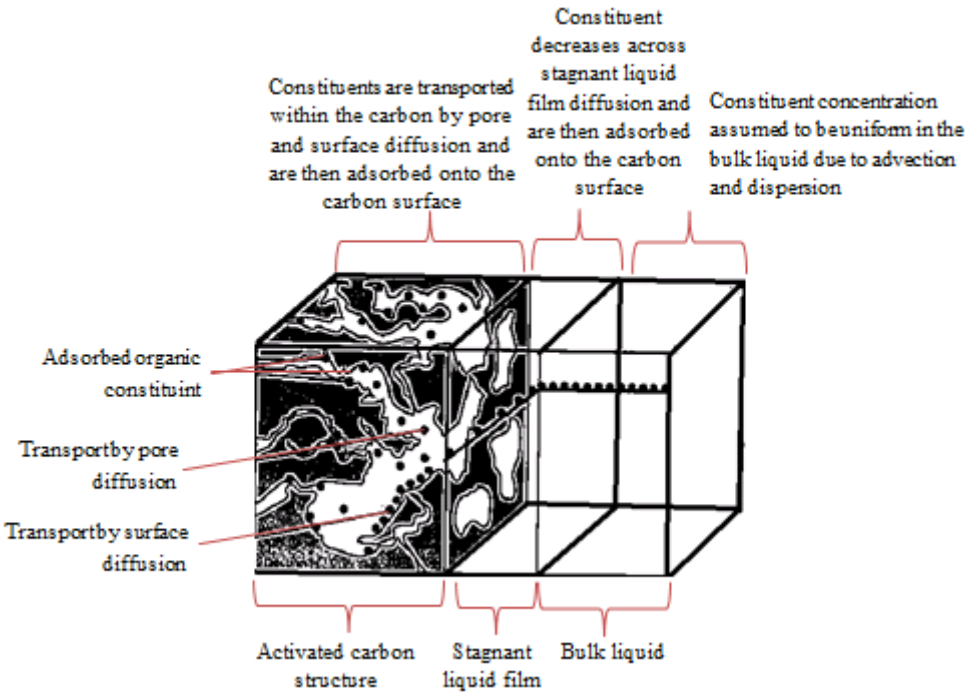

Figure 2.8. Definition sketch for the adsorption of an organic constituent with activated carbon (adapted from Metcalf and Eddy, 2003).

Bulk solution transport involves the movement of the material to be adsorbed through the bulk liquid to the boundary layer of fixed film of liquid surrounding the adsorbent, typically by convection and dispersion in carbon contactors. *Film diffusion transport* involves the transport by diffusion of the material through the stagnant liquid film to the entrance of the pores of the adsorbent. *Pore transpor*t involves the transport of the material to be adsorbed through the pores by a combination of molecular diffusion through the pore liquid and/or by diffusion along the surface of the adsorbent. *Adsorption* involves the attachment of the material to be adsorbed to the adsorbent at an available adsorption site (Snoeyink and Summers, 1999).

These steps are influenced by a range of factors. Step (1) (*bulk solution transport*) is affected by the molecular dimensions and shape of the adsorbate, but proper mixing may minimize these effects. In step (2) (*film diffusion transport*), diffusion depends on flow rate (the higher the flow, the shorter the distance), and on adsorbate dimensions and shape, although it is generally considered to be fast under proper mixing. Step (3) (*Pore transport*) is affected by pore structure (both external and internal), and molecular dimensions and shape of the adsorbate. In practical situations, step (3) is most likely to be rate limiting (Newcombe and Cook, 2004). Step (4) (*adsorption*) is very rapid for physical adsorption and, in that case, one of the preceding diffusion steps controls the adsorption rate. When chemical adsorption occurs, step (4) may be slower than the diffusion steps and may therefore control the rate of compound uptake (Snoeyink and Summers, 1999).

Kinetic and isotherm modeling is essential to design and optimize the water treatment.

2.4.5.1. Isotherm models

One of the most important characteristics of an adsorbent is the quantity of adsorbate it can accumulate. The constant-temperature equilibrium relationship between the quantity of adsorbate per unit of adsorbent q_e and its equilibrium solution concentration C_e is called the **adsorption isotherm** (Snoeyink and Summers, 1999). The equilibrium adsorption capacity, q_e (e.g. µg/mg), at different adsorbate concentrations is determined by a mass balance (equation 2.1).

$$\boldsymbol{q_e = \frac{(C_0 - C_e)V}{m}} \quad \textbf{[2.1]}$$

where C_0 (µg/L) is the initial concentration, Ce (µg/L) is the equilibrium concentration in the liquid phase, V is the volume of liquid phase (L), and m is the mass of adsorbent (mg).

Plotting the solid phase concentration against the liquid phase concentration graphically depicts the equilibrium isotherm. The theoretical adsorption capacity of a carbon for a particular contaminant can be determined by developing the adsorption isotherm as described below.

The common equations for single-solute adsorption are the **Freundlich** and the **Langmuir** equations. The **Freundlich** equation is an empirical equation that is very useful because it accurately describes much adsorption data. This equation has the form

$$\boldsymbol{q_e = K C_e^{1/n}} \quad \textbf{[2.2]}$$

and can be linearized as follows:

$$\boldsymbol{\log q_e = \log K + \frac{1}{n} \log C_e} \quad \textbf{[2.3]}$$

The parameters q_e (with units of mass adsorbate/mass adsorbent, or mole adsorbate/mass adsorbent) and C_e (with units of mass/volume, or moles/volume) are the equilibrium surface and solution concentrations, respectively. The terms *K* and *1/n* are constants for a given system; *1/n* is dimensionless, and the units of *K* are determined by the units of q_e and C_e.

The parameter *K* in the Freundlich equation is related primarily to the capacity of the adsorbent for the adsorbate, and *1/n* is a function of the strength of adsorption. For fixed values of C_e and *1/n*, the larger the value of *K*, the larger the capacity q_e. For fixed values of *K* and C_e, the smaller the value of *1/n*, the stronger is the adsorption bond. As *1/n* becomes very small, the capacity tends to be independent of C_e, and the isotherm plot approaches the horizontal level; the value of q_e is then essentially constant, and the isotherm is termed irreversible. If the value of *1/n* is large, the adsorption bond is weak, and the value of q_e changes markedly with small changes in C_e (Snoeyink and Summers, 1999).

The Freundlich equation cannot be applied to all values of C_e, however. As C_e increases, for example, q_e increases (in accordance with Equation 2.2) only until the adsorbent approaches saturation. At saturation, q_e is constant, independent of further increases in C_e, and the Freundlich equation no longer applies. Also, no assurance exists that adsorption data will conform to the Freundlich equation over all concentrations below saturation, so care must be exercised in extending the equation to concentration ranges that have not been tested (Snoeyink and Summers, 1999).

The **Langmuir** equation, is as follows

$$\boldsymbol{q_e = \frac{q_{max} b C_e}{1 + b C_e}} \qquad \textbf{[2.4]}$$

whose linear form is

$$\boldsymbol{\frac{C_e}{q_e} = \frac{1}{q_{max} b} + \frac{C_e}{q_{max}}} \qquad \textbf{[2.5]}$$

where b (volume/mass adsorbate) and q_{max} (mass adsorbate/mass adsorbent) are the Langmuir constants. The constant q_{max} corresponds to the surface concentration at monolayer coverage and represents the maximum value of q_e that can be achieved as C_e is increased. The constant b is related to the energy of adsorption and increases as the strength of the adsorption bond increases. The Langmuir equation often does not describe adsorption data as precisely as the Freundlich equation.

2.4.5.2. Kinetic models

In order to investigate the mechanism of adsorption and potential rate controlling steps such as chemical reaction, diffusion control and mass transport processes, kinetic models have been used to test experimental data (Ip et al., 2010). Some kinetic models are commonly employed, namely the **pseudo first-order kinetic model**, the **pseudo second-order kinetic model**, the **intraparticle diffusion model** and the **homogeneous surface diffusion model** (HSDM).

Both the **pseudo first-order** and **pseudo second-order models** assume that the difference between the surface concentration at equilibrium and the average surface concentration is the driving force for adsorption. They generally represent well experimental kinetic data where the adsorbate interactions are expected to be negligible. The diffusional mass transport models, in particular, the **intraparticle diffusion model**, are important in processes where ion exchange and ionic bonding are not as prevalent as in chemisorption processes. The intraparticle mass

transport model accounts for the adsorption mechanism in many well stirred adsorption systems (Yang and Al-Duri, 2005).

Recently, the linear forms of the pseudo-first order and the pseudo-second order equations were widely used due to the simplicity in estimation. When using the linear form, experimental adsorption kinetics should be linearized for the least-squares regression to estimate the model parameters. It has been reported that transformation of non-linear equations to linear forms implicity alter their error structure in the measurement of model parameters. As a result, one may obtain different kinetic parameters when using different forms of model equations for a given adsorption phenomenon (Junxiong and Wang, 2009).

There are, however, few studies comparing the linear and non-linear forms of pseudo-first order and pseudo-second order models estimating the kinetic parameters for the adsorption of MC-LR on activated carbon. Junxiong et al.,(2009) detailed a comparative analysis between the linear and non-linear method in determining the kinetic parameters. This study shows that the best fitting non-linear forms of pseudo-first order and pseudo-second order kinetic models were superior to the linear forms. Subramanyam and Das (2009) also concluded that it is always better to find the isotherm coefficients by non-linear method, as far as practicable. In case of linearized models application, at least, the results must be accepted as approximate, not exact.

Consequently, in this thesis the non-linear forms of pseudo-first order and pseudo-second order kinetic models will be used.

Lagergreen (1898) proposed a rate equation for the sorption of a solute from a liquid solution based on the adsorption capacity. The Lagergreen equation is the most widely used rate equation in liquid phase sorption and this kinetic model is expressed as:

$$\frac{dq_t}{dt} = k_1(q_e - q_t) \qquad \textbf{[2.6]}$$

Integrating the above equation for the boundary conditions t = 0 to t = t and $q_t = q_t$ gives:

$$\ln (q_e - q_t) = \ln\ q_e - k_1\, t \qquad \textbf{[2.7]}$$

Where q_e (µg/mg) is the surface concentration at equilibrium, q_t (µg/mg) is the average surface concentration at time t. The pseudo-first order rate constant k_1 (h^{-1}) can be determined by plotting ln (q_e - q_t) against t (linear form of the model).

However, as what is measured experimentally is the concentration that is in water, it seems to be more correct to analyze the kinetics in terms of concentration of liquid phase. For that purpose, equation 2.1 may be substituted in equation 2.6:

$$\frac{dC}{dt} = -\frac{k_1 m}{V}(q_e - q_t) = -k_1\left[\frac{m}{V}q_e - (C_0 - C)\right] \quad \textbf{[2.8]}$$

Ho and McKay (1999) developed a second-order equation based on adsorption capacity. This kinetic model can be written as:

$$\frac{dq_t}{dt} = k_2\,(q_e - q_t)^2 \quad \textbf{[2.9]}$$

Integrating the above equation for the boundary conditions t = 0 to t = t and $q_t = 0$ to $q_t = q_t$ gives:

$$\frac{1}{q_e - q_t} = \frac{1}{q_e} + k_2\,t \quad \textbf{[2.10]}$$

Where k_2 (mg/(μg.h) is the pseudo-second order rate constant of sorption. A linear form of this equation was shown as:

$$\frac{t}{q_t} = \frac{1}{k_2 q_e^2} + \frac{1}{q_e}t \quad \textbf{[2.11]}$$

The applications of this model are widely used in fitting the kinetic data for various systems (Ip et al., 2010). The pseudo-second-order equation is in agreement with chemisorption being the rate controlling step (Badmus et al.,2007).

In order to concentration of liquid phase we obtain:

$$\frac{dC}{dt} = \frac{-mk_2(q_e - q_t)^2}{V} = \frac{-mk_2(q_e - (C_0 - C)\frac{V}{m})^2}{V} \quad \textbf{[2.12]}$$

For using this methodology, a fixed q_e must be known. This q_e must be the one that best defines the equilibrium isotherm. Since the equilibrium equations are non-linear and are complex, it is not possible to calculate q_e analytically. It has therefore to be calculated numerically. It is necessary to solve the following system of equations:

$$\begin{cases} q_e = \frac{q_{max} b C_e}{1 + b C_e} \\ C_e = C_0 - \frac{q_e m}{V} \end{cases} \quad \textbf{[2.13]}$$

Table 2.6 presents all linear and non-linear forms of pseudo-first order and pseudo-second order equations.

Table 2.6. Linear and non-linear forms of pseudo-first order and pseudo-second order equations.

Kinetic model	Linear equation	Non-linear equations
Pseudo-first order	$\ln(q_e - q_t) = \ln(q_e) - k_1 t$	$q_t = q_e(1 - e^{-k_1 t})$ $\frac{dq_t}{dt} = k_1(q_e - q_t)$ $\frac{dC}{dt} = -\frac{mk_1}{V}\left(q_e - \frac{V}{m}(C_0 - C)\right)$
Pseudo-second order	$\frac{t}{q_t} = \frac{1}{k_2 q_e^2} + \frac{1}{q_e} t$ $q_t = q_e - \frac{1}{k_2 q_e}\frac{q_t}{t}$ $\frac{q_t}{t} = k_2 q_e^2 - k_2 q_e q_t$	$q_t = \frac{k_2 q_e^2 t}{1 + k_2 q_e t}$ $\frac{dq_t}{dt} = k_2(q_e - q_t)^2$ $\frac{dC}{dt} = \frac{-mk_2(q_e - (C_0 - C)\frac{V}{m})^2}{V}$

Weber and Morris presented the intraparticle diffusion equation as follows:

$$\boldsymbol{q_t = k_p t^{1/2}} \quad \textbf{[2.14]}$$

where k_p (µg/(mg.h$^{1/2}$)) is the intraparticle diffusion rate constant and q_t (µg/mg) is the amount adsorbed at time t (min). Equation 2.14 can be represented in a plot of q_t vs. $t^{1/2}$, and a straight line passing through the origin should indicate that the adsorption process follows the intraparticle diffusion model. The slope of the straight line is k_p, the rate constant.

If this plot is linear but does not pass through the origin (equation 2.15), the external mass transfer may not be neglected and the constant C is proportional to the boundary layer thickness, the larger the intercept the greater the contribution of the surface sorption to the rate limiting step.

$$\boldsymbol{q_t = k_p t^{1/2} + C} \quad \textbf{[2.15]}$$

Such plots may present a number of linear portions implying that two or more steps occur. The first sharper portion is the external surface adsorption stage, indicating the boundary layer effect, while the second linear portion is defined as the intraparticle diffusion or pore diffusion. The third portion is the final equilibrium stage (Choy and Porter, 2004). The slope of the second line has been defined as the intraparticle diffusion parameter k_p (µg/(mg.h)). If the intra-particle diffusion is the rate limiting step of adsorption, the line will pass through the origin, otherwise, external mass transfer resistance may not be neglected.

The kinetic data could be additionally analyzed using the kinetics expressions derived by Boyd, Adamson and Myers (Reichenberg, 1953).

$$F = \frac{q}{q_e} = 1 - \frac{6}{\pi^2} \times \sum_{n=1}^{\infty} \frac{1}{n^2} \times e^{-n^2 \times Bt} \quad \textbf{[2.16]}$$

where B (1/s, if t is in s) is given by

$$B = \frac{\pi^2 \times D_i}{r^2} \quad \textbf{[2.17]}$$

and Di (cm^2/s) is the effective diffusion coefficient and r (cm) is the particle radius, assuming spherical particles.

According to Reichenberg (1953), for values of F < 0.85, equation 2.16 can be simplified to:

$$B\,t = 6.28318 - 3.2899\,F - 6.28318\,(1 - 1.0470\,F)^{\frac{1}{2}} \quad \textbf{[2.18]}$$

If the Bt versus t plot is a straight line passing through the origin, the intraparticle transport is the rate-limiting step. If the plot does not pass through the origin, external mass transport is rate-limiting (Kumar et al., 2005).

These kinetic models were applied to a high number of compounds. With respect to cyanotoxins Huang and Cheng (2007) and Costa (2010) applied the kinetic intraparticle diffusion model to the adsorption of MC-LR onto AC, and the results indicated that pore diffusion might not be the only rate-controlling step in the removal of MC-LR.

Along with the previous models, the homogeneous surface diffusion model (HSDM) is often used. In this model, porous diffusion is neglected, so that internal mass transfer is only due to surface diffusion. It predicts the diffusion of a molecule from the external surface of the adsorbent particle through the pore surface, to the adsorption site. The other three mass transfer steps taking place during adsorption, transfer from bulk liquid to surface film surrounding the particle, transfer through this surface film, and the adsorption step, are not considered rate-limiting in this model. The AC particles are considered to be spherical and of homogeneous structure, and Fick's first law of diffusion is applied for the calculation of the adsorbent surface concentration as a function of the radial position within the particle. The change in bulk liquid phase concentration with time is then calculated using a mathematical model, appropriate for the configuration of the system (Newcombe et al., 2003).

Although with some limitations, the HSDM model has been used to predict the dosages of PAC to use in full-scale systems, including the removal of microcystins (Newcombe et al., 2003).

2.4.6. Competitive adsorption

Background water NOM strongly affects the adsorption of other organic microcontaminants, specifically through competition mechanisms. The greatest competition is expected to be between compounds of similar molecular size (Jain and Snoeyink ,1973; Costa, 2010).
NOM competition was found for trichloroethylene (TCE), atrazine, 2-methylsoborneol (MIB) and MC-LR (Donati et al., 1994; Lambert et al., 1996).

The Langmuir and Freundlich equations are often used to determine the AC adsorption capacity in single-solute solutions, namely organic compounds at very low concentrations.
However, AC performance for microcontaminant removal is greatly affected by NOM competitive adsorption. This competition reduces the adsorption sites and the adsorption capacity for the target compounds with **direct site competition** and **pore blockage** considered the most likely competing mechanisms.

Direct competition is responsible for a reduction in the adsorption capacity for the target compound (Snoeyink and Summers, 1999) and occurs when i) the competing compounds are able to access the same sites (when the target and the competing compounds have similar size), or ii) the target compound adsorbs in a larger pore (with lower adsorption energy) and the larger competing compound (with higher adsorption energy) is able to displace it (Newcombe et al., 2002).

Sometimes, competing molecules may not adsorb on the same sites as the target compound, because pores are too small, but are capable of **constricting or blocking pores** and disturb the target compound transport to final adsorption sites, reducing its rate of adsorption (Snoeyink and Summers, 1999). The NOM fraction larger than the target compound may **reduce/block** the pores entrance.

Several authors concluded that an increase of AC pore size distribution could reduce, and even avoid pore blockage by NOM (Donati et al., 1994; Newcombe et al., 1997; Li et al., 2002). Other studies have showed that the smaller NOM compounds may also participate in pore constriction/blockage (Newcomb et al., 2002). As suggested by Kilduff et al. (1998), these two mechanisms become indistinguishable as the competing and target compounds become closer in size.

The subsequent reduction of the carbon capacity for the target contaminant is reflected by reduced Langmuir (q_{max}) and Freundlich (K) parameters. The comparison of the *1/n* values in single-solute and in competition conditions provides insight on the leading competition mechanism (Pelekani and Snoeyink, 1999). If *1/n* does not vary (i.e. there is no change in site heterogeneity) target compound is adsorbed on the same porous range and therefore its adsorption capacity decreases proportionally to the number of pores blocked/constricted by the larger competing NOM fraction. On the other hand, if *1/n* increases the adsorption is taking place in a wider range of pore sizes and direct site competition between the target compound and the NOM fraction of similar size is most probably the dominant mechanism (Pelekani and Snoeyink, 1999). In most cases these models may not be applicable.

The application of kinetic models is used for single-solute data. However, for practical purposes, it is interesting to apply these models to natural waters in order to find variation in the kinetic parameters due to the competition mechanisms. Direct competition for sites should have no effect on adsorption kinetics (diffusion rates) if competing molecules have approximately the same size, but pore constriction/blockage should significantly change adsorption diffusivity if the competitive molecules have different sizes. To elucidate the competitive mechanism an integrated approach with kinetic and isotherm models should be undertaken.

Furthermore, during use, **NOM preloads AC**, which significantly inhibits microcontaminant adsorption by blocking the pores' access and or by adsorbing onto the sites to be used by the microcontaminants, in both cases reducing the number of available adsorption sites (Pelekani and Snoeyink, 1999; Newcombe et al., 2002).

2.5. ACTIVATED CARBON APPLICATION FOR MICROCYSTIN-LR CONTROL

The equilibrium between the solution phase and carbon-adsorbed MC-LR is described below (Pendleton et al., 2001):

$$MC - LR\ (solution) + AC \leftrightarrow MC - LR\ (adsorbed) - AC$$

Published studies on MC-LR adsorption onto activated carbon show that the removal efficiency depends upon the type of activated carbon and the water background matrix (Donati et al., 1994).

Table 2.7. Maximum capacity of some AC for removing MC-LR from ultrapure water.

AC type	C_0 (µg/L)	Maximum capacity, q_e (µg/mg)	Literature
Coconut-based	2500	20-40	(Donati et al., 1994)
Wood-based	2500	220-280	(Donati et al., 1994)
Wood-based	300000	177±12	(Pendleton et al., 2001)
Extruded Peat	116	6.04	(Costa, 2010)

The wood-based carbons tested by Donati et al., (1994) (Table 2.7) seemed to be more effective for the removal of MC-LR than the coal or the coconut-based carbons. The same authors indicate the carbon mesopore (2–50 nm) volume to be responsible for the MC-LR adsorption. Newcombe and Nicholson (2004) obtained a linear relationship between the pore volume of AC and the MC-LR adsorption, finding poor influence of the surface chemistry of the carbons.

Between the numerous types of AC investigated, Falconer et al., (1989) and Costa (2010) found the peat-based NORIT 0.8 SUPRA carbon very efficient for the removal of MC-LR. Consequently, NORIT 0.8 SUPRA was the carbon selected for the present study.

PAC addition is a common option used in drinking water treatment due to the simplicity of operation and efficiency (as discussed in section 2.4.2). PAC and GAC efficiency depends in both cases on the AC and the target contaminant, as well as on water background matrix, namely, NOM content, pH and ionic make-up.

The literature reports limited lifetime of the GAC for the removal of microcystins, as for other microcontaminants. However, this parameter can be increased by biodegradation, since in practice microorganisms colonize the filters (Newcombe and Nicholson, 2004). The biologically active carbon filters (BAC) are promising for the removal of cyanotoxins (Mesquita et al., 2006; Mesquita, 2011).

The first consideration in the design of any activated carbon system is the carbon selection. Selection depends on the ability of a given carbon to remove the contaminants of concern and to meet other system requirements related to pressure drop, carbon transport, and reactivation. A number of granular activated carbons are commercially available, and the most appropriate type for a given application is usually determined by laboratory and pilot testing based on isotherms (Clark and Lykins, 1989).

For MC-LR adsorption it is important to take into consideration first that MC-LR is a relatively large molecule (section 2.2; Figure 2.3) and second that it is a complex aggregate of amino acids rendering hydrophobic character to its aqueous solution properties (Pendleton et al., 2001). Consequently, the correct selection of an AC for MC-LR removal from an aqueous solution, prior to any adsorption measurements, requires an appreciation of these two properties combined with a detailed knowledge of the adsorbent's physical and surface chemical properties.

Four types of commercial activated carbons were considered for selection based on literature: **Filtrasorb 400** (from Calgon Corporation), **Filtrasorb 200** (from Calgon Corporation), **Norit Row 0.8 Supra** (from NORIT) and **Norit GAC 1240** (from NORIT). Henceforth, these coals will be called: **F200**, **F400**, **NOR 0.8** and **NOR 1240**. The properties of the screened ACs that were found in literature are summarized in Table 2.8 and Table 2.9.

Table 2.8. Properties of the studied AC based on literature (Rivera-Utrilla and Sánchez-Polo, 2002; Sánchez-Polo et al., 2006; Lyubchik et al., 2008; Costa 2010; Sze e McKay, 2010).

	F400	**F200**	**NOR 0.8**	**NOR 1240**
Material	Bituminous coal	Bituminous coal	Extruded-peat	Bituminous coal
S_{BET} (m^2/g)	825	714	900	770
V_{micro} (cm^3/g)	0.387	0.32	0.38	0.39
V_{meso} (cm^3/g)	0.104	0.14	0.25	0.25
V_{total} (cm^3/g)	0.491	0.48	0.66	0.4
S_{micro} (m^2/g)	768	631	747	729
S_{meso} (m^2/g)	57	83	153	41
pH_{pzc}	7.91	7.1	9.5	6.92

NOR 0.8 is the activated carbon selected for the present study. As discussed previously in section 2.5, this carbon was selected due to its efficiency for MC-LR removal (Falconer et al., 1989; Donati et al., 1994; Lambert et al., 1996; Costa, 2010).

Table 2.9. Elemental analysis (wt %) of the NOR 0.8 (Costa, 2010).

N (%)	C (%)	H (%)	S (%)	O (%)	Ash (%)
0.5	87.2	0.4	0.5	11.5	6.0

According to the manufacturer (Table 2.10), NOR 0.8 is an extruded carbon, suitable for a wide range of applications in the food, chemical and bulk pharmaceutical industries. Its structure makes it suitable for the removal of compounds that give color and smell to water, organic microcontaminants and other dissolved organic compounds and for the removal of chlorine and ozone (NORIT, 2007).

Table 2.10. Product specifications given by manufacturer (NORIT, 2007).

Product specifications for NORIT 0.8 SUPRA	
Iodine Number (mg/g)	1100
Particle size (average) (µm)	600
Methylene blue adsorption (g/100g)	24
Surface area, BET (m^2/g)	1300
Apparent density (g/mL)	0.40
Ash (%)	7

3. MATERIALS AND METHODS

3.1. RESEARCH STRATEGY

In order to achieve the central objective of this thesis (defined in section 1.2), the adsorption of MC-LR onto different types of activated carbon was studied and interpreted. The research strategy (Figure 3.1) developed for the study of MC-LR adsorption, TA adsorption and their competitive adsorption onto different types of activated carbon includes:

- **Carbon selection** (based on literature review);

- **Treatment of the studied activated carbon including:**
  - Carbon preparation: Grinding (two different particle sizes: 125-180 μm and 63-90 μm with the aim of studying the adsorption kinetics), sieving and washing the selected activated carbon;
  - Carbon modification: modification of the surface chemistry making it more basic (decreasing oxygen content);
  - Carbon preloading with tannic acid, a NOM surrogate with similar characteristics (similar size, charge and hydrophobicity), i.e. a strong competitor with MC-LR.

- **Chemical** (elemental analysis, ash content, surface charge by carbon titration) **and textural** (porous structure and distribution) **characterization of the studied carbons** (virgin: two particle sizes, modified and after TA-preloading);

- **Batch adsorption tests – kinetic and isotherm** experiments and respective evaluation with kinetic and isotherm models, to study the influence of the structure and surface chemistry of activated carbon on the adsorption of microcystins, and on its competitive adsorption in the presence of NOM, in controlled conditions of temperature, pH and ionic strength (soft natural water: 2.5 mM IS electrolyte – 1 mM IS KCl + 1.5 mM $CaCl_2$).

- **Non-linear models** for kinetic and isotherm adsorption modeling were used due to its better fit and lower associated errors.

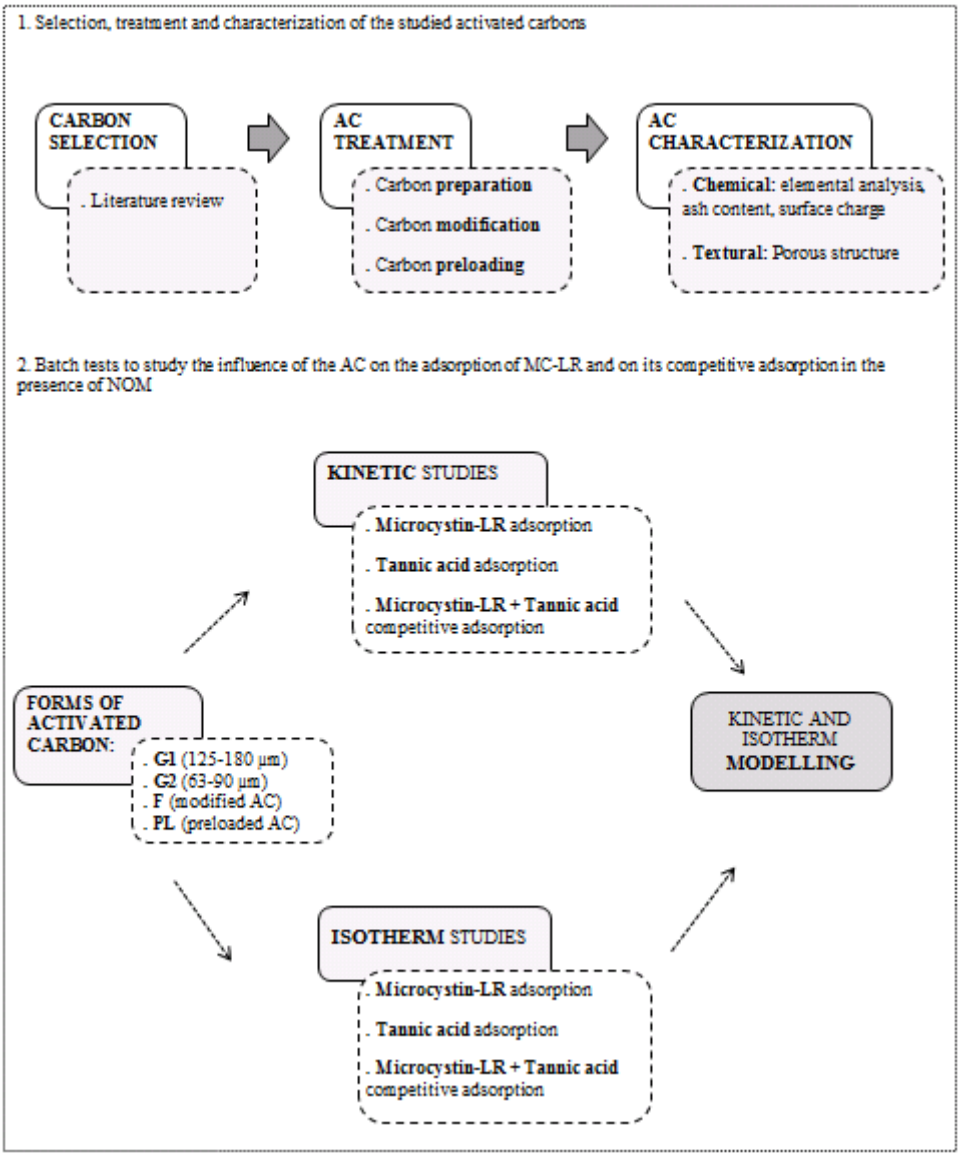

Figure 3.1. Strategy of the thesis.

3.2. ACTIVATED CARBON

3.2.1. Carbon preparation

NOR 0.8 was used in this study in four forms: two particle sizes: **G1** (125–180 µm) and **G2** (63–90 µm); modified G1 (125–180 µm): **F**; preloaded G1 (125–180 µm): **PL**.

NOR 0.8 was obtained from suppliers in extruded form with dimensions bigger than those intended. To obtain the AC in the form of granules with the size to be used in the experiments (125-180 µm and 63-90 µm), it was subjected to prior preparation which consists of grinding, sieving, washing and drying the activated carbon.

NOR 0.8 was crushed in a ceramic Ball Mill (*The Pascall Enginerering Co, Ltd*) for 10 min at 30 rpm, and sequentially sifted through 180 µm and 125 µm sieves (*Retsh, ASTM E-11*), until the desired particle size. A fraction of NOR carbon sifted through 90 µm and 63 µm sieves was also obtained and was treated identically until a reasonable amount was produced.

Figure 3.2. *Retsh Sieves (ASTM E-11)(*a); Ceramic Ball Mill (*The Pascall Enginerering Co, Ltd)* (b); and Ceramic Ball Mill holder (c) (Chemistry Department of the Faculty of Sciences and Technology – New University of Lisbon).

Afterwards, the AC was washed with ultrapure water (Milli-Q® water) to remove fines.

For this purpose, the amount of activated carbon sieved to **125-180 µm G1** (34.8 g) or to **63-90 µm G2** (17.8 g) was placed in Erlenmeyer flasks of 500 mL with140 mL and 70 mL, respectively, of Milli Q® water, corresponding to a ratio of coal: water of **1:4**. The mixture was subjected to manual stirring for a few seconds, the carbon allowed to sediment and the washing water discarded. The washing was repeated until the conductivity of the washing water presented a constant value and was not visually noticeable particles in suspension. This procedure ensured that any residual, physically adsorbed, activating chemicals were removed prior to use, providing a reproducible surface for adsorption studies (Pendleton et al., 2002). After washing, the carbons were dried in an oven at 100°C for 24h, and were stored in a desiccator until use.

3.2.2. Carbon surface chemistry modification

General

To examine the influence of carbon surface chemistry on MC-LR adsorption, it is desirable to develop methods to modify functional groups with no significant effect on the textural properties. Heating is a direct way to remove carbon-oxygen structures from a carbon (Considine et al., 2001). Carbon dioxide, carbon monoxide, water and hydrogen are the main products released during heating. Surface chemical groups, such as carboxylic acid or lactone, which involve CO_2, are less stable and decompose at temperatures as low as 300°C. Phenol or quinone-like structures are more stable and involve CO_2 at temperatures > 500°C. Bansal and Dhami (1977) demonstrate that heating in a vacuum or in nitrogen atmosphere (as in the present study) is superior to heating in a CO_2 atmosphere since the surface oxide reduction occurs to in the former atmosphere.

Heating in N_2 atmosphere

A mass of 3.00 grams of NOR 0.8 was put into a tubular reactor with a porous plate and this reactor was then placed in a tubular oven at 800°C for 3 h under a nitrogen flow rate of 80 mL/min. The final mass of AC was weighted, being the recovered mass 2.75 g.

Figure 3.3. Tubular oven used in the experiment (Chemistry Department of the Faculty of Sciences and Technology – New University of Lisbon).

3.2.3. Carbon preloading

A mass of 5.00 grams of activated carbon was put into a brown stoppered glass flask with 2 L of a solution of tannic acid (1 g/L with 2.5 mM ionic strength). Preloading carbon with tannic acid was carried out during 20 days until all activated carbon is saturated.

The preloaded AC was dried at 100ºC for 24 h and stored in a desiccator until use.

3.3. ADSORBATES

3.3.1. Microcystin-LR

Microcystin-LR was previously extracted from a culture of *Microcystis aeruginosa* and maintained in laboratory. The solubility of microcystin-LR in water is higher than 1 g/L (Rivasseau et al., 1998). The general characteristics of the studied microcystin are present in Table 3.4.

Table 3.1. Characteristics of the microcystin MC-LR used in this study (Antoniou et al., 2005 and Ho et al., 2011).

Characteristic	MC-LR
Amino acids (X | Y)	Leucine | Arginine
Molecular weight (g/mol)	995
Diameter (nm)	3
Net charge, 6 < pH < 8.5	-1
LD_{50} (µg/kg body weight)	50
Hydrophobicity	Hydrophobic

3.3.1.1. Preparing aqueous solutions of microcystin-LR

Aqueous solutions prepared from methanol extracts of biomass *Microcystis aeruginosa*, and stored at -18ºC were used in study.

For the removal of cellular waste, the methanolic suspensions were centrifuged twice for 10 minutes at 4000 rpm (Sigma 3K30 centrifuge, rotor 12157), in vials of 10 mL, discarding the sediment. The final supernatant was further filtered through glass microfiber filters GF/F, 47 mm (Whatman), transferred to glass flasks and stored at -18°C.

The concentration of MC-LR in methanol solution (75%) was determined by HPLC/PDA (High Performance Liquid Chromatography/Photodiode Array Detector).

All experimental tests with MC-LR were performed with the toxin in aqueous solution. Its preparation from solutions of MC-LR in methanol involved the evaporation of the solvent and dissolving the residue (MC-LR) in the electrolyte solution. The elimination of methanol was carried out by air sparging.

3.3.2. Tannic acid

Tannic acid (Sigma Chemicals) was selected as NOM surrogate, being representative of hydrophobic organics with a molecular weight of approximately 1700 g/mol. It contains phenolic groups and is expected to have a stronger competitive adsorption with MC-LR due to their similar molecular weight and charge (Campinas and Rosa, 2006). TA has an estimated diameter of 5.7 nm (between 3 - 8.4 nm) (Muhlpford, 1982), and carries a negative net charge at the pH range of the experiments (Bjelopavlic et al., 1999). Its chemical structure is represented in Figure 3.4.

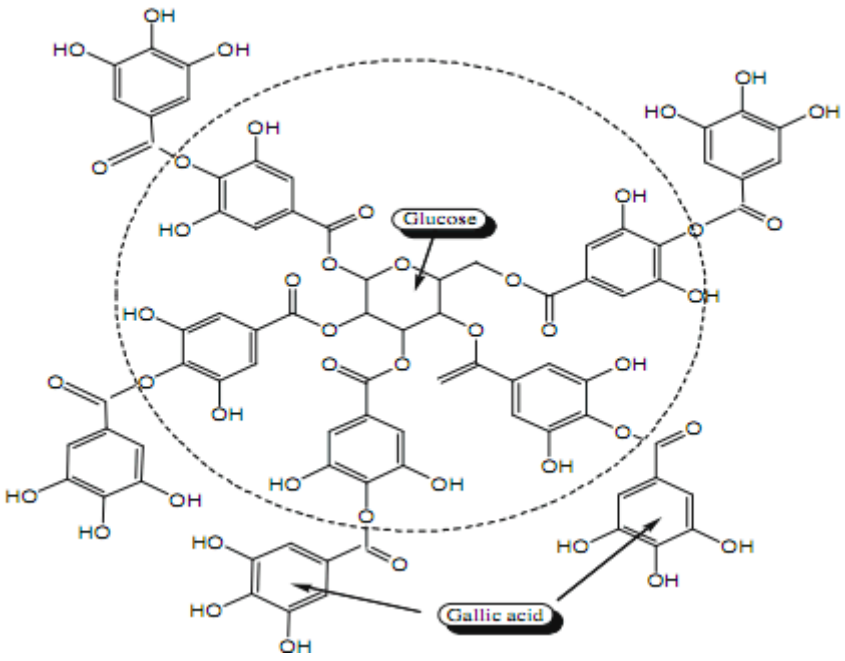

Figure 3.4. Chemical structure of tannic acid (adapted from Gülçin et al., 2010).

3.4. ASSAYED WATERS

The assayed waters in this study have a constant pH and ionic strength. The electrolyte solution was prepared to give conductivity similar to the soft natural waters, less than 60 mg/L $CaCO_3$. Electrolyte solution characteristics are described in Table 3.2.

This solution is prepared with ultrapure water and salts of KCl and $CaCl_2$. Ultrapure water (UPW) (i.e. Milli-Q® water), was obtained from a Millipore system with a resistivity of 18.2MΩ.cm at 25°C and a total organic carbon (TOC) not exceeding 10 ppb.

The NOM model water was prepared with tannic acid to give a DOC concentration of approximately 3 mgC/L.

Table 3.2. Characteristics of electrolyte solution used in all experiments.

Electrolyte (2.5 mM IS – 1mM IS KCl + 1.5 mM IS $CaCl_2$)			
$CaCl_2$		**KCl**	
mM	mg/L	mM	mg/L
0,5	55.5	1	74.6

Table 3.3. General characteristics of the assayed waters before spiking with MC-LR.

Water type	**pH**	**EC (µS/cm)**
Electrolyte solution	5-6	250-290
TA solution (TA + electrolyte solution)	5.5-6.5	230-280

3.5. METHODS FOR WATER ANALYSIS

3.5.1. pH and conductivity

The pH and the electrical conductivity (EC) were measured with a Consort C863 multi-parameter analyzer at 20°C and 25°C using standard methods of analysis (Eaton et al., 2005).

3.5.2. Quantification of microcystin-LR

3.5.2.1. Sample concentration (Solid phase extraction)

Prior to analysis, microcystin samples were concentrated by solid phase extraction (Figure 3.5) in isolute C18 cartridges (1 g in a 6 mL reservoir, from Argonaut Technologies) according to

the standard operation procedure developed by Meriluoto and Spoof (2005) with the adaptation introduced by Ribau Teixeira and Rosa (2005), as follows. The cartridges were first conditioned with 10 mL methanol followed by 10 mL of water at a flow rate not exceeding 10 mL/min, without letting it dry during conditioning. The cartridge was then washed with 4 mL methanol 20% (v/v) and dried during 2 min. The microcystins were recovered from the C18 cartridges with 4 mL of acetonitrile containing 0.05% trifluoracetic acid (v/v). The eluate was evaporated by air sparging.

Figure 3.5. Solid phase extraction apparatus used in the experiments (Sanitary Engineering Laboratory (LABES) of the Urban Water Division (NES) of LNEC´s Hydraulics and Environment Department (DHA)).

3.5.2.2. High performance liquid chromatography (HPLC-PDA)

Reversed-phase HPLC on C_{18} phases is a common choice for separating small peptides, and the mobile phases for peptides often consist of acetonitrile gradients in the presence of perfluorinated alkyl carboxylic acids, usually trifluoroacetic acid (TFA). Microcystins make no exception, they chromatograph perfectly under these conditions. Neutral ammonium acetate – acetonitrile based effluents commonly used in preparative toxin separations. Using retention time and spectrum match, the major microcystins variants, such as LR, RR, and YR are practically and easy to identify by HPLC combined with photodiode array detection (Meriluoto and Spoof, 2003).

Microcystins analysis by high performance liquid chromatography with photodiode-array detection (HPLC/PDA) followed Meriluoto and Spoof (2005) is method with adaptation introduced by Ribau Teixeira and Rosa (2005).

A Dionex Summit HPLC-PDA system was used. A C18 column (Merck Purospher STAR RP-18 endcapped, 3-µm particles, LiChro-CART 55 × 4 mm) was used and the mobile phase consisted of a gradient of two eluents designated as A and B (Table 3.4): TFA (Uvasol, Merck) 0.05% (v/v) in Milli-Q water (eluent A) and TFA (Uvasol, Merck) 0.05% (v/v) in acetonitrile (Lichrosolv, Merck) (eluent B) (Table 3.6).

The flow of the mobile phase and the oven temperature was kept at 1 mL/min and 40ºC, respectively. The microcystin was identified based on retention time and UV absorbance spectrum.

Table 3.4. Gradient program of mobile phase for analysis of MC-LR.

Time (min)	Eluent A (%)	Eluent B (%)
0	75	25
5	30	70
6	30	70
6.1	75	25
9	STOP	

Chromatograms were analyzed between 180 and 900 nm, with a main detection at 238 nm for the typical microcystin´s spectrum (Meriluoto and Spoof, 2005).

3.5.2.3. Preparation of standard solutions of MC-LR for HPLC calibration

The calibration curve was prepared with standard MC-LR extract of *Microcystis* (provided by DHI Laboratory). Standard solutions were prepared in methanol 75% (v/v) by successive dilution of a solution 11.5 µg MC-LR/mL. Standard solutions of MC-LR were prepared to cover the range of concentrations of 0.3 and 5 µg MC-LR/mL and were analyzed in duplicate.

Calibration of HPLC systems with microcystin-LR is based on the spectrophotometric determination of microcystin-LR concentration. Chromatograms were analysed between 180-900 nm with a main detection at 238 nm for the typical microcystins spectra and calibration curve was established according to Meriluoto and Spoof (2003) (Annex I).

3.5.3. Quantification of tannic acid

3.5.3.1. UV spectrophotometry

For the quantification of tannic acid, its UV absorbance was measured using a Hitachi 2000 UV/Vis spectrophotometer at 215 nm (UV_{215}).

The absorption spectrum of tannic acid in 2.5 mM IS electrolyte solution with an ionic strength of 2.5 mM and the calibration curve between UV absorbance and TA concentration were performed (Annex II).

3.6. CHEMICAL AND TEXTURAL CHARACTERIZATION OF THE ACTIVATED CARBONS

3.6.1. Surface charge characterization

Surface charge titration gives an important indication of how the (surface) ionizable groups respond to pH changes. The point of zero charge (pH_{pzc}) represents the pH condition where the surface ionic groups are neutralized, to give an effectively uncharged surface (Pendleton et al., 2001). The surface charge of NOR 0.8 (125-180) is determined by direct pH measurements according to Moreno-Castilla et al. (2000).

One gram of carbon was weighted and placed in a glass flask, and 10 mL of ultrapure water was added. The carbon suspension in N_2 atmosphere was stirred (*Edmund-Bühler* orbital shaker) for 48 h (at 200 rpm, after which the stirring was stopped and the pH of the solution was measured at 20ºC in a Crison GLP22 pH meter. The carbon suspension was immersed in nitrogen atmosphere to purge the solution of dissolved CO_2 and to prevent further dissolution of CO_2. The value obtained was taken as the pH of the point of zero charge, $\mathbf{pH_{pzc}}$ (Moreno-Castilla et al., 2000). The procedure was repeated three times to obtain an average value.

3.6.2. Characterization of the surface functional groups

Elemental analysis of nitrogen, carbon, hydrogen and sulphur was carried out on an Eager 300 micro elemental analyzer. The ash content of the activated carbons was determined by the mass of the residue obtained after combustion of samples to air, according to the procedure adapted from the Spanish Standard UNE 32 111 October 1995. A furnace was used (Lenton Thermal designs, Ltd.) for carbonization of the samples and the mass loss of samples was determined on an analytical balance (AE Adam equipment WP 250) with 0.001g accuracy.

The activated carbon was dried overnight in an oven at 100°C, then one gram of activated carbon was put in a vessel and the sample was introduced into the furnace for complete combustion of the carbonaceous matrix. The heating method used was as follows: the first 10 minutes the temperature increased up to to 500 °C and was maintained for the next 30 minutes; then was again increased to 800 ºC for 15 minutes and maintained for 2.5 h.
After cooling to a temperature near 150 °C, the sample was removed from the furnace and stored in a desiccator to reach room temperature and then weighed again. The ash content is

determined based on the dry weight of activated carbon and the mass of residue after air combustion. The ash content value was calculated as the average of three results.

3.6.3. Textural characterization

The analytical determination of the activated carbons' porous structure was performed by Professor Isabel Fonseca's research group from the Chemistry Department of FCT/UNL.

The physical characteristics of the activated carbons, which included the specific surface area, the micropore area, the total pore volume, the micropore volume and the pore size distribution, were measured by N_2 adsorption in a ASAP 2010 Pore Structure Analyser (Micromeritrics, USA), at 77 K with liquid N_2 (Costa, 2010).

3.7. BATCH STUDIES OF ACTIVATED CARBON ADSORPTION

3.7.1. General procedure

The apparatus used in the kinetic and isotherm batch experiments was an *Edmund-Bühler* KM–2 orbital shaker (Figure 3.6). The stirring speed used in all the experiments was 200 rpm, a value previously found to be satisfactory to prevent settling and loss of carbon in the bottle surface. The temperature was kept constant at 24°C.

Figure 3.6. Apparatus used in the kinetic and isotherm batch experiments (*Edmund-Bühler* orbital shaker).

The glass flasks had 100, 250 or 500 mL capacity. The 250 and 500 mL flasks were used in order to detect lower toxin concentration.

The general experimental procedure for the kinetic and isotherm assays was as follows: a predetermined amount of AC was accurately weighted into the glass flasks (duplicates of each experimental condition were always performed), and the water sample spiked with toxin, tannic acid or both (toxin and tannic acid) was added to the flasks. The flasks were sealed with plastic paraffin film - *Parafilm* or stoppered and placed in the shaker at 24°C and 200 rpm. Flasks were collected at predetermined time intervals.

In the isotherm tests, flasks were sealed and stirred at constant temperature for the necessary period to reach equilibrium. The equilibrium time was determined in preliminary experiments. For kinetics tests, flasks were sealed and stirred at a constant temperature and samples were taken at predetermined time (30 min, 1 h, 2 h, 4 h, 6 h, 8 h, 10 h and 24 h).

The clarified volume was filtered through a 0.7 µm glass fiber filter (GF-C *Whatman*), and the filtrate was passed through a SPE cartridge to extract the toxin for analysis by HPLC/PDA. TA quantification was performed by UV_{215nm}.

Blanks, consisting of glass bottles containing no AC but treated identically to the samples containing AC, were also tested during the same period of the equilibrium experiments to check for possible toxin degradation.

Summary of the experimental conditions were represented in Table 3.5.

Table 3.5. Summary of the experimental conditions tested.

		Assay	Activated carbons [a]	Volume of assayed water (mL)	NORIT range (mg)	NORIT range (mg/L)	Solution
STUDIES	**KINETIC**	**MC-LR extract** (C_0 = 100 µg/L)	G1, G2, F, PL	200	6.4	32	**Electrolyte (2.5 mM)** (1mM IS KCl + 1.5 mM IS $CaCl_2$) [b]
		Tannic Acid (C_0 = 5.6 mg/L)	G1, F	80	2.6	32	
		MC-LR extract (C_0 = 100 µg/L) + **Tannic Acid** (C_0 = 5.6 mg/L)	G1, F, PL	200	6.4	32	
	ISOTHERM	**MC-LR extract** (C_0 = 100 µg/L)	G1, G2, F, PL	200 200 500 500 500	2.5 5.0 15 20 25	12.5 25 30 40 50	
		Tannic Acid (C_0 = 5.6 mg/L)	G1, G2, F, PL	200 200 200 200 200	2.5 5.0 6.0 8.0 10	12.5 25 30 40 50	
		MC-LR extract (C_0 = 100 µg/L) + **Tannic Acid** (C_0 = 5.6 mg/L)	G1, G2, F, PL	200 200 500 500 500	2.5 5.0 15 20 25	12.5 25 30 40 50	

[a] **G1:** 125-180 µm, **G2:** 63-90 µm; **F:** modified G1; **PL:** Preloaded G1 ; [b] 55.5 mg/L $CaCl_2$ + 74.6 mg/L KCl

3.7.2. Studies for determining the MC-LR equilibrium time

Equilibrium time for MC-LR adsorption was tested for NOR carbon (G1: 125-180 µm) in electrolyte solution (2.5 mM IS) spiked with MC-LR. The experimental conditions used are presented in Table 3.6.

Amounts of the same mass of AC were weighted into 100 mL glass flasks. Then, 80 mL of electrolyte solution spiked with 36 µg MC-LR/L were added (Table 3.6). The flasks were sealed and stirred as previously described.

After a predetermined time-interval of shaking, the correspondent flask was withdrawn and the sample was filtered through a 0.7 µm glass fiber filter (GF-C *Whatman*) for AC particles retention and the filtrate was passed through a SPE cartridge to extract the toxin for MC-LR quantification by HPLC-PDA.

Equilibrium was assumed to occur when the concentration no longer changed with time (no more than 10% variation).

Table 3.6. Characteristics of activated carbon and assayed water used in the MC-LR adsorption kinetic for determining the MC-LR equilibrium time.

Electrolyte solution (2.5 mM IS)	**C_0 (µg MC-LR/L)**	**EC (µS/cm)**	**pH**
	36	276	6.1
NOR 0.8 (125-180 µm)	**m_{NOR} (mg)**	**$V_{assayed\ water}$ (mL)**	**C (mg_{NOR}/L)**
	1	80	12.5
Time-intervals for sampling	30 min, 2 h, 4 h, 7 h, 24 h, 48 h, 52 h, 120h		

3.7.3. Adsorption kinetic studies of MC-LR

The MC-LR adsorption kinetic studies were performed with NOR 0.8 two size grades (G1 and G2), modified (F) and preloaded (PL) activated carbons, using the experimental conditions presented in Table 3.7 and Table 3.8.

Table 3.7. Characteristics of the assayed water used in the MC-LR adsorption kinetic studies.

AC	**Electrolyte solution (2.5 mM IS)**		
	C_0 (µg MC-LR/L)	EC (µS/cm)	pH
NOR 125-180	104	280	6.0
NOR 63-90	85.0	240	5.8
Modified NOR 125-180	99.8	270	6.2
TA-preloaded NOR 125-180	90.0	210	5.5

Table 3.8. Characteristics of the activated carbon used in the MC-LR adsorption kinetic studies.

AC	$V_{assayed\ water}$ (mL)	m_{NOR} (mg)	C (mg_{NOR}/L)
G1, G2, F and PL	200	6.4	32
Time-intervals for sampling	1 h, 2 h, 4 h, 6 h, 8 h, 24 h		

3.7.4. Adsorption kinetic studies of TA

TA adsorption kinetic studies were performed with the NOR 0.8 grade G1 and with modified (F) activated carbons, using the experimental conditions presented in Table 3.9 and Table 3.10.

Table 3.9. Characteristics of the assayed water used in the TA adsorption kinetic studies.

AC	Electrolyte solution (2.5 mM IS)		
	C_0 (mg TA/L)	EC (µS/cm)	pH
NOR 125-180	5.3	234	5.5
Modified NOR 125-180	5.5	238	5.7

Table 3.10. Characteristics of the activated carbon used in the TA adsorption kinetic studies.

AC	$V_{assayed\ water}$ (mL)	m_{NOR} (mg)	C (mg_{NOR}/L)
G1 and F	80	2.6	32
Time-intervals for sampling	30 min, 1 h, 2 h, 4 h, 6 h, 8 h, 24 h		

3.7.5. Kinetic studies of competitive adsorption between MC-LR and TA

Kinetic studies of competitive adsorption were performed with NOR 0.8 grade G1, modified (F) and preloaded (PL) activated carbon, using the experimental conditions presented in Table 3.11 and Table 3.12.

Table 3.11. Characteristics of the assayed water used in the kinetic studies for competitive adsorption of MC-LR and TA.

AC	Electrolyte solution (2.5 mM IS)			
	C_0 (µg MC-LR/L)	C_0 (mg TA/L)	EC (µS/cm)	pH
NOR 125-180	78.0	5.1	221	5.5
Modified NOR 125-180	104	5.8	215	5.4
TA-preloaded NOR 125-180	96.3	5.2	213	5.3

Table 3.12. Characteristics of the activated carbon used in the kinetic studies for competitive adsorption of MC-LR and TA.

AC	$V_{assayed\ water}$ (mL)	m_{NOR} (mg)	C (mg_{NOR}/L)
G1, F and PL	200	6.4	32
Time-intervals for sampling	30 min, 1 h, 2 h, 4 h, 6 h, 8 h, 24 h		

3.7.6. Isotherm studies for MC-LR adsorption

The MC-LR adsorption isotherm studies were performed with NOR 0.8 two size grades (G1 and G2), modified (F) and preloaded (PL) activated carbons, using the experimental conditions presented in Table 3.13 and Table 3.14.

Table 3.13. Characteristics of the assayed water used in the MC-LR adsorption isotherm studies.

AC	Electrolyte solution (2.5 mM IS)		
	C_0 (µg MC-LR/L)	EC (µS/cm)	pH
NOR 125-180	104	272	6.3
NOR 63-90	87.3	245	6.5
Modified NOR 125-180	97.3	272	6.2
TA-preloaded NOR 125-180	78.4	216	5.5

Table 3.14. Characteristics of the activated carbon used in the MC-LR adsorption isotherm studies.

AC	$V_{assayed\ water}$ (mL)	m_{NOR} (mg)	C (mg_{NOR}/L)
G1, G2, F and PL	200	2.5	12.5
	200	5.0	25
	500	15	30
	500	20	40
	500	25	50
Time-intervals for sampling	120 h		

3.7.7. Isotherm studies for TA adsorption

The TA adsorption isotherm studies were performed with NOR 0.8 two size grades (G1 and G2), modified (F) and preloaded (PL) activated carbons, using the experimental conditions presented in Table 3.15 and Table 3.16.

Table 3.15. Characteristics of the assayed water used in the TA adsorption isotherm studies.

AC	Electrolyte solution (2.5 mM IS)		
	C_0 (mg TA/L)	EC (µS/cm)	pH
G1, G2, F and PL	4.7	281	5.8

Table 3.16. Characteristics of the activated carbon used in the TA adsorption isotherm studies.

AC	$V_{assayed\ water}$ (mL)	m_{NOR} (mg)	C (mg_{NOR}/L)
G1, G2, F and PL	200	2.5	12.5
	200	5.0	25
	200	6.0	30
	200	8.0	40
	200	10	50
Time-intervals for sampling	72 h		

3.7.8. Isotherm studies of competitive adsorption between MC-LR and TA

Isotherm studies of competitive adsorption were performed with NOR 0.8 two size grades (G1 and G2), modified (F) and preloaded (PL) activated carbons, using the experimental conditions presented in Table 3.17 and Table 3.18.

Table 3.17. Characteristics of the assayed water used in the competitive adsorption isotherm studies of MC-LR and TA.

AC	Electrolyte solution (2.5 mM IS)			
	C_0 (µg MC-LR/L)	C_0 (mg TA/L)	EC (µS/cm)	pH
NOR 125-180	103	5.1	221	5.5
NOR 63-90	42.0	5.0	220	5.3
Modified NOR 125-180	90.0	5.2	215	5.4
TA-preloaded NOR 125-180	96.0	5.0	213	5.3

Table 3.18. Characteristics of the activated carbon used in the competitive adsorption isotherm studies of MC-LR and TA.

AC	$V_{assayed\ water}$ (mL)	m_{NOR} (mg)	C (mg_{NOR}/L)
G1, G2 F and PL	200	2.5	12.5
	200	5.0	25
	500	15	30
	500	20	40
	500	25	50
Time-intervals for sampling	120 h		

3.7.9. Calculation methods

The software package Scientist ^{TM} from MicroMath^{R} was used to perform the non-linear fitting calculations. This software allies the capability of performing non-linear fittings and solving both integral and differential equations. The least squares and the simplex algorithms were used.

4. RESULTS AND DISCUSSION

4.1. CHEMICAL AND PHYSICAL CHARACTERIZATION OF THE ADSORBENT

The efficiency of a carbon for removing a given pollutant depends on both its adsorption capacity and its surface chemistry (Considine et al., 2001). The relatively large adsorption capacity of an AC is usually attributed to its internal pore volume (Donati et al., 1994; Huang and Cheng, 2007). A carbon containing numerous pores in the size range of the contaminant is expected to be efficient due to the enhancement of the adsorption potential for such conditions (Gregg and Sing, 1982).
In drinking water treatment the effect of the adsorbent surface chemistry is also important, since adsorption proceeds via the displacement of the existing water covered surface by the dissolved contaminant molecules (Considine et al., 2001).

In this study, the characterization of the AC intended to understand the role of pore size distribution and of specific surface properties (point of zero charge, type of surface functional groups) of the AC's on the adsorption of MC-LR.

For this purpose, NOR carbon of two particle sizes, 125-180 μm (G1) and 63-90 μm (G2) were tested. The surface chemistry of carbon NOR 125-180 was modified by careful thermal treatment (as described in section 3.2.3) in order to obtain different surface properties with minimal changes in PSD. This AC (NOR 125-180) was also preloaded with tannic acid.

4.1.1. Surface charge of the activated carbon

The surface charge of the tested activated carbons was determined by direct pH measurement (described in section 3.6.1). The results are presented in Table 4.1.

Table 4.1. Point of zero charge of the studied carbons.

pHpzc measured by	pH_{pzc}		
	NOR 125-180 (G1)	**Modified NOR 125-180 (F)**	**NOR 63-90 (G2)**
Moreno-Castilla et al. (2000) method	9.1	12.1	9.1
Literature (Costa, 2010)	9.5 ± 0.40	-	-

The results for NOR 125-180 carbon agree with those determined recently by Costa (2010).

Results presented in Table 4.1 show that the $pH_{pzc,}$ i.e,. the basicity (Pendleton et al., 2002) of the carbons varies in the order **F > (G1, G2)**. As it was previously observed, carbon surfaces

acquire a basic character upon high – temperature (> 973K) treatment (Menendez et al., 1996), so the results obtained for the modified carbon, which is treated with N_2 at 1073 K, is in agreement with what was predicted.

As expected, crushing the AC to obtain a smaller particle size does not affect its pH_{pzc}.

This also indicates that at the pH of the tested waters (5-7) the carbon's surface charge is always positive. As a positively charged carbon favors the adsorption of negatively charged molecules and hinders the adsorption of positively charged adsorbates, this means that all studied carbons show a good potential for the adsorption of microcystins, since at the tested pH values (5-7), it always carry a net positive charge whereas the microcystin-LR is negatively charged.

4.1.2. Functional Groups

The results of the elemental analysis of the activated carbons (G1, G2 and F) are presented in Table 4.2. The oxygen content of the AC samples was calculated by difference:

$$\boldsymbol{O}\ (\%) = \{\mathbf{100} - [\boldsymbol{N}(\%) + \boldsymbol{C}(\%) + \boldsymbol{H}(\%) + \boldsymbol{S}(\%)]\} \quad \textbf{[4.1]}$$

The ash content value indicated in Table 4.2 was obtained by the method described in section 3.6.2.

Table 4.2. Elemental analysis (wt%) of the studied activated carbons.

	N (%)	C (%)	H (%)	S (%)	O (%) [(a)]	Ash (%)
NOR 125-180	1.14	79.6	0.340	0.550	18.4	5.50
Literature (Costa, 2010)	0.500	87.2	0.400	0.500	11.5	6.00
NOR 63-90	0.410	84.1	0	0.570	15.0	-
Modified NOR 125-180	0.450	89.6	0	0	9.90	-

[(a)] obtained from subtraction of total C, N, H, S.

The three carbons have relatively different surface chemistries, i.e. they differ on the type and amount of surface groups, as shown by their oxygen and nitrogen contents. The oxygen content of NOR 125-180 is attributed to carbonyl and lactone groups (Costa, 2010). A portion of oxygen was also attributed to N-containing groups, which had the highest content of nitrogen (Table 4.2).

The heat-treated AC shows a decrease in oxygen content. Oxygen is the most frequently encountered and important element, forming various functional groups on the AC surface.

The acidic character as well as the hydrophobicity of an AC is related to the oxygen contents. The higher the oxygen content of an activated carbon the stronger is its acidic character (Li et

al., 2002), so the lower oxygen content the stronger is its basic character. As it seen in Table 4.2, the heat-treated carbon (F) has the lowest oxygen content, so it is the more basic carbon, which agrees with the pH_{pzc} presented in Table 4.1.

Reducing the oxygen content of NOR 125-180 carbon increases its hydrophobic character (Pendleton et al., 2002) and its basic character (Li et al., 2002).

According with Considine et al. (2001), Pendleton et al. (2002), Huang and Cheng, (2007) and taking into account only the surface chemistry of AC, it is expected that this heat-treated carbon, with the larger amount of basic surface groups, higher pH_{pzc} and stronger hydrophobicity have the higher MC-LR adsorption capacity.

4.1.3. Textural Characterization

The textural characterization of the studied activated carbons included **pore size distribution**, **apparent surface area**, **total microporous volume**, **specific external area**, **total volume of pores**, **specific microporous surface area** and **volume of macropores and mesopores** (performed using a Micromeritrics ASAP 2010 instrument) (Costa, 2010).

The **pore size distribution** was determined by the Density Functional Theory (DFT) (data presented in Annex III). The apparent surface area was calculated by the BET method (A_{BET}). The **total microporous volume** and the **external area** (i.e. the mesoporous surface area, A_{ext}) were determined by the t-plot. The **total volume of pores** was determined by the Gurvitsch rule. The **specific microporous surface area** was computed by subtracting the external surface area to the BET surface area. All the previously mentioned parameters are specific areas and volumes, i.e. per unit mass weight. The calculations for A_{BET} (valid for $0.05 < P/P_0 < 0.30$), microporous volume, A_{ext} and total volume of pores (for saturation, i.e. $P/P_0 = 0.98$) (methods presented in Annex IV). The volume of macropores and mesopores was calculated from the BJH method. The data are presented in Figure 4.1, Figure 4.2 and Table 4.3.

Since higher and stronger adsorption can be expected within pores of dimensions similar to the molecular dimension of the MC-LR (Huang and Cheng, 2007), carbon pore size distributions were examined.

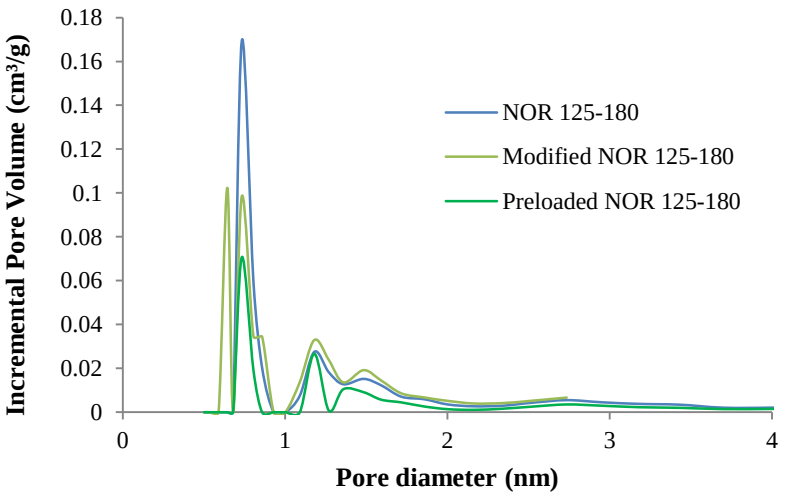

Figure 4.1. Pore size distribution (microporous structure) of NOR 125-180 virgin, modified and preloaded.

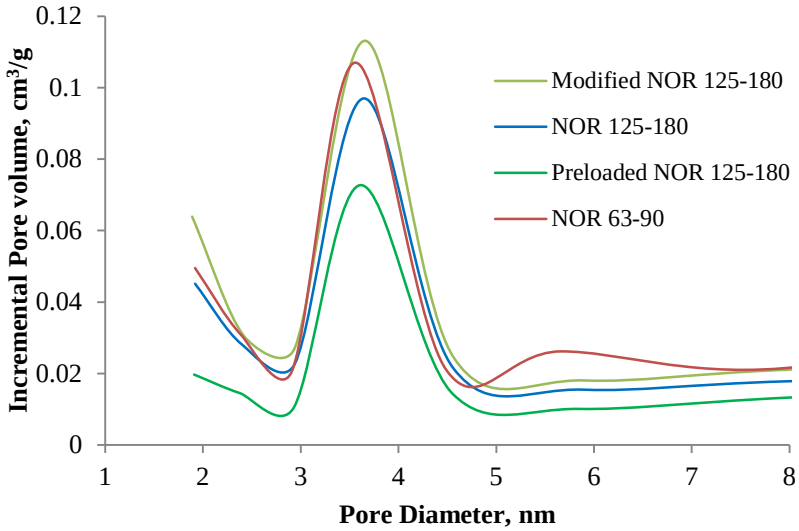

Figure 4.2. Pore size distribution (mesoporous structure) of the studied activated carbons.

Figure 4.1 shows that the three carbons are essentially microporous in nature but Figure 4.2 shows the mesoporous structure of the activated carbons, being this one the most important in the MC-LR adsorption.

Table 4.3. Textural properties of the studied NOR carbons.

Property	**Method**	**G1**	**G2**	**F**	**PL**
Apparent surface area (A_{BET}) (m^2/g)	BET	1035	1083	1191	464
Total microporous volume (cm^3/g)	t-plot	0.35	0.36	0.39	0.14
External area (mesopores) (A_{ext}) (m^2/g)	t-plot	301.7	346.4	374.9	175.8
Total volume of pores (cm^3/g)	Gurvitsch rule	0.66	0.74	0.77	0.36
Microporous surface area (m^2/g)	$A_{BET} - A_{ext}$	734	737	816	288
Volume of macropores and mesopores (cm^3/g)	BJH	0.34	0.4	0.4	0.23

Most suppliers claim that a high specific surface area available for adsorption is important for the removal of a particular adsorptive. But a recent study (Considine et al., 2001) on 2-methylisoborneol (MIB) adsorption analysis suggests that this assumption must be made with caution, having no conclusion about this.

As it is seen in Table 4.3, the heat-treated AC shows a modified porous structure, with an increase in the volume of micro and mesopores. Due to this, this **heat-treated** activated carbon was then called **modified NOR 125-180**. According to the literature (Donati et al., 1994; Pendleton et al., 2002; Newcombe and Cook, 2004) this increase in carbon's mesoporosity may be advantageous for MC-LR adsorption. From the data presented in Table 4.3, among the three studied carbons, modified NOR 125-180 has the highest surface area and (together with G2) the highest BJH adsorption cumulative pore volume, i.e. has the largest number of mesopores and macropores. These results, together with those from the surface charge characterization, suggest that this carbon should be very adequate for the removal of microcystins.

NOR 125-180 and NOR 63-90 present quite similar characteristics although NOR 63-90 with a slightly higher pore volume, and therefore may present a higher adsorption capacity.

Regarding the TA-preloaded NOR 125-180, the specific surface area is lower when compared with AC source (NOR 125-180). That was expected, since when loading with tannic acid, the pores are blocked, making the AC less porous particularly, less microporous). This AC will later be used for competition studies.

4.2. ADSORPTION OF MICROCYSTIN-LR ONTO ACTIVATED CARBON

4.2.1. Equilibrium time for MC-LR adsorption

The objective of this experimental study (experimental conditions detailed in section 3.7.2) was to evaluate the time needed for MC-LR adsorption to reach the equilibrium, in order to ensure that the equilibrium is reached in all isotherm adsorption experiments.

NOR carbons exhibit fast kinetics in early stages (first hours of the run), as expected taking into account AC characteristics. Figure 4.3 shows that the equilibrium is reached after approximately 48h contact for NOR 125-180 µm (G1), but based on other studies and similar conditions (Costa, 2010) it was expected a higher adsorption of MC-LR.

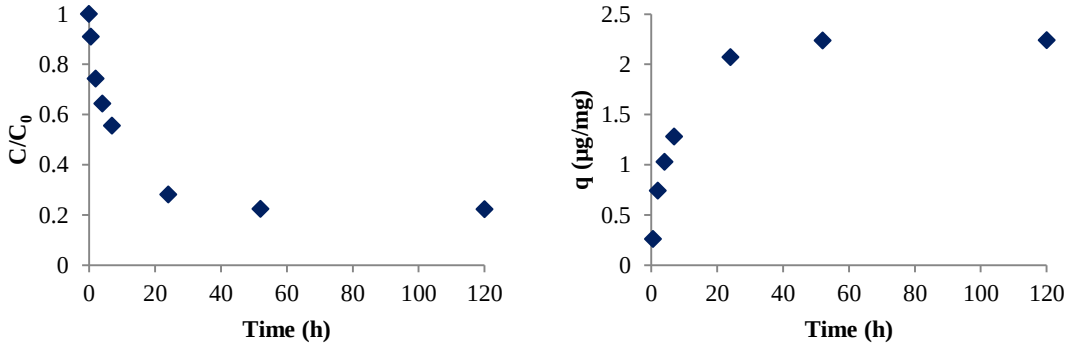

Figure 4.3. Adsorption kinetics of MC-LR (extract) in 2.5 mM IS electrolyte (1 mM IS KCl + 1.5 mM IS $CaCl_2$) onto NOR 125-180 for determining the MC-LR adsorption equilibrium time.

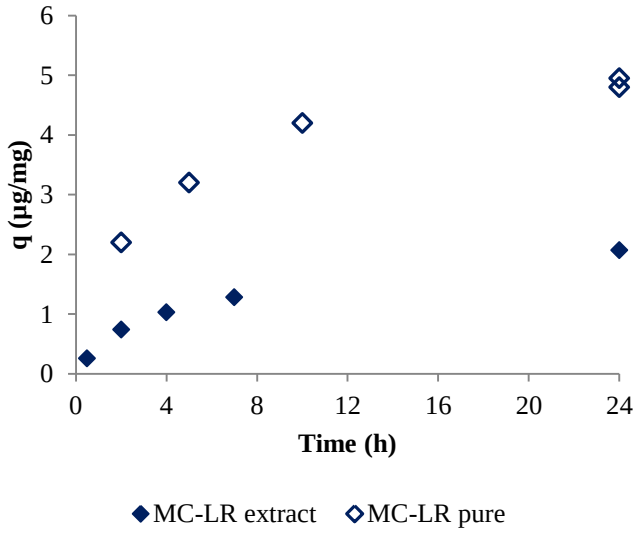

Figure 4.4. Comparison between the adsorption kinetic of MC-LR (extract in 2.5 mM IS electrolyte (♦)) and pure MC-LR in ultrapure water (◊) (results from Costa, 2010).

Microcystins were produced and extracted from *Microcystis aeruginosa* laboratory grown culture. As these extracts were not purified, they must have some algogenic organic matter (AOM) and other types of microcystins, which may be affecting the adsorption of MC-LR, competing with it. The TOC analysis justifies the presence of AOM (2.1 mg C/L). The literature regarding the cyanotoxin adsorption by AC suggests that different toxins have distinct removal efficiencies (Campinas and Rosa, 2006). The microcystin variants detected in HPLC chromatograms (Figure 4.5) were MC-LR, MC-LY, MC-LW and MC-LF based on retention times, but the dominant microcystin variant was MC-LR (main peak), which leads to the conclusion that other types of microcystins are present in all experiments in this thesis.

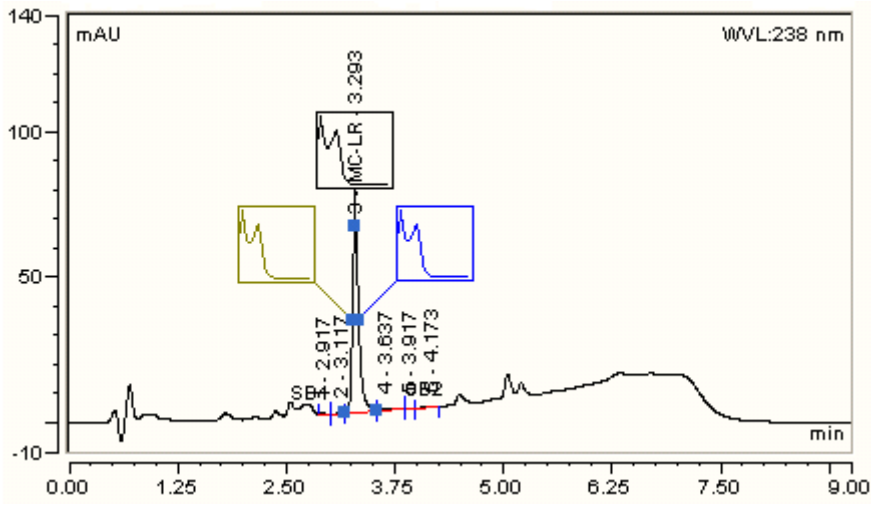

Figure 4.5. HPLC chromatogram of MC-LR (extract of *Microcystis aeruginosa*) result of this first experiment.

Some properties of the most common MC are summarized in Table 4.4.

Table 4.4. Properties of microcystin variants (adapted from Campinas and Rosa, 2006).

	MC-LR	**MC-LY**	**MC-LW**	**MC-LF**
Amino acids (X and Z)	Leucine, arginine	Leucine, tyrosine	Leucine, trytophane	Leucine, phenylalanine
Molecular Weight	994	1001	1024	985
Net charge, pH 7	-1	-2	-2	-2
	→ Increasing Hydrophobicity			

So, in this work, the extracts used in all kinetic and isotherm adsorption experiments contained a mixture of microcystin variants, and not pure microcystin-LR, fact that was not ignored during analysis/discussion of the results.

4.2.2. Adsorption of MC-LR onto NOR 125-180

Equilibrium isotherms onto NOR 125-180 carbon were performed with 104 µg/L MC-LR initial concentration in 2.5 mM IS electrolyte (1 mM IS KCl + 1.5 mM IS $CaCl_2$) and AC concentrations between 12.5-50 mg/L during five days (experiments detailed in section 3.7.6). The fitting of adsorption isotherm curve is illustrated in Figure 4.6 and Table 4.5 presents the isotherm parameters.

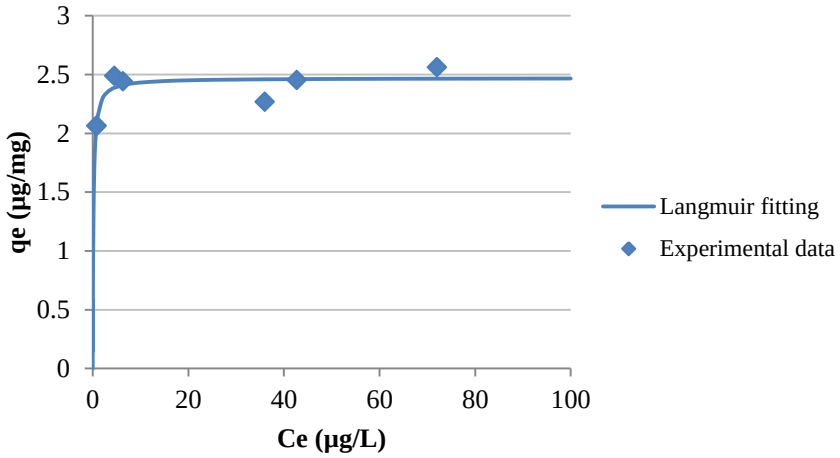

Figure 4.6. Langmuir isotherm fitting for MC-LR adsorption onto NOR 125-180 (2.5 mM IS electrolyte).

For MC-LR adsorption, only the Langmuir model was applied. The isotherm shows a plateau (q_e became constant regardless of additional increases of C_e), and therefore the Freundlich equation does not apply (Snoeyink and Summers, 1999). This indicates the adsorption of a complete monolayer.

Table 4.5. Langmuir isotherm parameters with 95% confidence interval for NOR 125-180 adsorption of MC-LR from 2.5 mM IS electrolyte solution.

q_{max} (µg/mg)	b (L/µg)	R^2
2.47 ± 0.14	6.38 ± 4.60	0.770

The objective of the kinetic experiments was to evaluate the limiting steps of the MC-LR adsorption. Three kinetic models were used to study these processes and to investigate the mechanisms and the potential rate-controlling step(s) of MC-LR adsorption, such as mass transport (**intraparticle diffusion model**) and chemical reaction (**pseudo-first and pseudo-second order models**).

The pseudo-first order and pseudo-second order kinetic model fittings are presented in Figure 4.7 and Table 4.6.

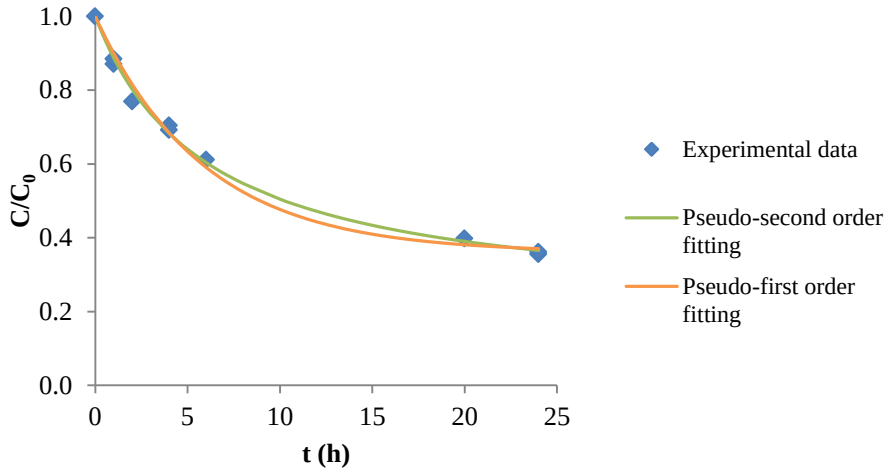

Figure 4.7. Pseudo-first order and pseudo-second order adsorption kinetic models for MC-LR adsorption onto NOR 125-180 (2.5 mM IS electrolyte).

Table 4.6. Adsorption kinetics constants with 95% confidence interval for pseudo-first order and pseudo-second order models for MC-LR adsorption onto NOR 125-180 (2.5 mM IS electrolyte).

	Pseudo-first order model		**Pseudo-second order model**	
$\mathbf{q_{e\_calc}}$ (µg/mg)	$\mathbf{k_1}$ (h^{-1})	$\mathbf{R^2}$	$\mathbf{k_2}$ (mg/(µg/h))	$\mathbf{R^2}$
2.47	0.17 ± 0.02	0.990	0.064 ± 0.008	0.996

For the full range of contact time studied, the experimental kinetic data of NOR 125-180 carbon is best described by the pseudo-second order model, with very good correlation (R^2=0.996). The pseudo-first order model also describes the MC-LR adsorption kinetics onto NOR 125-180 µm data in the full range of contact time, but does not have a so good correlation (R^2=0.990). In most cases published in literature, the pseudo-first order model does not fit well the data in the full range of contact time, and is often applicable only in the first period of the sorption process (Ho and McKay, 1999). As the MC-LR adsorption kinetic data are best fitted by the pseudo-second order model, this indicates the chemisorption as the adsorption mechanism, which is consistent with adsorption well-described by the Langmuir model.

The pseudo-second order adsorption kinetic model fitting of C (µg/L) and q (µg/mg) for MC-LR adsorption onto NOR 125-180 is shown in Figure 4.8.

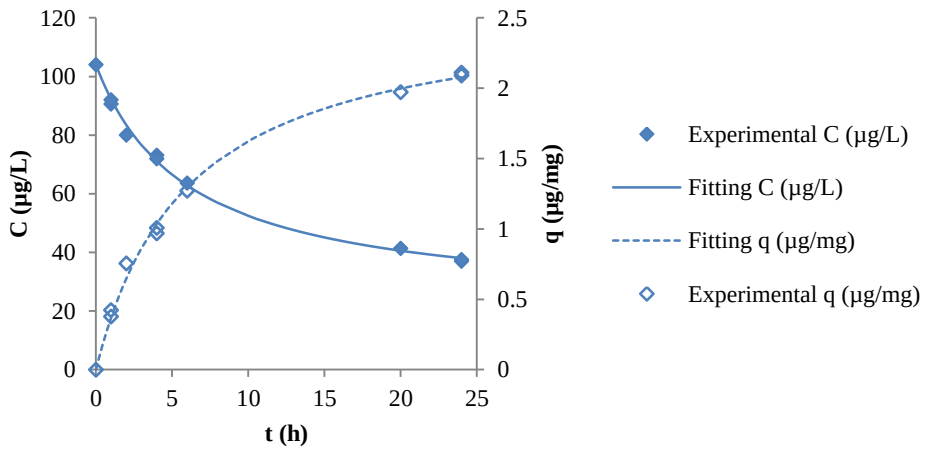

Figure 4.8. Pseudo-second order adsorption kinetic model fitting of C (µg/L) and q(µg/mg) for MC-LR adsorption onto NOR 125-180 (2.5 mM IS electrolyte).

With respect to diffusion models, according to numerous studies (Wang and Li, 2007; Ip et al., 2010) external mass transfer (film diffusion) or intraparticle diffusion (particle diffusion) are often the rate-limiting steps in the sorption process.

A classic approach to analyze if an adsorption process is controlled by intraparticle diffusion is to plot the amount adsorbed versus the square root of time, $t^{1/2}$ (Figure 4.9a). If the plot is linear and passes through the origin, the intraparticle diffusion is controlling the rate of adsorption. Some authors (Hameed and Daud, 2008; Khaled et al., 2009) have shown that if there is an initial external mass transfer or chemical reaction, then the plot will still be linear but it will not pass through the origin.

The intraparticle diffusion model approach is shown in Figure 4.9 and Table 4.7.

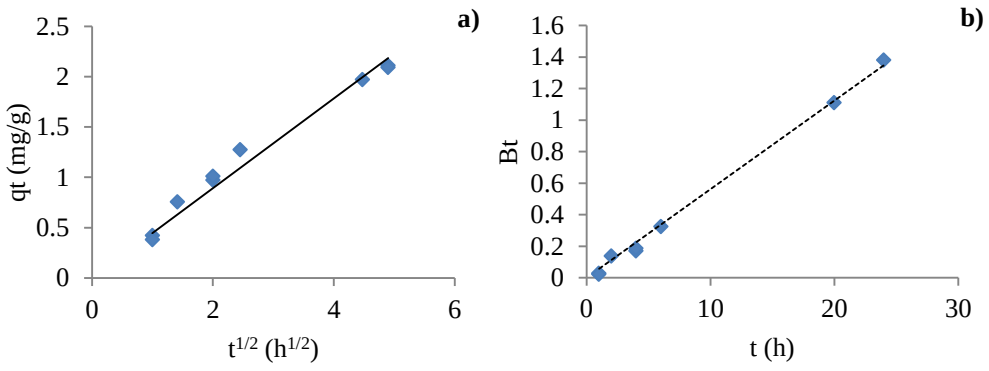

Figure 4.9. Intraparticle diffusion model (a), and Boyd plot (diffusion coefficient) (b), for MC-LR adsorption onto NOR 125-180 (2.5 mM IS electrolyte).

The associated error for the C parameter is high (C=0.098 ± 0.154), so it is assumed that this equation passes the origin. So, neglecting this value, it is forced that this equation passes the origin. The same goes for the Boyd plot (b=0.03 ± 0.03).

Table 4.7. Parameters for intraparticle diffusion model and Boyd plot for MC-LR adsorption onto NOR 125-180.

Intraparticle diffusion model		**Boyd et al. (1947) equation**			
kp (μg/mg.$h^{1/2}$)	$\mathbf{R^2}$	$\mathbf{r_{AC}}$ (μm)	**Equation**	**Di** (cm^2/s)	$\mathbf{R^2}$
0.446 ± 0.026	0.977	76.25	Bt = (0.056 ± 0.003) t	$9.16x10^{-11}$	0.996

NOR 125-180 carbon exhibits only one linear portion. The linear portion passes through the origin indicating that the intraparticle diffusion is the rate controlling step for the adsorption.

In order to confirm this analysis, the data were also analyzed by the kinetic expressions given by Boyd et al., 1947.

The calculated Bt values were plotted against time t and are shown in Figure 4.9b. The linearity of this plot is used to distinguish which transport mechanism, external transport or intraparticle, controls the adsorption rate. The plot presented in Figure 4.9b is linear and pass through the origin. These results validate the previous conclusion based on the intraparticle diffusion model consequently demonstrating that the rate-limiting step is the intraparticle diffusion for NOR 125-180 carbon.

The diffusion coefficients of MC-LR through studied carbons were determined by equation 2.17, assuming spherical particles.

4.2.3. Adsorption of MC-LR onto NOR 63-90

Equilibrium isotherms onto NOR 63-90 carbon were performed with 87.3 µg/L MC-LR initial concentration in 2.5 mM IS electrolyte (1 mM IS KCl + 1.5 mM IS $CaCl_2$) and AC concentrations between 12.5-50 mg/L during five days (experiments detailed in section 3.7.6). The fitting of adsorption isotherm curve is illustrated in Figure 4.10 and Table 4.8 presents the Langmuir parameters.

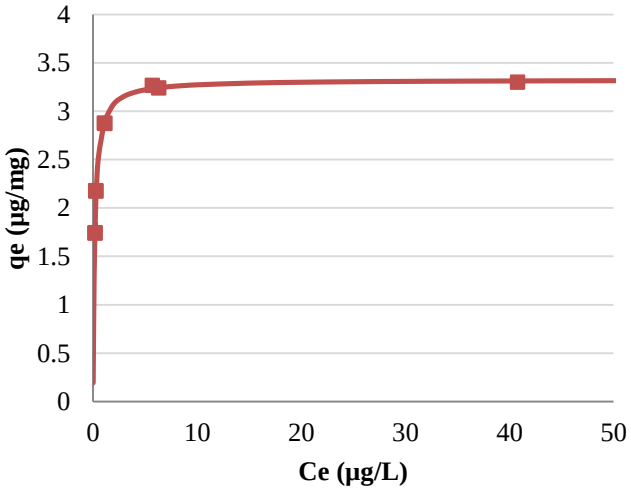

Figure 4.10. Langmuir isotherm fitting for MC-LR adsorption onto NOR 63-90 (2.5 mM IS electrolyte).

The Freundlich model was not applied since the experimental data are out of the range of model applicability (Snoeyink and Summers, 1999). So, the Langmuir equation were applied to this experiment with a good correlation coefficient (R^2=0.992) indicating the adsorption of a complete monolayer, as it was previously found for NOR 125-180.

Table 4.8. Langmuir isotherm parameters with 95% confidence interval for MC-LR adsorption onto NOR 63-90 (2.5 mM IS electrolyte).

q_{max} (µg/mg)	b (L/µg)	R^2
3.33 ± 0.08	6.13 ± 0.70	0,992

NOR 63-90 has a higher adsorption capacity (3.33 ± 0.08 vs 2.47 ± 0.14) when compared with NOR 125-180.

The pseudo-first order and pseudo-second order kinetic model fittings are presented in Figure 4.11 and the results are presented in Table 4.9.

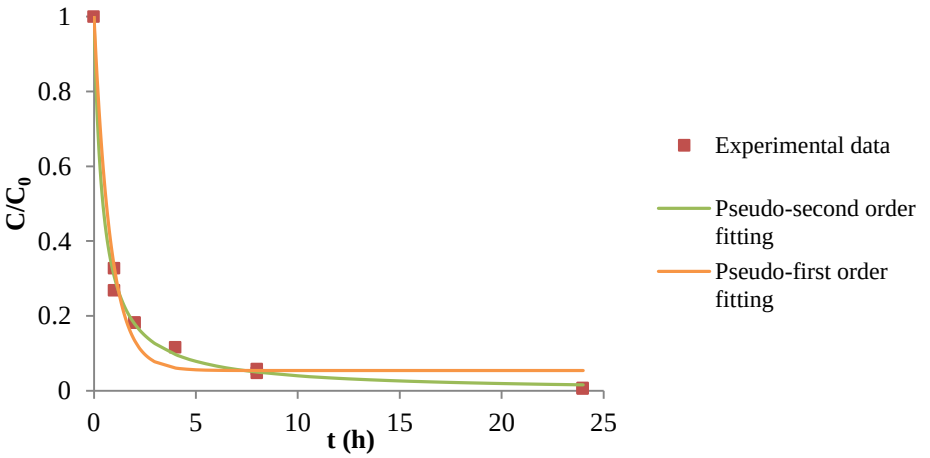

Figure 4.11. Pseudo-first order and pseudo-second order adsorption kinetic models for MC-LR adsorption onto NOR 63-90 (2.5 mM IS electrolyte).

Table 4.9. Adsorption kinetics constants with 95% confidence interval for pseudo-first order and pseudo-second order models for MC-LR adsorption onto NOR 63-90 (2.5 mM IS electrolyte).

	Pseudo-first order model		**Pseudo-second order model**	
$\mathbf{q_{e\_calc}}$ (µg/mg)	$\mathbf{k_1}$ (h^{-1})	$\mathbf{R^2}$	$\mathbf{k_2}$ (mg/(µg/h))	$\mathbf{R^2}$
3.33	1.24 ± 0.170	0.987	0.852 ± 0.091	0.998

For the full range of contact time studied, the experimental kinetic data of NOR 63-90 carbon is best described by the pseudo-second order model, with very good correlation (R^2=0.998), much better than the pseudo-first order model, that does not describe the MC-LR adsorption kinetics in the full range of contact time. Like in most cases published in literature, the pseudo-first order model is applicable only in the first period of the sorption process (Ho and McKay, 1999), in this case, in the first 2 h. As the MC-LR adsorption kinetic data are best fitted by the pseudo-second order model, this indicates that the chemisorption is the adsorption mechanism, which is consistent, as it was seen previously for NOR 125-180, with adsorption well-described by the Langmuir model.

The pseudo-second order adsorption kinetic model fitting of C (µg/L) and q (µg/mg) for MC-LR adsorption onto NOR 63-90 is shown in Figure 4.12.

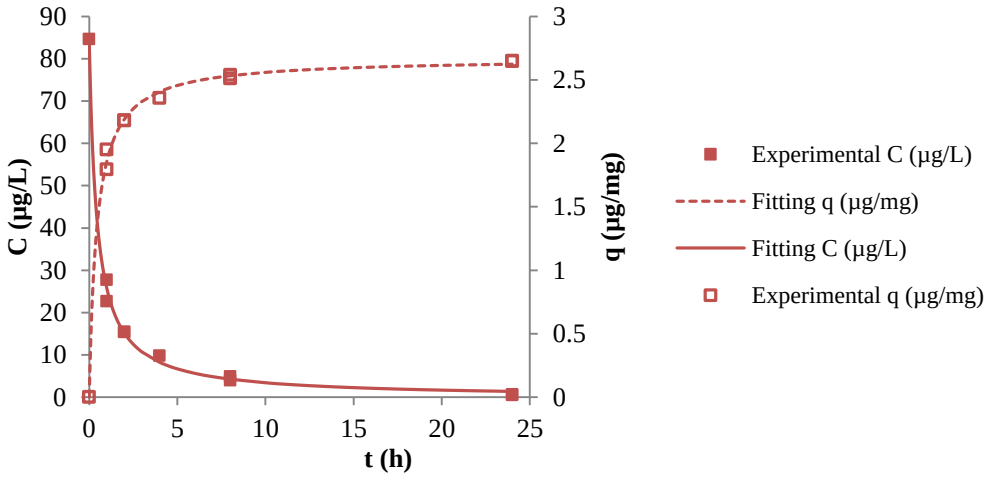

Figure 4.12. Pseudo-second order adsorption kinetic model fitting of C (µg/L) and q(µg/mg) for MC-LR adsorption onto NOR 63-90 (2.5 mM IS electrolyte).

NOR 63-90 carbon shows faster kinetics than NOR 125-180 carbon, as expected. In addition to a shorter intraparticle path, crushing the carbon apparently opens pores a little bit (Table 4.3), which causes the faster adsorption of microcystin-LR. The intraparticle diffusion model approach is shown in Figure 4.13 and Table 4.10.

The plot of q_t versus $t^{1/2}$ may present multi-linearity (Ip et al., 2010), which indicates that two or more rate controlling steps occur in the adsorption processes (the external mass diffusion, the intraparticle diffusion and the equilibrium).

The slope of the second linear plot characterizes the rate parameter corresponding to the intraparticle diffusion (k_p) while the intercept C is proportional to the boundary layer thickness, i.e. the larger the value of the intercept of the second linear plot, the greater is the boundary layer effect on the adsorption kinetics.

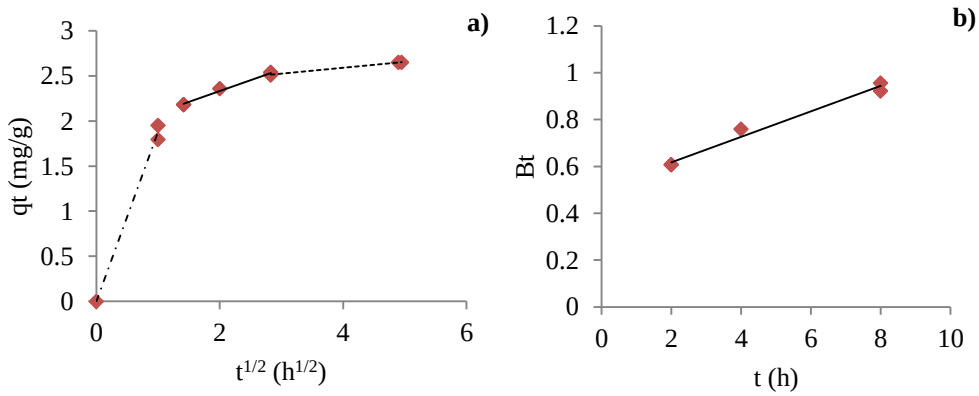

Figure 4.13. Intraparticle diffusion model for MC-LR adsorption (a) and Boyd plot (diffusion coefficient) (b) onto NOR 63-90 (2.5 mM IS electrolyte).

Table 4.10. Parameters for intraparticle diffusion model and Boyd plot for MC-LR adsorption onto NOR 63-90 (2.5 mM IS electrolyte).

Intraparticle diffusion model			**Boyd et al. (1947) equation**			
$\mathbf{k_p}$ (μg/mg.$h^{1/2}$)	**C** (μg/mg)	$\mathbf{R^2}$	$\mathbf{r_{AC}}$ (μm)	**Equation**	**Di** (cm^2/s)	$\mathbf{R^2}$
0.242 ± 0.047	1.85 ± 0.102	0.989	38.25	Bt = (0.054 ± 0.013) t + (0.508 ± 0.072)	$2.22x10^{-11}$	0.983

In this case, three segments can be observed and the second linear segment has a significant intercept (C=1.85 ± 0.102 μg/mg, (Figure 4.13a)) which represents the boundary layer thickness. The multilinearity analysis of q_t versus $t^{1/2}$ plot then indicates a significant contribution of the external mass transfer to the MC-LR adsorption kinetics onto NOR 63-90 μm carbon.

These conclusions agree with the carbons' particle grade. The smaller the particle size the greater the importance of the external mass transfer over intraparticle diffusion. This is, the MC-LR adsorbate may easily diffuse through the internal pores of the small particles of NOR 63-90 μm, and external diffusion becomes the rate-limiting step for this AC. MC-LR has to travel a shorter path through the NOR 63-90 μm particles compared to the 125-180 μm particles, and the external film diffusion is thus more relevant to the overall kinetics than the intraparticle diffusion. These results are in accordance with Mohan et al., (2004) and with Costa (2010), concluding that the external transport is the rate-limiting step in systems where the particle sizes are smaller, which is the case of NOR 63-90 μm carbon.

Consequently, it does not make sense to apply the Boyd model to the adsorption data of NOR 63-90 μm.

4.2.4. Adsorption of MC-LR onto modified NOR 125-180

Equilibrium isotherms onto modified NOR 125-180 carbon were performed with 97.3 μg/L MC-LR initial concentration in 2.5 mM IS electrolyte (1 mM IS KCl + 1.5 mM IS $CaCl_2$) and AC concentrations between 12.5-50 mg/L during five days (experiments detailed in section 3.7.6). The fitting of adsorption isotherm curve is illustrated in Figure 4.14 and Table 4.11 presents the Langmuir parameters.

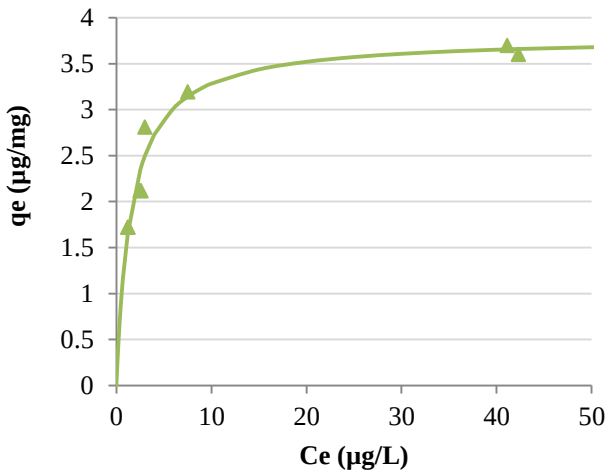

Figure 4.14. Langmuir isotherm fitting for MC-LR adsorption onto modified NOR 125-180 (2.5 mM IS electrolyte).

The curve fitting was obtained with the Langmuir equation (R^2=0.951). The Freundlich model was not applied once more, since the experimental data are out of the range of model applicability (Snoeyink and Summers, 1999).

Table 4.11. Langmuir isotherm parameters with 95% confidence interval for MC-LR adsorption onto modified NOR 125-180 (2.5 mM IS electrolyte).

q_{max} (µg/mg)	b (L/µg)	R^2
3.79 ± 0.350	0.64 ± 0.20	0.951

The pseudo-first order and pseudo-second order kinetic models fittings are presented in Figure 4.15 and the results are presented in Table 4.12.

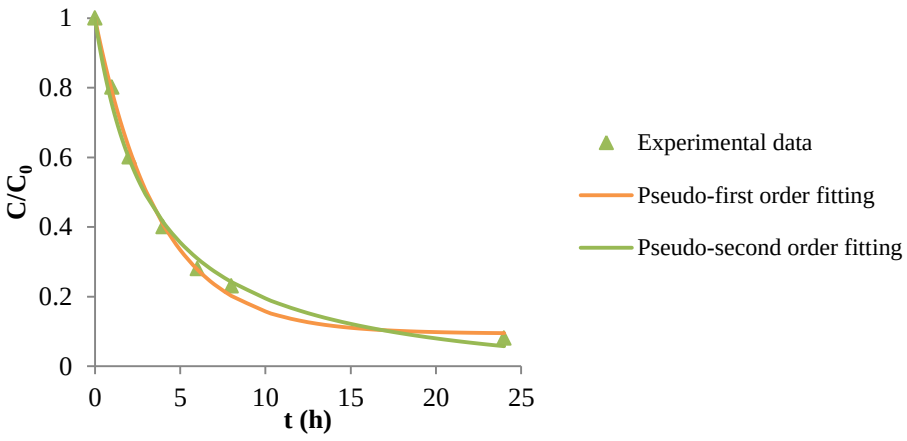

Figure 4.15. Pseudo-first order and pseudo-second order adsorption kinetic models for MC-LR adsorption onto modified NOR 125-180 (2.5 mM IS electrolyte).

Table 4.12. Adsorption kinetic constants with 95% confidence interval for pseudo-first order and pseudo-second order models for MC-LR adsorption onto modified NOR 125-180 (2.5 mM IS electrolyte).

	Pseudo-first order model		Pseudo-second order model	
$q_{e\ calc}$ (µg/mg)	k_1 (h^{-1})	R^2	k_2 (mg/(µg/h))	R^2
3.77	0.265 ± 0.020	0.997	0.089 ± 0.020	0.994

For this carbon, both the pseudo-first and -second order models fit the kinetic data.

The pseudo-second order adsorption kinetic model fitting of C (µg/L) and q (µg/mg) for MC-LR adsorption onto modified NOR 125-180 is shown in Figure 4.16.

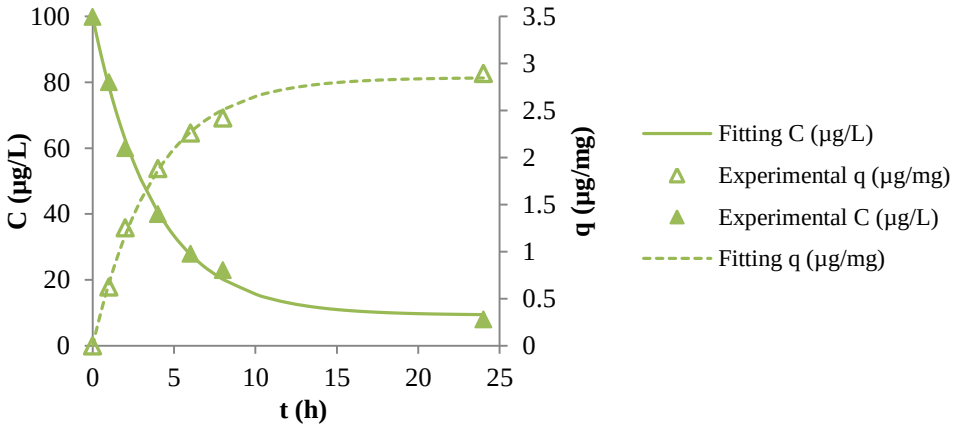

Figure 4.16. Pseudo-second order adsorption kinetic model fitting of C (µg/L) and q(µg/mg) for MC-LR adsorption onto modified NOR 125-180 (2.5 mM IS electrolyte).

The intraparticle diffusion and Boyd's models approach is shown in Figure 4.17 and Table 4.13.

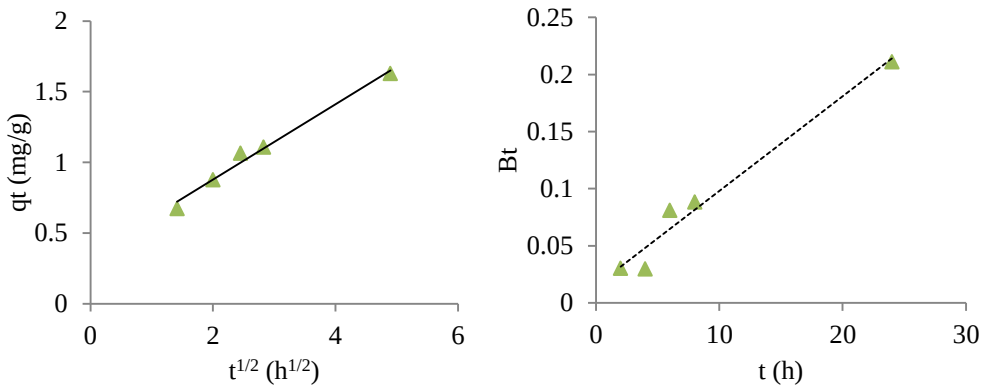

Figure 4.17. Intraparticle diffusion model (a), and Boyd plot (diffusion coefficient) (b), for MC-LR adsorption onto modified NOR 125-180 (2.5 mM IS electrolyte).

Table 4.13. Parameters for intraparticle diffusion model and Boyd plot for MC-LR adsorption onto modified NOR 125-180 (2.5 mM IS electrolyte).

Intraparticle diffusion			**Boyd et al. (1947) equation**			
k_p (µg/mg.$h^{1/2}$)	C (µg/mg)	R^2	r_{AC} (µm)	Equation	Di (cm^2/s)	R^2
0.27 ± 0.06	0.35 ± 0.18	0.985	76.25	Bt = (0.08 ± 0.015) t + (0.015 ± 0.032)	$1.35x10^{-11}$	0.969

Modified NOR 125-180 carbon exhibits only one linear portion. The linear portions do not pass through the origin indicating that the intraparticle diffusion is not the only rate controlling step for the adsorption. This conclusion is confirmed by Boyd's analysis.

4.2.5. Comparative analysis of the three NOR carbons for MC-LR adsorption

In this section, the difference of adsorption kinetics and capacities are described and related to the characteristics of the ACs. The adsorbed capacity by each carbon is represented and summarized in Figure 4.18 and Table 4.14.

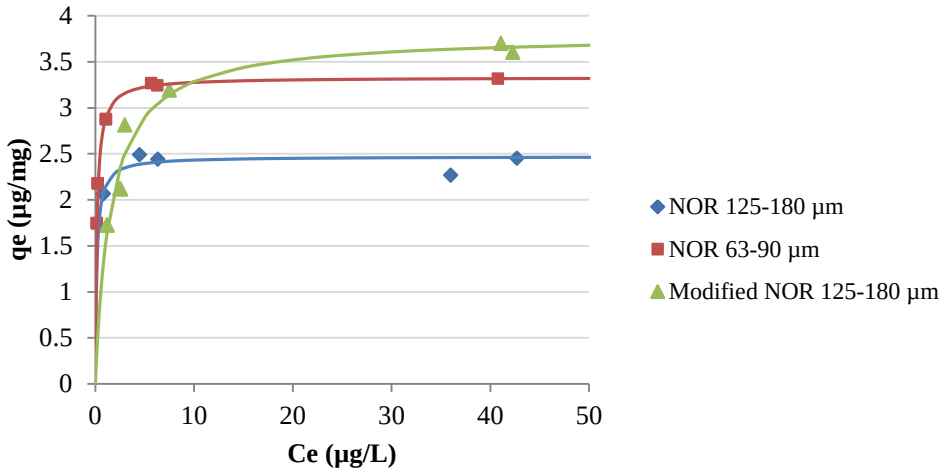

Figure 4.18. Langmuir isotherm fitting for adsorption of MC-LR onto the studied ACs.

Table 4.14. Langmuir isotherm parameters with 95% confidence interval for adsorption of MC-LR onto the studied ACs.

AC	**Langmuir fitting**		
	q_{max} (µg/mg)	**b** (L/µg)	**R^2**
NOR (125-180 µm) (♦)	2.47 ± 0.14	6.38 ± 4.60	0.770
NOR (63-90 µm) (▪)	3.33 ± 0.08	6.13 ± 0.70	0.992
Modified NOR (125-180 µm) (▲)	3.79 ± 0.35	0.64 ± 0.20	0.951

The isotherms were reasonably well fitted using the Langmuir adsorption model. Figure 4.18 shows how the NOR 63-90 and the modified NOR 125-180 carbons exhibit a higher affinity for MC-LR (during adsorption from 2.5 mM IS electrolyte solution) than NOR 125-180.

Comparing the results for the three activated carbon (Table 4.14) and taking into account the characteristics of the different activated carbons, modified NOR 125-180 is clearly the most effective adsorbent, adsorbing a maximum of 3.79 μg/mg carbon, as indicated by the plateau of the adsorption isotherm, followed by NOR 63-90 which adsorbs a maximum of 3.33 μg/mg carbon.

Table 4.15 summarizes relevant chemical and textural properties of the three activated carbons.

Table 4.15. Summary of activated carbon properties.

AC	Micropore volume (cm^3/g)	BJH volume (cm^3/g) (macro + mesopores)	pH_{pzc}	Oxygen content, %
NOR 125-180	0.35	0.34	9.10	18
NOR 63-90	0.36	0.40	9.10	15
Modified NOR 125-180	0.39	0.40	12.1	9.9

The surface created by crushing NOR 125-180 apparently causes an increase in the capacity of NOR 63-90 carbon. Donati et al. (1994) proposes that MC-LR maximum adsorption for the AC's is directly related to the pore volume in the mesopore region and the most effective MC-LR adsorbent bears the largest mesopore volume.

The size and the shape of MC-LR molecule, which is dependent on the overall configuration of the hepto-peptide ring and side-chains (Lanaras et al., 1991), is important when considering the relevance of the above correlation. With the assistance of molecular models (Lanaras et al., 1991), the diameter of the molecule was estimated to be between 1.2 and 2.6 nm. For the removal of microcystin-LR, literature indicates that the mesopore structure (2-50 nm) is consistent with the microcystin size (1.2-2.6 nm) (Donatiet al., 1994, Newcombe and Nicholson, 2004), so a high MC-LR adsorption capacity would require a high mesopore volume. The present results corroborate this. Figure 4.19 shows the correlation between the maximum adsorption of MC-LR onto the studied ACs and their BJH (a) and micropore (b) volumes.

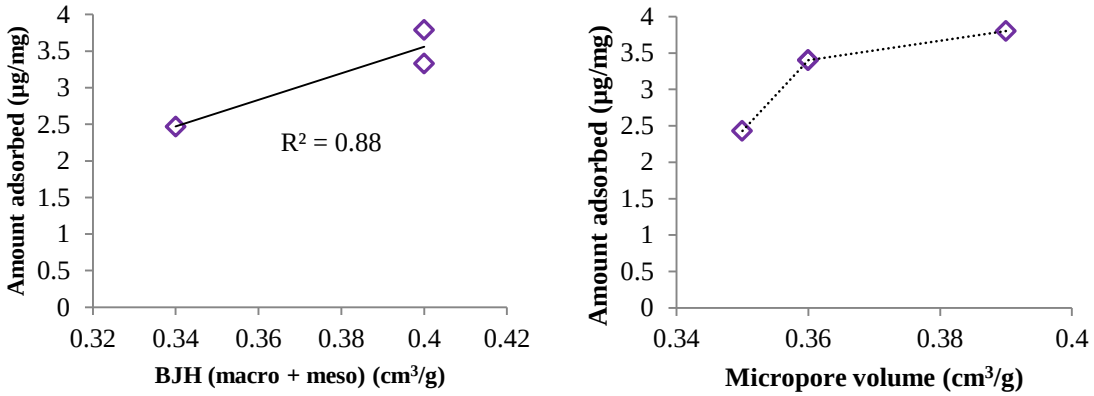

Figure 4.19. Correlation of the q_{max} of the MC-LR adsorbed with the mesopore and macropore volumes (BJH) and with micropore volume.

The amount adsorbed by each AC is directly proportional to the BJH volume, whereas there is no correlation with the micropore volume. This result suggests the importance of mesopores in the adsorption of MC-LR (with a reasonably correlation coefficient of 0.88).

This observation is consistent with those previously made for MIB adsorption by AC (Newcombe et al., 1997) and for surfactant adsorption (Pendleton et al., 2002) by AC. The micropores (< 1nm) in carbon offer only a nominal internal surface for adsorption (Huang and Cheng, 2007).

However, Figure 4.19a shows that the same BJH volume may be associated to different adsorption capacities, other factors must therefore be contributing to the higher adsorption capacity shown by the modified carbon. Actually the isotherms show a trend of increasing affinity with decreasing the oxygen content (Figure 4.20), which is also in agreement with results of Considine et al. (2001); Pendleton et al. (2002) and Costa, 2010.

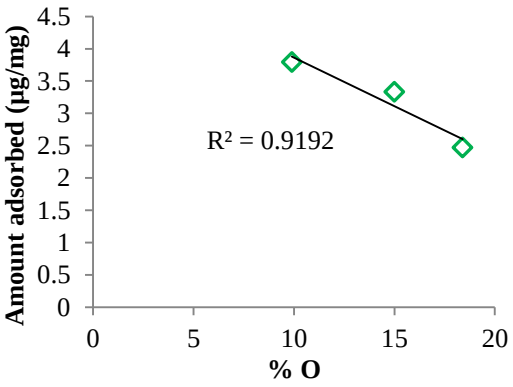

Figure 4.20. Correlation between the amounts of MC-LR adsorbed with oxygen content on AC´s (2.5 mM IS electrolyte).

A good linear correlation between MC-LR adsorption capacity and the oxygen content (Figure 4.20) of the activated carbons is also an interesting finding – the higher the AC oxygen content, the lower the capacity for adsorbing MC-LR. Wu and Pendleton (2001) observed this type of trend for the adsorption of a relatively hydrophobic low molecular weight anionic surfactant on different activated carbons. They found a linear decrease of the adsorption capacity with increasing oxygen content of the carbonaceous adsorbent. Also Considine et al., (2001) shows that increasing surface oxygen content at a constant pore volume leads to a decrease in the amount adsorbed of MIB.

The pH_{pzc} is a good indicator of the carbon surface charge and therefore of its basicity. All the three carbons presented high pH_{pzc}, in the order NOR 125-180 = NOR 63-90 < modified NOR (9.1, 9.1 and 12.1, respectively) i.e. they were positively charged in all experiments (pH 5-7). At the pH of the experiences, microcystin-LR was negatively charged, with a -1 net charge, carrying two net negative charges (COO^-) and one net positive charge (NH_2^+).

When modified/functionalized, pH_{pzc} of NOR 125-180 increased (9.1 to 12.1), making this modified AC more alkaline and thus increasing the adsorption capacity.

From these observations, it is reasonable to conclude that the adsorption of MC-LR by AC from aqueous solution will be influenced not only by porosity, but also by the adsorbent surface chemistry.

A controlled increase or decrease in the oxygen content will lead to a controlled modification of the adsorbent surface chemistry (Considine et al., 2001). From these results, the heating method used in this work is an excellent and simple process for increasing the basicity and hydrophobicity of an AC and thereby enhancing the MC-LR adsorption capacity of the carbon.

Regarding the adsorption kinetics, the comparison is shown Figure 4.21 and in Table 4.16.

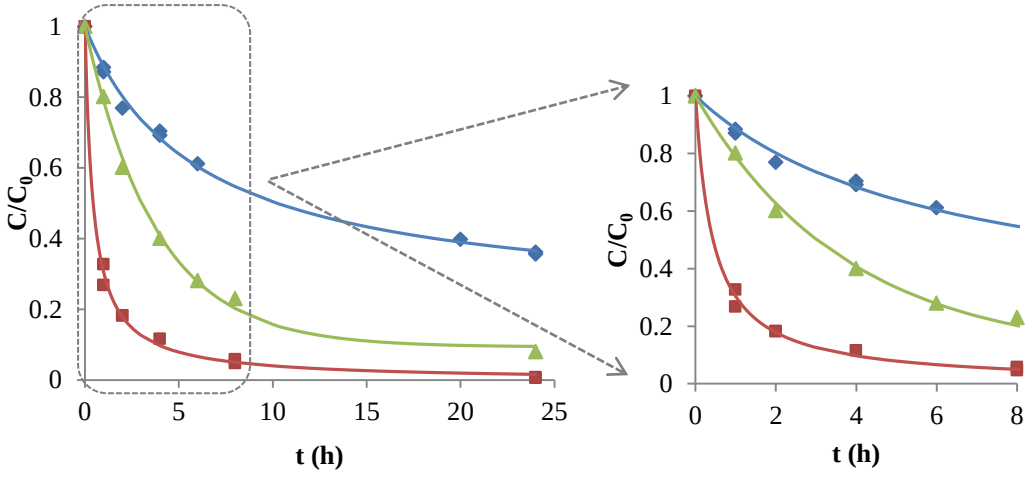

Figure 4.21. Adsorption kinetics for adsorption of MC-LR onto the studied ACs.

Table 4.16. Adsorption kinetic parameters with 95% confidence interval for adsorption of MC-LR onto the studied ACs (2.5 mM IS electrolyte).

AC	Pseudo-second order model		
	q_{e_calc} (µg/mg)	k_2 (mg/(µg/h))	R^2
NOR (125-180 µm) (♦)	2.47	0.064 ± 0.01	0.996
NOR (63-90 µm) (▪)	3.33	0.852 ± 0.09	0.998
Modified NOR (125-180 µm) (▲)	3.77	0.089 ± 0.02	0.994

The higher k_2 correspond to the NOR 63-90, demonstrating a faster adsorption of MC-LR, followed by modified NOR 125-180.

The kinetic data show an excellent agreement with the pseudo-second order model ($R^2 > 0.99$). These results corroborate those obtained in the isotherms. The adsorption kinetics was described by the pseudo-second order model, which is consistent with adsorption by chemisorption, and therefore well described by the Langmuir isotherm model.

Crushing carbon (NOR 63-90) has also a double effect. On one hand, the resistance to transport is lower because of the smaller particle size, and on the other hand apparently the crushing opens the pores, which facilities the adsorption.

The intraparticle diffusion and Boyd's models approach is shown in Figure 4.22 and Table 4.17.

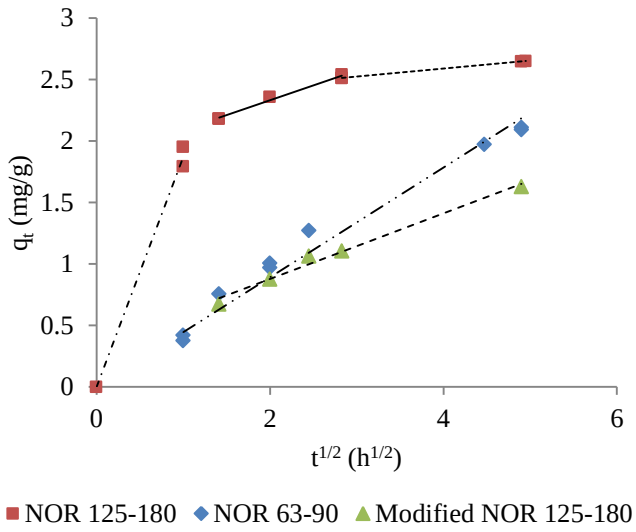

Figure 4.22. Intraparticle diffusion model for MC-LR adsorption onto the studied activated carbons (2.5 mM IS electrolyte).

Table 4.17. Intraparticle diffusion model parameters for MC-LR adsorption onto the studied activated carbons (2.5 mM IS electrolyte).

AC	Intraparticle diffusion model		
	kp (μg/mg.h$^{1/2}$)	**C** (μg/mg)	**R^2**
NOR 125-180 (♦)	0.446 ± 0.026	-	0.977
NOR 63-90 (♦)	0.242 ± 0.047	1.85 ± 0.102	0.989
Modified NOR 125-180 (♦)	0.270 ± 0.060	0.35 ± 0.18	0.985

In the case of MC-LR adsorption onto NOR 63-90 carbon the three linear segments above exposed can be notable and the second linear segment has a significant intercept (C=1.85 ± 0.102 μg/mg, Figure 4.22). The multilinearity analysis of q_t versus $t^{1/2}$ plot for the NOR 63-90 indicates a significant contribution of the external mass transfer to the MC-LR adsorption kinetics onto this carbon. NOR 125-180 carbon exhibits only one linear portion. The linear portion passes through the origin indicating that the intraparticle diffusion is the rate controlling step for the adsorption. Modified NOR 125-180 carbon exhibits only one linear portion, but this linear portion do not pass through the origin indicating that the intraparticle diffusion is not the only rate controlling step for the adsorption.

These conclusions agree with the carbons' particle grade. The smaller particle size, the greater is the importance of the external mass transfer over the intraparticle diffusion. This is, the MC-LR adsorbate may easily diffuse through the internal pores of the small particles of NOR 63-90 μm, and external diffusion becomes the rate-limiting step for this AC. MC-LR has to travel a shorter path through the NOR 63-90 μm particles compared to the 125-180 μm particles, and the external film diffusion is thus more relevant to the overall kinetics than the intraparticle diffusion. These results are in accordance with Mohan et al., (2004) and with Costa (2010), concluding that the external transport is the rate-limiting step in systems where the particle sizes of the adsorbate are smaller, which is the case of NOR 63-90 μm carbon.

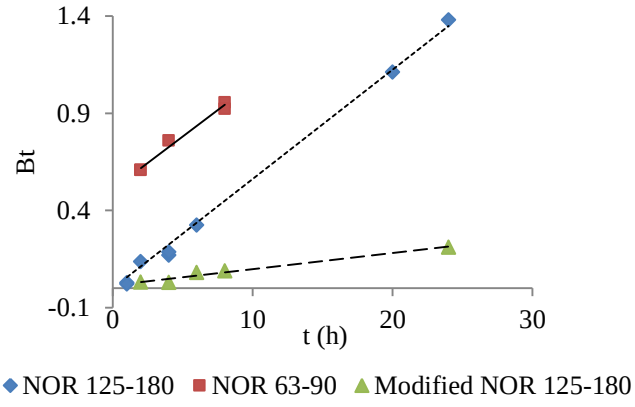

Figure 4.23. Diffusion coefficients of MC-LR through the studied ACs.

Table 4.18. Boyd's model parameters for MC-LR adsorption onto the studied activated carbons.

AC	Boyd et al. (1947) equation			
	r_{AC} (μm)	Equation	Di (cm^2/s)	R^2
NOR 125-180 (♦)	76.25	Bt = (0.056 ± 0.003) t	$9.16x10^{-11}$	0.996
NOR 63-90 (♦)	38.25	Bt = (0.054 ± 0.013) t + (0.508 ± 0.072)	$2.22x10^{-11}$	0.983
Modified NOR 125-180 (♦)	76.25	Bt = (0.08 ± 0.015) t + (0.015 ± 0.032)	$1.35x10^{-11}$	0.969

Boyd plots confirm the results obtained by intraparticle diffusion model.

The integrated analysis of the results of the chemical and textural characterization of the activated carbons shows that the carbon which presents the highest surface area (A_{BET}), external area (A_{ext}), pH_{pzc} value and the lowest oxygen content (and hence hydrophobicity), the modified NOR 125-180, has a higher capacity for adsorption of MC-LR. These characteristics explain the higher capacity for modified NOR 125-180 when compared with NOR 125-180.

The results showed that both physical and chemical properties simultaneously affect the adsorption process. In such a complex system the adsorption of MC-LR cannot be explained by structure of AC or surface chemistry effects alone.

4.3. ADSORPTION OF TANNIC ACID ONTO ACTIVATED CARBON

4.3.1. Comparative analysis of the MC-LR adsorption and TA adsorption as single-solutes

The single solute isotherms were conducted with MC-LR and TA dissolved in 2.5 mM IS electrolyte solution. The initial concentrations were 104 μg MC-LR/L for microcystins and 5 mg TA/L for NOM model compound.

Is important to note again, that the MC-LR isotherm cannot be called single-solute, since an extract was used. Figure 4.24 represents single-solute isotherms of MC-LR and TA adsorption onto NOR 125-180.

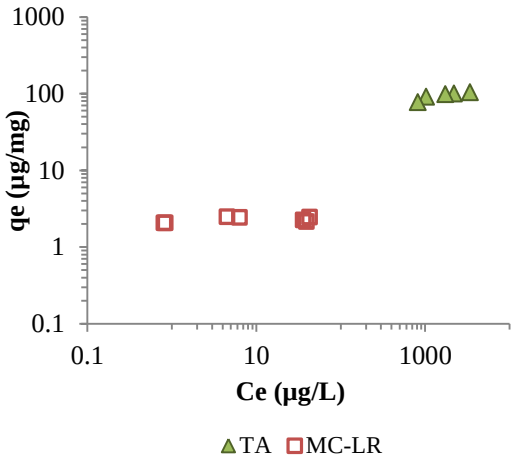

Figure 4.24. Single-solute isotherms (Langmuir plot) of MC-LR and TA adsorption onto NOR 125-180 (2.5 mM IS background electrolyte).

Table 4.19. Single-solute isotherms (Langmuir parameters) of MC-LR and TA adsorption onto NOR 125-180 (2.5 mM IS background electrolyte).

	q_{max} (µg/mg)	**b** (L/µg)	R^2
MC-LR	2.5 ± 0.14	6.4 ± 4.6	0.770
TA	117.4 ± 17.2	0.003 ± 0.002	0.908

Parameters of TA adsorption were not comparable to those of MC-LR. According to Campinas and Rosa (2006) and Campinas (2009), the parameters relative to tannic acid adsorption onto PAC SA-UF should be comparable to those of microcystins, with a slightly lower adsorption capacity and intensity, and these results provided good evidence of a similar access to a range of adsorption sites for both MC-LR and TA.

Regardind the kinetic study, no major differences were observed in the velocity profile between MC-LR and TA adsorption (Figure 4.25), although it was expected a faster adsorption of MC-LR.

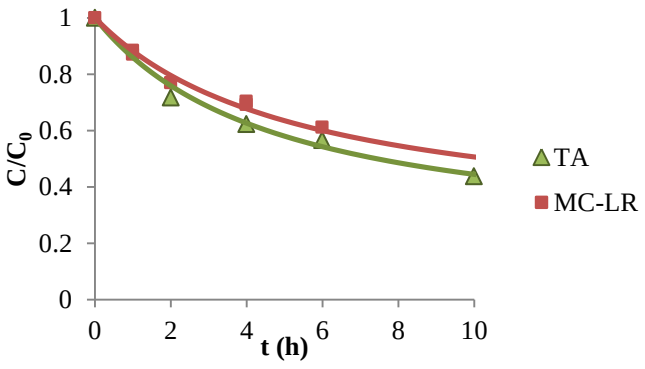

Figure 4.25. Single-solute adsorption kinetics of MC-LR and TA adsorption in the presence of 2.5 mM IS background onto NOR 125-180 µm.

Table 4.20. Single-solute adsorption kinetics of MC-LR and TA adsorption in the presence of 2.5 mM IS background onto NOR 125-180 µm.

	k_2 (mg/(µg/h))	R^2
MC-LR + IS	0.064 ± 0.008	0.996
TA + IS	0.002 ± 0.001	0.975

It is then expected competition between both solutes and consequently a lower adsorption capacity in the competitive adsorption tests (presented in section 4.4).

4.3.2. Comparative analysis of the three NOR carbons for TA adsorption

Equilibrium isotherms and kinetic studies of tannic acid onto the studied ACs were detailed in sections 3.7.4 and 3.7.7. The fittings of the adsorption isotherm curves are illustrated in Figure 4.26 and Table 4.21 presents Langmuir parameters for the three NOR carbons. For NOR 125-180 and for NOR 63-90, the isotherms show a reasonably plateau, thus the Freundlich equation does not apply. For the modified NOR 125-180 both isotherm models were tested but the Langmuir still produces the best fitting, and consequently only the Langmuir isotherm fitting is presented.

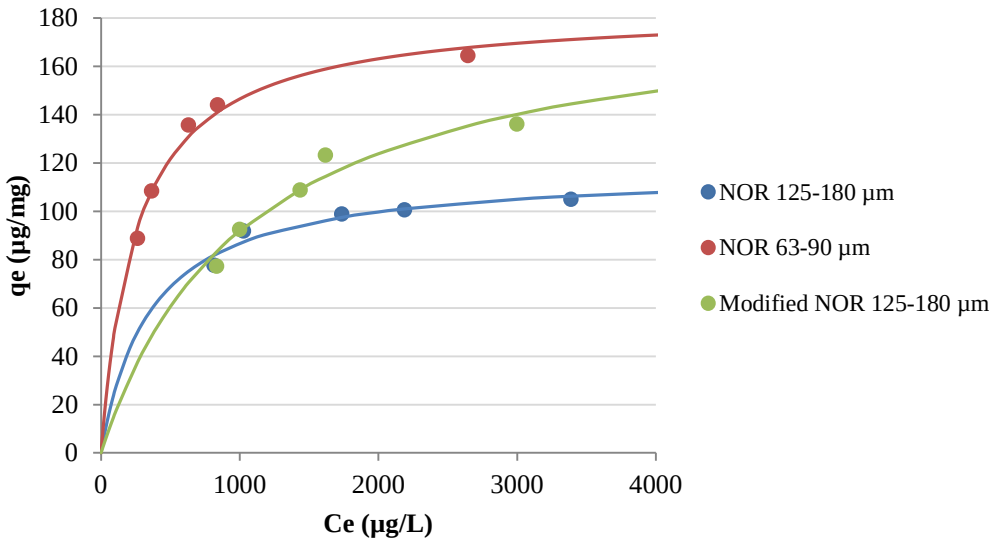

Figure 4.26. Langmuir isotherm fitting for adsorption of TA onto the studied ACs (2.5 mM IS electrolyte).

Table 4.21. Langmuir isotherm parameters with 95% confidence interval for adsorption of TA onto the studied ACs (2.5 mM IS electrolyte).

AC	Langmuir fitting		
	q_{max} (µg/mg)	**b** (L/µg)	R^2
NOR (125-180 µm) (●)	117 ± 17	0.003 ± 0.002	0.908
NOR (63-90 µm) (●)	184 ± 19	0.004 ± 0.001	0.982
Modified NOR (125-180 µm) (●)	190 ± 63	0.001 ± 0.0007	0.941

Figure 4.26 and Table 4.21 shows that TA adsorption increases approximately with increasing the available pore volume (mesopore and macropore): **NOR 125-180 < NOR 63-90 < modified NOR 125-180.** These results were consistent with the findings of Bjelopavlic et al. (1999). Again, available pore volume is not the only factor influencing adsorption. Chemical factors must therefore be involved in the adsorption mechanisms, probably associated to the surface chemistry and associated functional groups of the ACs.

The factors influencing adsorption seems to be the same for MC-LR and for TA. TA is negatively charged at pH of the experiments and electrostatic interactions became significant.

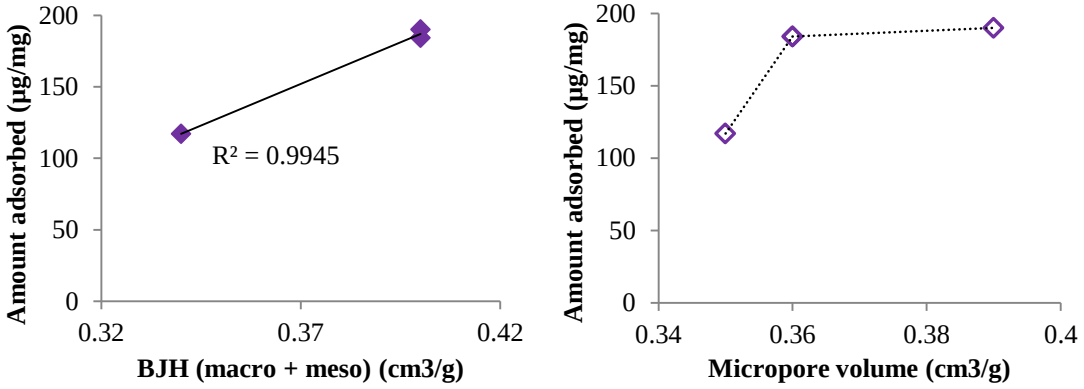

Figure 4.27. Correlation of the qmax of the TA adsorbed with the mesopore and macropore volumes (BJH) and with micropore volume.

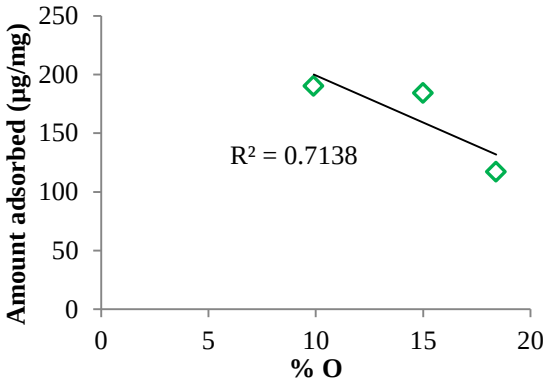

Figure 4.28. Correlation between the amounts of TA adsorbed with oxygen content on AC´s (2.5 mM IS electrolyte).

As observed in Figure 4.27 and Figure 4.28, make sense to say that just changing the oxygen content of an AC keeping its structure, MC-LR adsorption can be increased when in the presence of TA, making this a factor of selectivity.

Modified NOR 125-180 displays significantly higher adsorption than NOR 125-180 and has much higher positive surface charge than NOR 125-180 at the pH of the experiments. The adsorption of TA appears to be attributable, as adsorption of MC-LR, to a number of factors.

As for adsorption of MC-LR, the objective of the kinetic studies for TA adsorption was to evaluate the limiting steps of the TA adsorption. The same kinetic models were used to study these processes and to investigate the mechanisms and the potential rate-controlling step(s) of TA adsorption, such as mass transport (**intraparticle diffusion model**) and chemical reaction (**pseudo first and second order models**). It was observed that the pseudo-first order model fitting shows poor correlation, consequently, it is not presented here (Figure 4.29). As the TA adsorption kinetic data are best fitted by the pseudo-second order model, this indicates the chemisorption as the adsorption mechanism.

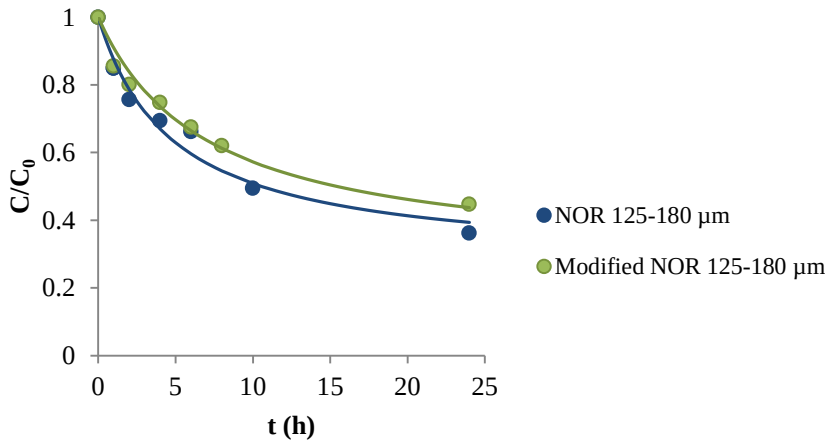

Figure 4.29. Pseudo-second order adsorption kinetics fitting for adsorption of TA onto NOR 125-180 and modified 125-180 (2.5 mM IS electrolyte).

The pseudo-second order adsorption kinetics model fitting of C (µg/L) and q (µg/mg) for TA adsorption onto NOR 125-180 and modified NOR 125-180 are shown in Figure 4.30.

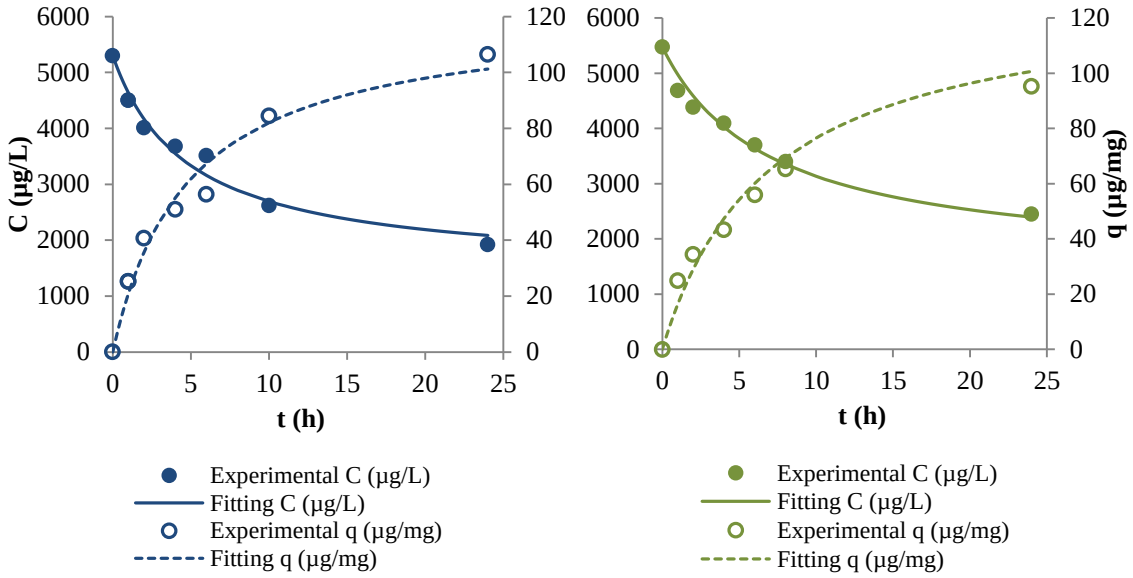

Figure 4.30. Pseudo-second order fitting of C (µg/L) and q(µg/mg) for NOR 125-180 (●) and for modified NOR 125-180 (●) adsorption of TA (2.5 mM IS electrolyte).

Table 4.22. Adsorption kinetics parameters with 95% confidence interval for adsorption of TA onto NOR 125-180 and modified NOR 125-180 (2.5 mM IS electrolyte).

AC	Pseudo-second order model		
	q_{e_calc} (µg/mg)	k_2 (mg/(µg/h))	R^2
NOR (125-180 µm) (●)	122 ± 14	0.0020 ± 0.00070	0.971
Modified NOR (125-180 µm) (●)	130 ± 17	0.0010 ± 0.00050	0.975

TA is present in much higher concentration than MC-LR (5 mg/L vs 100 µg/L, i.e. 50 times higher) and has a strong negative surface charge at the studied pH values (Moreno-Castilla et al., 2004), leading to strong TA-AC electrostatic attraction.

The intraparticle diffusion and Boyd's models approach is shown in Figure 4.31 and Table 4.23.

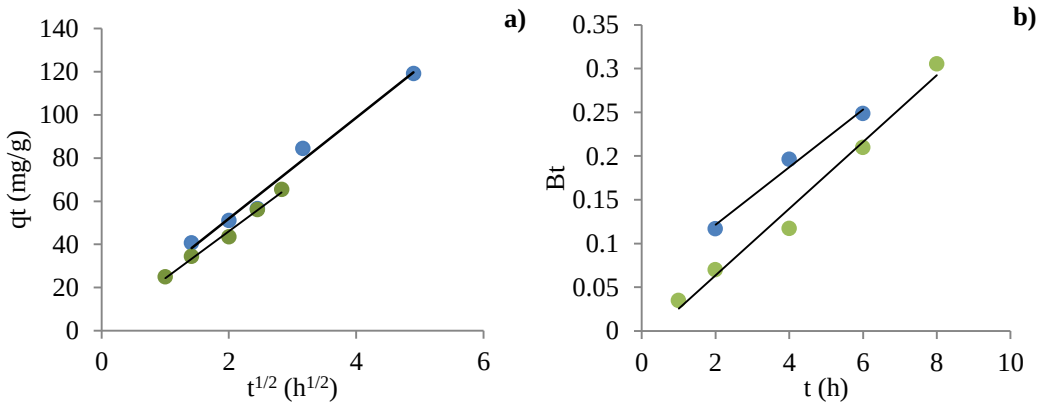

Figure 4.31. Intraparticle diffusion model (a), and Boyd plot (diffusion coefficient) (b), for TA adsorption onto NOR 125-180 (●) and modified NOR 125-180 (●) (2.5 mM IS electrolyte).

Table 4.23. Intraparticle diffusion and Boyd's parameters for TA adsorption onto NOR 125-180 and modified NOR 125-180 (2.5 mM IS electrolyte).

AC	Intraparticle diffusion model			Boyd et al. (1947) equation			
	kp ($\mu g/mg.h^{1/2}$)	C ($\mu g/mg$)	R^2	r_{AC} (μm)	Equation	Di (cm^2/s)	R^2
NOR 125-180 (●)	23.4 ± 5.79	5.2 ± 17.6	0.982	76.25	Bt = (0.03±0.05) t + (0.05±0.22)	$5.4x10^{-11}$	0.986
Modified NOR 125-180 (●)	21.8 ± 3.96	2.6 ± 8.2	0.991	76.25	Bt = (0.04±0.01) t – (0.012±0.05)	6.2×10^{-11}	0.982

The experimental data for TA adsorption show the same tendency as the results for MC-LR adsorption. Modified NOR 125-180 proved to be more effective in TA adsorption.

Considering the intraparticle diffusion model for TA adsorption, NOR 125-180 carbon exhibits only one linear portion. The linear portions do not pass through the origin indicating that the intraparticle diffusion is not the only rate controlling step for the adsorption (Table 4.23).

In the case of TA adsorption onto modified NOR 125-180 carbon also one linear segment can be observed. But the errors associated with the parameters are so high, that we cannot guarantee that the intercepts is not zero, thus controlling the intraparticle diffusion (Table 4.23).

In order to get a perceptive of the step that controls the TA adsorption kinetics; the data were also analyzed by the kinetic expressions given by Boyd et al. (1947).

The calculated Bt values were plotted against time t and are shown in Figure 4.31b. The linearity of this plot is used to distinguish which transport mechanism, external transport or intraparticle, controls the adsorption rate. The plot presented in Figure 4.31b is linear but do not pass through the origin. These results validate the previous conclusion based on the intraparticle diffusion model consequently demonstrating that the rate-limiting step can be the intraparticle diffusion for TA adsorption onto NOR 125-180 carbon and modified NOR 125-180.

The diffusion coefficients of TA through studied carbons were determined by equation 2.17, assuming spherical particles.

4.4. COMPETITIVE ADSORPTION BETWEEN MC-LR AND TA

4.4.1. Competitive adsorption between MC-LR and TA onto NOR 125-180

Figure 4.32 presents the competitive adsorption isotherms of extract of MC-LR (103 µg/L in 2.5 mM IS (1 mM IS KCl + 1.5 mM IS $CaCl_2$) background electrolyte) and tannic acid (5 mg TA/L) onto NOR 125-180. The experimental conditions were detailed in section 3.7.8.

For easier analysis of the effect of TA competition, previous data relative to NOR adsorption of MC-LR from 2.5 mM electrolyte (single solute isotherm, Figure 4.6) are also shown in Figure 4.32.

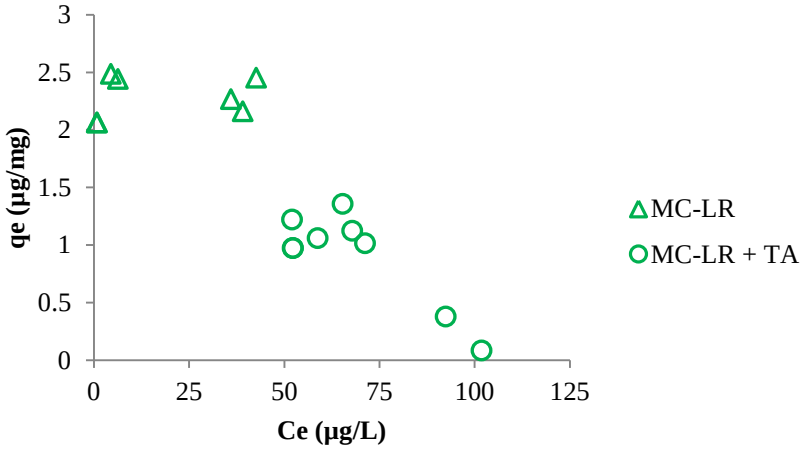

Figure 4.32. Competitive and single-solute adsorption isotherms of MC-LR onto NOR 125-180 (2.5 mM IS electrolyte)

The competitive adsorption isotherm of MC-LR onto NOR 125-180 in the presence of tannic acid presents a negative slope, and consequently the Freundlich and Langmuir models did not fit the experimental data.

Only a 48% MC-LR removal was achieved, in contrast with the 98% removal found in "single solute" conditions.

Pelekani and Soeyink (2000) identified this phenomenom in a study where the presence of methylene blue strongly affected atrazine adsorption to activated carbon fiber, resulting in a negative slope in the adsorption isotherm of atrazine. They atributed this to direct competition for the same adsorption sites in the micropore region.

In this case, the competition is in the mesopores region, which has the adequate size for these molecules (TA is 1700 g/mol and MC-LR is 994 g/mol). TA is present in much higher concentration than MC-LR (5 mg/L vs 100 µg/L, i.e. 50 times higher) and has a strong negative surface charge at the studied pH values (Moreno-Castilla et al., 2004), leading to strong TA-AC electrostatic attraction.

Considering this and by observing the Figure 4.32 it is believed that there was no adsorption of MC-LR, due to the presence of TA and consequently strong competition.

These results show that tannic acid has a strong influence on the MC-LR adsorption onto NOR 125-180 carbon. As both TA and MC-LR molecules have similar molecular weights and carry net negative charges at the pH of the experience, these similar characteristics point to the fact that there would be competition for the positively charged activated carbon. The shape of the MC-LR isotherm (Figure 4.32) with a negative slope is indicative of the strongly competing effects between the two adsorbates (Pelekani and Snoeyink, 2000).

TA molecules are small enough to access small mesopores and may therefore directly compete with MC-LR for the same adsorption sites. However, TA molecules may block the MC-LR access to even small mesopores where MC-LR can fit whereas TA is size-excluded.

When pore blockage by TA is a dominant effect, both adsorption kinetics and adsorption equilibrium will be affected (Matsui et al., 2003).

Kinetic tests were then performed (Figure 4.33). As can be seen in Figure 4.33a), when in competition, although a reducing AC capacity for MC-LR and for TA had been previously observed they have similar kinetics, so direct competition seems to be the dominant effect.

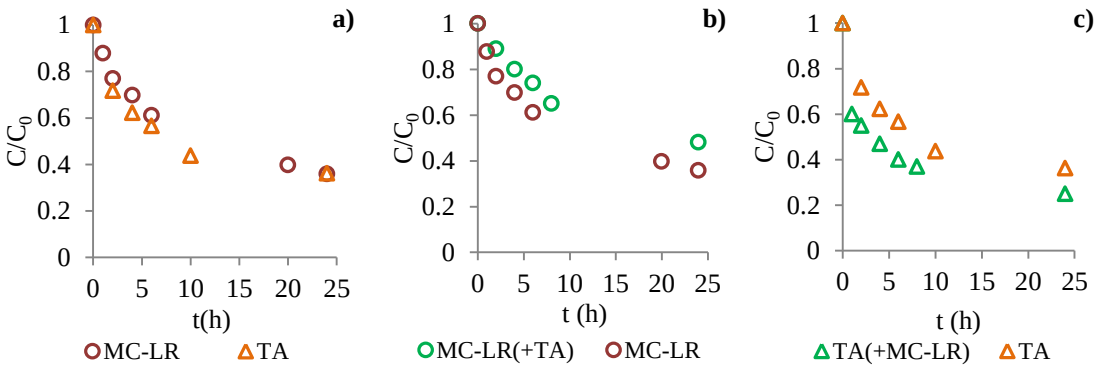

Figure 4.33. Single-solute adsorption kinetics of MC-LR and TA (a), Competitive adsorption kinetics of MC-LR in the presence of TA (b), and competitive adsorption kinetics of TA in the presence of MC-LR (c) onto NOR 125-180.

Visibly, direct competition can only occur when the competing compounds are able to access the same sites. This situation will arise when the compounds are of the same size and compete for the same pores, or when the target compound adsorbs in a larger pore (with lower adsorption energy) and the larger competing compound (with a higher adsorption energy) is able to displace it (Newcombe et al., 2002). As suggested by Kilduff et al., (1998), direct competition and pore blockage become indistinguishable as the competing and target compounds become closer in size.

4.4.2. Competitive adsorption between MC-LR and TA onto NOR 63-90

Figure 4.34 presents the competitive adsorption isotherms of extract of MC-LR (42 µg/L in 2.5 mM IS (1 mM IS KCl + 1.5 mM IS $CaCl_2$) background electrolyte) and tannic acid (5 mg TA/L) onto NOR 63-90. The experimental conditions were detailed in section 3.7.8.
For easier analysis of the effect of TA competition, previous data relative to NOR 63-90 adsorption of MC-LR from 2.5 mM electrolyte (single solute isotherm, Figure 4.10) are also shown in Figure 4.34.

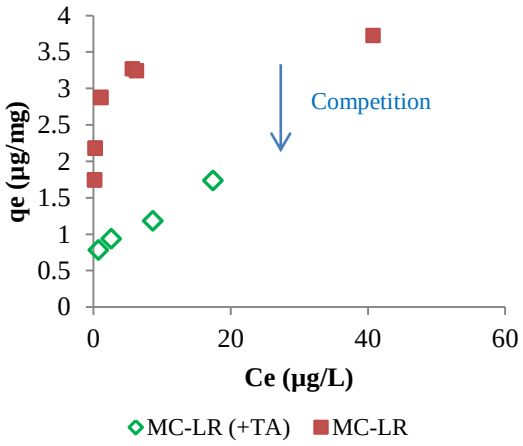

Figure 4.34. Competitive and single-solute adsorption isotherms of MC-LR onto NOR 63-90 carbon from electrolyte solution.

Figure 4.34 suggests that for NOR 63-90 the same type of direct competition occurs, but this isotherm show a decreasing on adsorption, but not as notorious for NOR 125-180.

For comparison purposes with NOR 125-180, isotherms were both represented on the same graph (Figure 4.35).

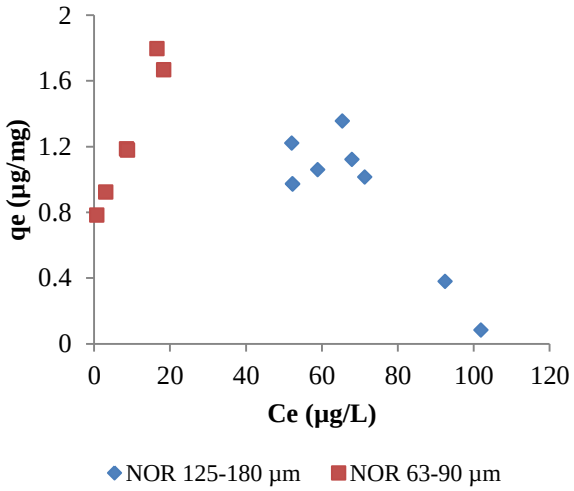

Figure 4.35. Comparison between NOR 125-180 and NOR 63-90 carbons in the adsorption of MC-LR in the competitive adsorption between MC-LR and TA.

As can be observed and expected, NOR 63-90 has a higher adsorption capacity than NOR 125-180, even in competitive adsorption.

4.4.3. Competitive adsorption between MC-LR and TA onto modified NOR 125-180

Figure 4.36 presents the competitive adsorption isotherms of extract of MC-LR (90 µg/L in 2.5 mM IS (1 mM IS KCl + 1.5 mM IS $CaCl_2$) background electrolyte) and tannic acid (5 mg TA/L) onto modified NOR 125-180. The experimental conditions were detailed in section 3.7.8. For easier analysis of the effect of TA competition, previous data relative to modified NOR 125-180 adsorption of MC-LR from 2.5 mM electrolyte (single solute isotherm, Figure 4.14) are also shown in Figure 4.36.

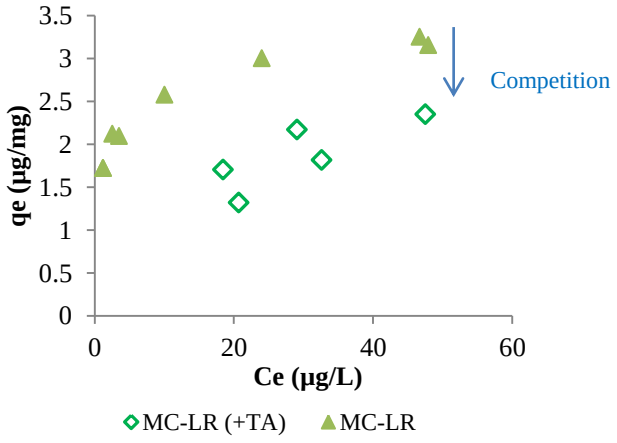

Figure 4.36. Competitive and single solute adsorption isotherms of MC-LR onto modified NOR 125-180 carbon.

Again, for comparison purposes with NOR 125-180 isotherms were both represented on the same graph (Figure 4.37). When in presence of TA, equilibrium capacity decreases.

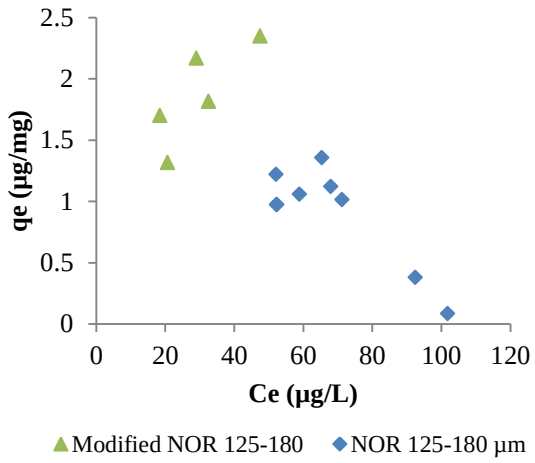

Figure 4.37. Comparison between NOR 125-180 and modified NOR 125-180 carbons in adsorption of MC-LR in the competitive adsorption between MC-LR and TA.

As can be observed and expected once more, modified NOR 125-180 has a higher adsorption capacity than NOR 125-180, even in competitive adsorption.

Kinetic tests were then performed and are shown in Figure 4.38.

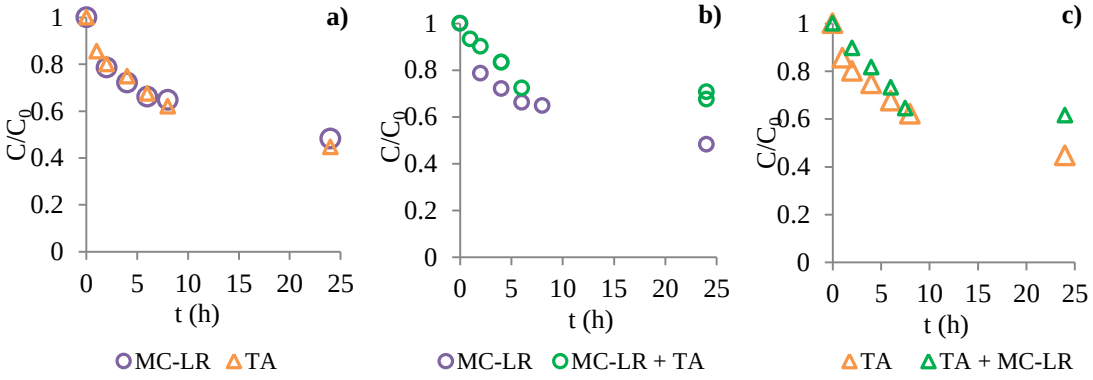

Figure 4.38. Single solute adsorption kinetics of MC-LR and TA (a), Competitive adsorption kinetics of MC-LR in the presence of TA (b), and competitive adsorption kinetics of TA in the presence of MC-LR (c) onto modified NOR 125-180 µm.

Single-solute adsorption kinetics of MC-LR and TA (Figure 4.38a) are very similar. When in competition, although a reducing AC capacity for MC-LR and for TA had previously observed, they have similar kinetics, so direct competition seems to be the dominant effect.

4.5. COMPETITIVE ADSORPTION BETWEEN MC-LR AND TA ONTO PRELOADED NOR 125-180

4.5.1. General

Adsorption isotherms with preloaded NOR 125-180 were performed to evaluate the competitive adsorption of MC-LR in the presence of background NOM on preloaded carbon. For that purpose, the NOM surrogate TA dissolved in an inorganic background matrix approaching that of soft-moderately hard natural water (2.5 mM IS (1 mM IS KCl + 1.5 mM IS $CaCl_2$)) was investigated. The organic matrix (TA) concentration was always 50 times higher compared to MC-LR initial concentration. The conditions were detailed in sections 3.2.4 and 3.7.8.
Preloading carbon with tannic acid was carried out during 20 days until all activated carbon is saturated.

4.5.2. Adsorption of MC-LR onto TA-preloaded NOR 125-180 carbon

The adsorption isotherm of extract of MC-LR (96 µg/L) in electrolyte solution (2.5 mM IS (1 mM IS KCl + 1.5 mM IS $CaCl_2$)) onto TA-preloaded NOR 125-180 is depicted in Figure 4.39.

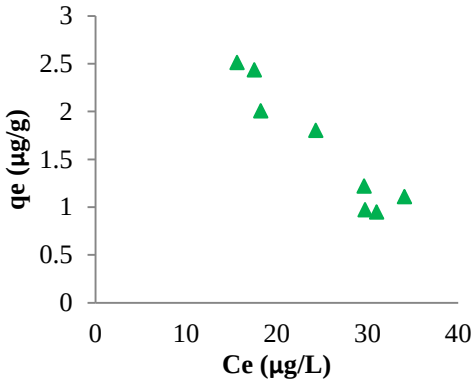

Figure 4.39. Single solute adsorption isotherm of MC-LR onto TA-preloaded NOR 125-180.

Similarly to competitive adsorption of MC-LR onto NOR 125-180 in the presence of TA, the adsorption isotherm of MC-LR onto TA-preloaded NOR carbon presents a negative slope and consequently the Freundlich and Langmuir models do not fit the experimental data.

As discussed earlier in section 4.4, the negative slope of the competitive adsorption isotherms of MC-LR onto both NOR 125-180 (G1 and PL) is indicative of a very strong direct site competition between TA and MC-LR (Pelekani and Snoeyink, 2000).

With preloading, the surface of the activated carbon can become more polar. This change may also alter the microcystin removal mechanism (Lambert et al.,1996).

Desorption, however, is generally "activated". Most small compounds might be expected to adsorb and desorb, practically instantaneously at the microscale (Pignatello and Xing, 1996).

Carter et al., (1992) studied the effect of preloading of NOM on the adsorption of trichloroethylene (TCE). Association between MC-LR and TA (micropollutant and NOM) molecules possibly will decrease adsorption (Carter et al., 1992).

Figure 4.40 shows a comparison between single solute isotherms of MC-LR onto NOR 125-180 and TA-preloaded NOR 125-180.

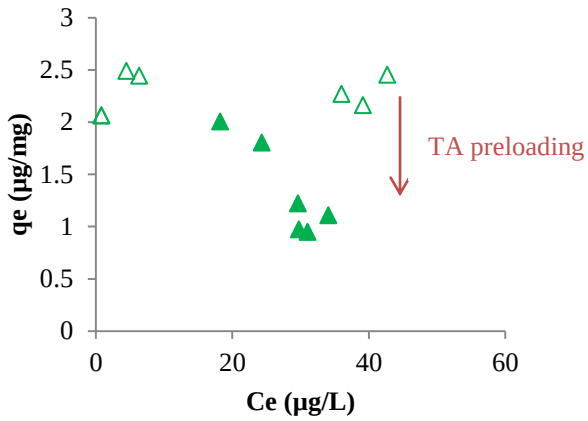

Figure 4.40. Single solute adsorption of MC-LR onto NOR 125-180 (Δ) and TA-preloaded NOR 125-180 (▲).

It is clearly in Figure 4.40, the effect of preloading NOR 125-180. AC capacity for MC-LR adsorption decreases, and it seems correlated with desorption phenomenon (negative slope of isotherm). Pores were already taken by TA, as it can be seen in Table 4.3 (preloaded NOR characterization).

Pore blockage and direct site competition are generally considered the most likely mechanisms affecting activated carbon adsorption in the presence of NOM (Newcombe et al., 2002). Using the data from a suite of preload and simultaneous adsorption experiments, Pelekani and Snoeyink (1999) concluded that the competitive mechanism depends strongly on the pore size distribution of the carbon, as well as the relative sizes of the target and competing compounds. They found that a wider pore size distribution in the adsorbent resulted in less pore blockage and consequently less evidence of competition.

The comparison between single solute adsorption kinetics of MC-LR onto NOR 125-180 and TA-preloaded NOR 125-180 is presented in Figure 4.41.

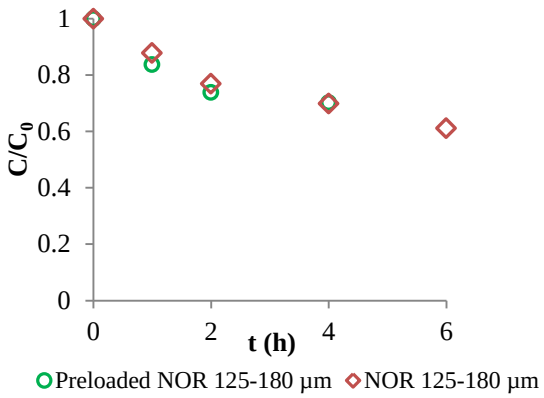

Figure 4.41. Single solute adsorption kinetics of MC-LR onto NOR 125-180 and TA-preloaded NOR 125-180.

As can be seen in Figure 4.41, when in TA-preloaded NOR 125-180, although a reducing AC capacity for MC-LR and for TA had been previously observed in Figure 4.40, they have similar kinetics, so direct competition seems to be the dominant effect also in preloaded AC.

4.5.3. Competitive adsorption between MC-LR and TA onto TA-preloaded NOR 125-180

The adsorption isotherms of MC-LR (extract) in 2.5mM IS (1 mM IS KCl + 1.5 mM IS $CaCl_2$) electrolyte with TA onto TA-preloaded NOR 125-180 are depicted in Figure 4.42. For comparison purposes, analogous data found with NOR 125-180 (originally presented in Figure 4.32) are also shown.

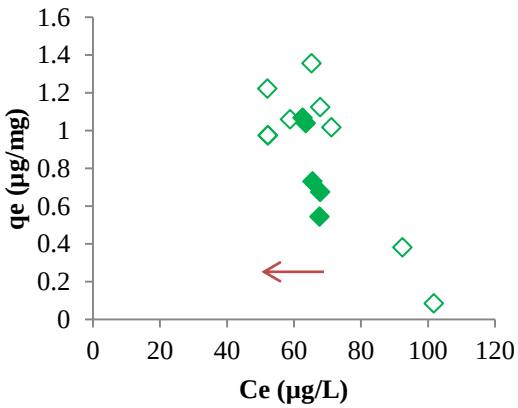

Figure 4.42. Competitive adsorption of MC-LR onto NOR 125-180 (◊) and TA-preloaded NOR 125-180 (♦) carbons.

The presence of NOM reduce significantly the efficiency of activated carbon, by competing with target MC-LR for adsorption sites, and thus reducing MC-LR uptake and rate of adsorption. It has been showed that the preloading phenomenon can significantly reduce the performance of activated carbon adsorption (Kilduff and Karanfil, 2002).

Both isotherms present a negative slope, which is indicative of a strong competition. The apparent displacement to the left of the curve with TA-preloaded NOR 125-180 means that the capacity of the AC decreased.

As can be observed, and as expected, the preloading of the carbon reduces its capacity to adsorb MC-LR.

5. CONCLUSIONS AND FUTURE DEVELOPMENTS

5.1. CONCLUSIONS

Cyanobacteria are common participants of the freshwater phytoplankton community in surface waters. They are of concern in drinking water because of their ability to produce toxins - cyanotoxins, tastes and odors which can significantly impair water quality. Excessive growth of cyanobacteria (blue-green algae) in drinking water reservoirs is an increasingly common problem associated with eutrophication. This poses an additional problem to our water treatment plants to the already challenge of converting water from various sources to good quality drinking water.

The presence of this risk posing cyanotoxins in surface waters used for drinking water production led several countries to develop specific guidelines and regulations for drinking water, including Portugal (DL 306/2007), motivating research into helpful water treatments addressing the removal of these pollutants.

It is possible that the treatment process may cause lysis and release the intracellular metabolites comprising toxins and taste and odor compounds. The present work aimed to understand the phenomena responsible for the activated carbon adsorption in removing the most frequently occurring cyanotoxins - microcystin-LR (MC-LR) from drinking water, by investigating the effects of activated surface chemistry and structure as well as the water background matrix making the main objective to study the key properties of activated carbon (trying to reveal which has more importance: the structure of AC or its surface chemistry) on the adsorption of MC-LR in drinking water treatment.

For MC-LR adsorption it is important to consider that first MC-LR is a large molecule (larger than most microcontaminants studied), and second that it is a complex aggregate of amino acids rendering hydrophobic character to its aqueous solution properties. Consequently, the correct selection of an AC for MC-LR removal from an aqueous solution, prior to any adsorption measurements, requires an appreciation of its properties combined with a detailed knowledge of the adsorbent's physical and chemical properties. Recent studies indicate that not only the mesoporosity of an AC is important, but also its surface chemistry (Costa, 2010). This question and consequently, this thesis arise with the problematic suggested by Costa, 2010.
For this purpose, this general objective comprehends:

- Modify activated carbon (NOR 0.8 SUPRA) in order to modify its surface chemistry: reducing the oxygen content making it more basic;

- Studying mechanisms of competitive adsorption with natural organic matter with similar characteristics to those of MC-LR (tannic acid) in waters with similar characteristics of those of "blooms" occur, soft natural water (2.5 mM IS electrolyte: 1 mM KCl + 1.5 mM $CaCl_2$);
- Tests with TA-preloaded activated carbon, as well as its textural characterization, in order to study the predominant effects of competition (pore blocking or direct competition);
- Non-linear modeling of kinetic and isotherm adsorption models.

To achieve these goals, a methodology was developed to evaluate activated carbon performance concerning the adsorption capacity for microcystin. The methodology included:

- **Carbon selection** (based on literature review);

- **Treatment of the studied activated carbon including:**
  - Carbon preparation: Grinding (two different particle sizes: 125-180 μm and 63-90 μm with the aim of studying the adsorption kinetics), sieving and washing the selected activated carbon;
  - Carbon modification: modification of the surface chemistry making it more basic (decreasing oxygen content);
  - Carbon preloading with tannic acid, a NOM surrogate with similar characteristics (similar size, charge and hydrophobicity), i.e. a strong competitor with MC-LR.

- **Chemical** (elemental analysis, ash content, surface charge by carbon titration) **and textural** (porous structure and distribution) **characterization of the studied carbons** (virgin: two particle sizes, modified and after TA-preloading);

- **Batch adsorption tests – kinetic and isotherm** experiments and respective evaluation with kinetic and isotherm models, to study the influence of the structure and surface chemistry of activated carbon on the adsorption of microcystins, and on its competitive adsorption in the presence of NOM, in controlled conditions of temperature, pH and ionic strength (soft natural water: 2.5 mM IS electrolyte – 1 mM IS KCl + 1.5 mM $CaCl_2$).

- **Non-linear models** for kinetic and isotherm adsorption modeling were used due to its better fit and lower associated errors.

The main conclusions regarding the objectives and subsequent research work are sequentially presented below.

The selection of the activated carbons used in this study was based on a literature review on microcystin adsorption. This study evaluated the MC-LR removal from water using commercial NORIT 0.8 SUPRA milled GAC. A large number of activated carbons are available in the market, but its evaluation in full-scale is relatively expensive and, with cyanotoxins it is an impossible mission, since these toxins are commercially very expensive.

The literature review indicated the peat based NORIT 0.8 SUPRA (NOR) granular carbon to be very effective for MC-LR removal. For NOR carbon, two different carbon sizes were tested, 125-180 μm (G1) and 63-90 μm (G2). The surface chemistry of carbon NOR 125-180 was modified by careful thermal treatment in order to obtain different surface properties. This AC (NOR 125-180) was also preloaded with tannic acid.

These activated carbons were characterized in terms of the key properties for toxin adsorption, i.e. surface chemistry and porous structure (textural characterization).

The chemical characterization revealed that the studied activated carbons are basic in nature (since the point of zero charge was always above seven), in the order NOR 125-180 = NOR 63-90 (pH_{pzc} 9.1) < modified NOR 125-180 (pH_{pzc} 12.1). The pH of the studied solutions ranged from five to seven, meaning that all carbons were carrying a net positive charge. In addition, the heteroatom content was also determined, since surface chemistry of activated carbons mainly depends on their surface oxygen content. As expected, crushing the AC to obtain a smaller particle size does not affect its pH_{pzc}.

The oxygen content of NOR 125-180 was mainly attributed to carbonyl and lactone groups and to carboxylic and phenolic groups.

The AC textural characterization indicated similarity in the pore size distribution of these carbons, composed mostly of mesopores and macropores (BJH volume), but also composed by a significant number of micropores.

The AC was also modified by heat treatment (changing its porous structure and increasing the volume of micro and mesopores). From the data, among the three studied carbons, modified NOR 125-180 has the highest surface area and the highest BJH adsorption cumulative pore volume, i.e., has the largest number of mesopores and macropores.

The preloaded AC was analyzed for surface area and pore volume distribution remaining after preloading with TA. When loading NOR 125-180, the pores congest, making it less porous and

consequently all pore volumes and surface areas show a decrease when compared with NOR125-180.

The BJH volume of these carbons correlated well with the carbon adsorption capacity for MC-LR adsorption, suggesting the importance of these pores in the adsorption of MC-LR. In addition, a major finding was the great correlation obtained between the amount of MC-LR adsorbed at equilibrium (q_{max} Langmuir parameter) and the oxygen content of the activated carbons.

The carbon characterization and its correlation to MC-LR adsorption showed that the surface chemistry of the carbons has a better influence on MC-LR adsorption than the carbon's porous structure usually referred in the literature as the dominant carbon property. However, we cannot say that a property is more important than another, because when changed the surface chemistry, porous structure also changed. To be able to say which of the two properties would have more importance, we should have considered separate variables, i.e., maintaining the porous structure constant and only changing the surface chemistry of AC or vice versa.

All experiments were made with an inorganic background matrix approaching that of soft-moderately hard natural water (2.5 mM). The impact of the water background matrix in terms of natural organic matter (NOM) content was assessed through kinetic and isotherm tests with model water (the NOM surrogate tannic acid dissolved in electrolyte solution with 2.5 mM) which allowed the evaluation of the carbons' performance.

An integrated analysis of kinetic and isotherm studies (based on Freundlich and Langmuir models) was used to investigate the effects of carbon physical and chemical properties on MC-LR adsorption, as well as the competitive adsorption of the MC-LR and NOM, both in simultaneous competition or in preloaded carbon conditions.

The MC-LR adsorption kinetics onto the activated carbons was studied using three kinetic models: pseudo-first order, pseud-second order and intraparticle diffusion models. The MC-LR adsorption from electrolyte solution is best described by the pseudo-second order model for all the studied forms of NOR 0.8. The TA adsorption onto the activated carbons was also studied using the same models, but TA adsorption is best described by the intraparticle diffusion model.

Another issue investigated was the influence of the natural organic matter with the same characteristics of MC-LR (TA) on the adsorption of MC-LR onto activated carbon. The results found for the studied carbons revealed a reduced MC-LR adsorption, as expected.

The competition mechanisms between the water background NOM and MC-LR were studied in detail. The results showed that similar sized NOM (represented by TA) strongly competes with MC-LR by direct site competition (isotherms with negative slope for NOR 125-180 were observed). The integrated analysis of adsorption kinetics and isotherms indicated that MC-LR adsorption is mostly influenced by a direct site competition mechanism with NOM, while the kinetic were not significantly affected.

In summary, the following important conclusions can be taken for the adsorption of MC-LR onto activated carbon:

- The surface chemistry of activated carbons is very important on their adsorption capacity for MC-LR, since a good correlation between adsorption capacity and surface oxygen content (inversely related to carbon hydrophobicity) was determined;

- The porous structure of activated carbons is not as important as surface chemistry in the MC-LR adsorption, although some correlation was found between the adsorption capacity and BJH (meso and macropore) volume;

- Modified NOR 125-180 was found to be more efficient on MC-LR removal, due to its high basicity (less oxygen content when compared with the other studied ACs) but also given its higher surface area and larger number of mesopores;

- From the results, the heating method used in this work is an efficient and simple process for reducing a relatively hydrophilic activated carbon and thereby enhancing the MC-LR adsorption capacity of the carbon;

- Crushing the carbon into a size range of 63-90 μm in addition to reducing the diffusional path contributed to pore opening facility the adsorption and consequently causing the faster adsorption of microcystin-LR. Furthermore, NOR 63-90 also shows to have higher adsorption capacity when compared with NOR 125-180. Apparently, the surface created by crushing NOR 125-180 causes an increase in the capacity of NOR 63-90 carbon;

- The intraparticle diffusion model showed that the smaller the particle size (i.e. for NOR 63-90), the greater is the importance of external mass transfer over intraparticle diffusion;

- Chemisorption was the adsorption mechanism for MC-LR adsorption for all the studied carbons, as expressed by the best fitting being the pseudo-second order kinetic model and for the Langmuir isotherm model, with the intraparticle diffusion being the rate-limiting step;

- NOR carbon, in all three forms (doses ranging from 12.5 to 50 mg/L) achieved very high removal efficiencies of microcystins (> 90%), ensuring the agreement with the Portuguese and the WHO drinking water guideline value for MC-LR (1 µg/L);

- Even in competition, modified NOR 125-180 and NOR 63-90 showed a better adsorption capacity for MC-LR removal;

- It has been shown that the preloading phenomenon can significantly reduce the performance of activated carbon adsorption. Since the quantification of TA in solution after the preloading was not performed, it was not possible to quantify it's desorption.

Table 5.1. Summary of removal percentage in the adsorption of MC-LR and TA onto the studied AC's.

AC	Single solute		Competition	
	MC-LR C_0= 85 -104 µg/L	**TA** C_0=5 mg/L	**MC-LR** C_0= 42-90 µg/L	**TA** C_0=5 mg/L
NOR 125-180 µm	> 90%	80%	48%	70%
NOR 63-90 µm	> 90%	90%	> 90%	> 90%
Modified NOR 125-180 µm	> 90%	80%	90%	85%
Preloaded NOR 125-180 µm	60%	50%	30%	80%

Considering these results, it is believed that the methodology developed in this work contributed to understand the phenomena responsible for activated carbon adsorption of MC-LR from drinking water. Also, it may be successfully used for studying other pollutants. The adequate choice of the activated carbon is an important factor to improve adsorption of microcontaminants and may also be evaluated with the proposed methodology. The main conclusion to be drawn is that although the two key properties to consider when choosing a carbon (structure and surface chemistry) are complementary, surface chemistry showed a better relationship with the amount adsorbed. Therefore, it is implicit that a fast, inexpensive and efficient way to enhance the rate of MC-LR removal is to modify the commercial activated carbon, making it more basic and/or more porous. Furthermore, crushing the carbon also demonstrated to be an effective form to improve MC-LR adsorption. From a combination of a careful modification of a carbon's surface chemistry and the carbon's structure, it is demonstrate that both properties play an important role in the adsorption process. Analyzing these results it

is appropriated to suggest that, although porous structure (mesoporosity) is a necessary condition (size exclusion) for MC-LR adsorption, the surface chemistry is very important property (more for MC-LR adsorption than for TA adsorption).

5.2. FUTURE DEVELOPMENTS

The research work presented in this dissertation contributed to an advance in the state of the art concerning the MC-LR removal from drinking water with activated carbon, although there are still some aspects that require additional investigation.

To be able to conclude what property has more influence in the choice of an activated carbon and to gain a better understanding of the influence of these properties to MC-LR adsorption, it is necessary to study which of the two properties would have more importance as two separable variables. Therefore, the development of a method that includes modification of a commercial AC, maintaining a constant property and studying separately the two would give more precise insight.

Complementary research for study the effect of AOM in adsorption of MC-LR onto activated carbon was also an interesting development.

The computer modeling of the kinetics of adsorption using the homogeneous surface diffusion model (HSDM) would be useful to predict the dosages of AC to use in full scale systems. It is interesting to explore this model, since it is already widely used for the prediction of adsorption kinetics of a range of microcontaminants and taste and odor compounds.

6. REFERENCES

Aksu, Z., and E. Kabasakal. "Adsorption characteristics of 2,4-dichlorophenoxyacetic acid (2,4-D) from aqueous solution on powdered activated carbon." *Journal of Environmental Science and Health Part B*, 2005: 545-570.

Antoniou, Maria G., Armah A. de la Cruz Cruz, and Dionysios D. Dionysiou. "Cyanotoxins: New generation of Water Contaminants." *Journal of Environmental Engineering*, 2005: 1239-1243.

Arnette, Verna J. "Cyanotoxin Removal in Drinking Water Treatment Processes." Master of Science Thesis in the department of Civil and Environmental Engineering of College of Engineering, Ohio Northern University, 2009.

Badmus, M., T. Audu, and B. Anyata. "Removal of lead ion from industrial wastewaters by activated carbon prepared from periwinkle shells (Typanotonus fuscatus)." *Turkish Journal Engineering Environmental Science*, 2007: 251-263.

Bansal, R., and T. Dhami. "Studies on adsorption from binary solutions-I: Adsorption on carbons from methanol-benzene solutions." *Carbon* 15 (1977): 153-156.

Bjelopavlic, M., G. Newcombe, and R. Hayes. "Adsorption of NOM onto activated carbon: effect of surface charge, ionic strenght, and pore volume distribution." *Journal of Colloid and Interface Science* 210 (1999): 271-280.

Boehm, H. P. "Some aspects of the surface chemistry of carbon blacks and other carbon." *Carbon*, 1994: 759-769.

Boyd, G., A. Adamson, and L. Myers. "The exchange adsorption of ions from aqueous solutions by organic zeolites. II Kinetics." *Journal of American Chemical Society* 69 (1947): 2836-2844.

Burch, M.D. "Chapter 36 - Effective doses, guidelines & regulations. In: Proceedings of the Interagency, International Symposium on Cyanobacterial Harmful Algal Blooms." *Advances in Experimental Medicine and Biology* (H.Kenneth Hudnell), 2007: 843-865.

Campinas, M. "Removal of cyanobacteria and cyanotoxins from drinking by powdered activated carbon adsorption/ultrafiltration." PhD , 2009.

Campinas, M., and M.J. Rosa. "The ionic strength effect on microcystin and natural organic matter surrogate adsorption onto PAC." *Journal of Colloid and Interface Science* 299 (2006): 520-529.

Carmichael, W.W. "Chapter 4 - A world overview - One-hundred-twenty-seven years of research on toxic cyanobacteria - where do we go from here? In: Proceedings of the Interagency, International Symposium on Cyanobacterial Harmful Algal Blooms." *Advances in Experimental Medicine and Biology* (H. Kenneth Hudnell), 2007.

Carmichael, W.W. "Cyanobacteria secondary metabolites: the cyanotoxins." *Journal of Applied Microbiology* 72 (1992): 445-459.

Carmichael, W.W. "The toxins of cyanobacteria." *Science Am.* 270 (2005): 78-86.

Carter, M.C., W.J. Weber, and K. P. Olmstead. "Effects of background dissolved organic matter on TCE adsorption by GAC." *J. Amer. Water Works Association* 84 (1992): 81-91.

Cecílio, T., E. Mesquita, H. Costa, and M.J. Rosa. "Processos Avançados de tratamento de água para consumo humano." *Águas & Resíduos*, 2007: 4-17.

Choy, K.K.H., and J.F., McKay, G. Porter. "Intraparticle diffusion in single and multi-component acid dye adsorption from wastewater onto carbon." *Chemical Engineering Journal*, 2004: 133-145.

Clark, R. M., and B. W. Lykins. *Granular Activated Carbon - Design, Operation and Cost.* Lewis Publishers, 1989.

Considine, R., R. Denoyel, P. Pendleton, R. Schumann, and S. Wong. "The influence of surface chemistry on activated carbon adsorption of 2-methylisoborneol from aqueous solution." *Colloids and Surfaces A: Physicochemical and Engineering aspects* 179 (2001): 271-280.

Considine, R., R. Denoyel, P. Pendleton, R. Schumann, and S. Wong. "The influence of surface chemistry on activated carbon adsorption of 2-methylsoborneol from aqueous solution." *Colloids and Surfaces* 179 (2001): 271-280.

Costa, H. "Activated carbon adsorption of cyanotoxins from natural waters." Ph.D. Thesis in Environmental Sciences and Technologies, Algarve University, Faro, 2010.

Dawson, R. M. "The toxicology of microcystins." *Toxicon* 36 (1998): 953-962.

documentation, Guidelines of Canadian Driking Water Quality:Supporting. *Cyanobacterial toxins - Microcystin-LR.* Guidelines of Canadian Driking Water Quality:Supporting documentation, Federal-Provincial-Territorial Committee on Driking Water, 2002.

Dombrowski, R. J., D. R. Hyduke, and C. M. Lastoskie. "Pore Size Analysis of Activated Carbons from Argon and Nitrogen Porosimetry Using Density Functional Theory." *Langmuir*, 2000: 5041-5050.

Donati, C., M. Drikas, R. Hayes, and G. Newcombe. "Microcystin-LR adsorption by powered activated carbon." *Water Research* 28 (1994): 1735-1742.

Drikas, M., C.W.K. Chow, J. House, and M. Burch. "Using coagulation, flocculation and settling to remove toxic cyanobacteria." *Journal AWWA*, 2001: 100-111.

Eaton, A. D., Clesceri. L. S., E. W. Rice, and A. E. Greenberg. *Standard methods for the examination of water & wastewater, 21st edition.* American Public Health Association, American Water Works Association, Water Environment Federation, 2005.

Edzwald, J. K. *Water Quality & Treatment - Handbook on Drinking Water, Sixth Edition - Chapter 14.* American Water Works Association, 1999.

Falconer, I. R. "Potential impact on human health of toxic cyanobacteria." *Phycologia* 335 (1996): 6-11.

Falconer, I., M. Runnegar, T. Buckley, V. Huyn, and P. Bradshaw. "Using activated carbon to remove toxicity from drinking water containing cyanobacterial blooms." *Journal American Water Works Association* 81 (1989): 102-105.

Figueiredo, J. L., and F. R. Ribeiro. *Catálise Heterogénea.* Lisboa: Fundação Calouste Gulbenkian, 2007.

Fonseca, I., and J. Vital. "wlherhweuhf." n.d.

Gregg, S., and K. Sing. "The physical adsorption of gases by porous solids." In *Adsorption, Surface area and porosity*, by S. Gregg and K. Sing, 121-194. London: Academic press, 1982.

Gülçin, I., H. Zübeyer, M. Elmastas, and H.Y. Aboul-Enein. "Radical scavenging and antioxidant activity of tannic acid." *Arabian Journal of Chemistry* 3 (2010): 43-53.

Himberg, K., A.M. Keijola, L. Hsvirta, H. Pyysalo, and K. Sivonen. "The effect of water treatment processes on the removal of hepatotoxins from Microcystis and Oscillatoria cyanobacteria: a laboratory study." *Water Research* 29 (1989): 979-984.

Ho, lionel, Paul Lambling, Heriberto Bustamante, Phil Duker, and Gayle Newcombe. "Application of powdered activated carbon for the adsorption of cylindrospermopsin and microcystin toxins from drinking water supplies." *Water Research*, 2011: 1-11.

Ho, Y.S., and G. McKay. "Pseudo-second order model for sorption processes." *Process Biochem* 34 (1999): 451-465.

Hrudey, S., M. Burch, M. Drikas, and R. Gregory. "Remedial Measures In: WHO - Toxic cyanobacteria in water - aguide to their public health consequences, monitoring, and management." 1999: 275-312.

Huang, W, Cheng. B., and Y. Cheng. "Adsorption of microcystin-LR by three types of activated carbon." *Journal of Hazardous Materials* 141 (2007): 115-122.

Ip, A.W.M., J.P. Barford, and G. McKay. "A comparative study on the kinetics and mechanisms of removal of Reactive Black 5 by adsorption onto activated carbons and bone char." *Chemical Engineering Journal*, 2010: 434-442.

Ip, Alvin W. M., John P. Bardford, and Gordon McKay. "A comparative study on the kinetics and mechanisms of removal of Reactive Black 5 by adsorption onto activated carbons and bone char." *Chemical Engineering Journal* 157 (2010): 434-442.

IUPAC. "Manual of symbols and terminology for physicochemical quantities and units. Appendix II - Terminology and Symbols." *Colloid and Surface Chemistry* 31 (2001).

Jain, S., and L. Snoeyink. "Adsorption from bisolut systems on active carbon." *Journal Water Pollution* , 1973: 2463-2479.

Junxiong, L., Wang, L. "Comparison between linear and non-linear forms of pseudo-first order and pseudo-second order adsorption kinetic models for the removal of methylene blue by activated carbon." *Environment Science Engineering* 3 (2009): 320-324.

Kasaini, H., G. Masahiro, and S. Furusaki. "Selective Separation of Pd(II), Rh(III), and Ru(III) ions from a mixed chloride solution using activated carbon pellets." *Separation science and technology* 35 (2000): 1307-1327.

Kilduff, J., and T. Karanfil. "Thrichloroethylene adsorption by activated carbon preloaded with humic substances: effects of solution chemistry." *Water Research* 36 (2002): 1685-1698.

Kilduff, J., T. Karanfil, and Jr.W. Weber. "Competitive effects of displaceable organic compounds on trichloroethylene uptake by activated carbon. II. Model verification and applicability to natural organic matter." *Journal of Colloid an Interface Science* 205 (1998): 280-289.

Kuiper-Goodman, Falconer, I., and J. Fitzgerald. "Toxic cyanobacteria in water - A guide to their public health consequences, monitoring and management." *E&FN Spon, WHO*, 1999: 113.

Kumar, K., V. Ramamurthi, and S. Sivanesen. "Modeling the mechanism involved during the sorption of methylene blue onto fly ash." *Journal of Colloid and Interface Science*, 2005: 14-21.

Lagergreen, S. "Zur theorie der sogenannten adsorption geloster stoffe." *Kungliga Sevenska Vetenskapsakademiens, Handlingar*, 1898: 1-39.

Lambert, T. W., C. F. B. Holmes, and S. E. Hrudey. "Adsorption of microcystin-LR by activated carbon and removal in full scale water treatment." *Water Research* 30 (1996): 1411-1422.

Lambert, T., C. Holmes, and S. Hrudrey. "Adsorption of microcystin-LR by activated carbon and removal in full scale water treatment." *Water Research* 30 (1996): 1411-1422.

Lambert, T.W., C.F.B. Holmes, and S.E. Hrudrey. "Microcystin class of toxins: health effects and safety of drinking water supplies." *Environmental Rev.* 2 (1994): 167-186.

Li, Lei, Patricia A. Quinlivan, and Detlef R.U. Knappe. "Effects of activated carbon surface chemistry and pore structure on the adsorption of organic contaminants from aqueous solution." *Carbon* 40 (2002): 2085-2100.

Lyubchik, Svetlana B., et al. "Simultaneous removal of 3d transition metals from multi-component solutions by activated carbons from co-mingled wastes." *Separation and Purification Technology* 60 (2008): 264–271.

Mara, Duncan, and Nigel Horan. *Handbook of Water and Wastewater Microbiology*. Academic Press, 2003.

Matsui, Y., Y. Fukuda, Inoue T., and T. Matsushita. "Effect of natural organic matter on powdered activated carbon adsorption of trace contaminants: characteristics and mechanism of competitive adsorption." *Water Research* 37 (2003): 4413-4424.

Menaia, José, and Maria João Rosa. *Cianobactérias e água para abastecimento público.* Carvoeiro: Florescências de algas e cianobactérias nas águas de captação - Curso AdP/LNEC, 2006.

Meriluoto, J., and L. Spoof. "Analysis of microcystins by high-performance liquid chromatography with photodiode array detection." *TOXIC*, 2003.

Meriluoto, J., and L. Spoof. "Preparation of standard solutions of microcystin-LR for HPLC calibration." *TOXIC*, 2003.

Meriluoto, J., and L. Spoof. "SOP: Solid Phase extraction of microcystins in water samples." *TOXIC Cyanobacterial Monitoring and Cyanotoxin Analysis*, 2005.

Mesquita, E., J. Menaia, M. J. Rosa, and V. Costa. "Microcystin-LR removal by bench-scale biologically activated carbon filters." *recent Progress in Slow Sand Alternative Biofiltration Processes*, 2006.

Mesquita, Elsa Alexandra Coutinho. "Remoção de cianotoxinas da água para consumo humano em filtros de carvão activado com actividade biológica." 2011.

Metcalf, and Eddy. *Wastewater Engineering - Treatment and Reuse.* McGraw-Hill Higher Education, 2003.

Moreno-Castilla, C.., M. V. López-Ramón, and F. Carrasco-Marín. "Changes in surface chemistry of activated carbons by wet oxidation." *Carbon* 38 (2000): 1995-2001.

Muhlpford, H. "The preparation of colloidal gold particles using TA as an additional reducing agent." *Experientia* 38 (1982).

Newcombe, G., and B. Nicholson. "Water treatment options for dissolved cyanotoxins." *Cyanobacteria - Management and implications for water quality*, 2004: 227-239.

Newcombe, G., and D. Cook. "Removal of natural microcontaminants from drinking water using activated carbon." *Encyclopedia of Surface and Colloid Science* , 2004.

Newcombe, G., and M. Drikas. "Adsorption of NOM onto activated carbon: electroestatic and non-electroestatic effects." *Carbon*, 1997: 1239-1250.

Newcombe, G., D. Cook, S. Brooke, L. Ho, and N. Slyman. "Treatment options for microcystin toxins: similarities and differences between variants." *Environmental Technology* 24 (2003): 299-308.

Newcombe, G., J. Morrison, C. Hepplewhite, and D.R.U Knappe. "Simultaneous adsorption of MIB and NOM onto activated carbon II. Competitive effects." *Carbon* 40 (2002): 2147-2156.

Newcombe, G., M. Drikas, and R. Hayes. "Influence of Characterised natural organic material on activated carbon adsorption: II. Effect on pore volume distribution and adsorption of 2-methylisoborneol." *Water Research* 31 (1997): 1065-1073.

Newcombe, Gayle, and Brenton Nicholson. "Water treatment options for dissolved cyanotoxins." *Journal of Water Supply: Research and Technology - AQUA* 53 (2004): 27-239.

NORIT. "Datasheet." 2007.

Osswald, J. "Ocorrência de cianobactérias produtoras de Anatoxin-A e avaliação do risco para a saúde pública, em Portugal." PhD Thesis, Faculty of Sciences, University of Porto, Portugal, 2007.

Pelekani, C., and V. Soeyink. "Competitive adsorption between atrazine and methylene blue on activated carbon: the importance of pore size distribution." *Carbon* 38 (2000): 1423-1436.

Pelekani, C., and V.L. Snoeyink. "Competitive adsorption in natural water: role of activated carbon pore size." *Water Research* 33 (1999): 1209-1219.

Pendleton, P., R. Schumann, and S. Hui Wong. "Microcystin-LR Adsorption by Activated Carbon." *Journal of Colloid and Interface Science* 240 (2001): 1-8.

Pendleton, P., S. Wu, and A. Badalyan. "Activated carbon oxygen content influence on water and surfactant adsorption." *Journal of Colloid and Interface Science* 246 (2002): 235-240.

Pignatello, J., and B. Xing. "Mechanisms of Slow Sorption of Organic Chemicals to Natural Particles." *Environmental Science & Technology* 30 (1996).

Pivokonsky, M., O. Kloucek, and L. Pivonska. "Evaluation of the production, composition and aluminium and iron complexation of algogenic matter." *Water Research* 40 (2006): 3045-3052.

Premazzi, G., and L. Volterra. *Microphyte toxins - A manual for toxin detection, environmental monitoring and therapies to counteract intoxications.* Environment Institute-Joint Research Centre, 1993.

Quality, Guidelines for Canadian Drinking Water. *Cyanobacterial toxins-Microcystin-LR.* Supporting Documentation, Federal-Provincial-Territorial Committee on Driking Water, 2002.

Reichenberg, D. "Properties of ion-exchange resins in relation to their structure. III. Kinetics of exchange." *Journal of Anerican Chemical Society*, 1953: 589-597.

Ribau Teixeira, M., and M.J. Rosa. "Comparing dissolved air flotation and conventional sedimentation to remove cyanobacterial cells of Microcystis aeruginosa." *Separation and Purification Technology* 53 (2007): 126-134.

Ribau Teixeira, M., and M.J. Rosa. "Comparing dissolved air flotation and conventional sedimentation to remove cyanobacterial cells of Microcystis aeruginosa: Part I: the key operating conditions." *Separation and Purification Technology* 53 (2006): 126-134.

Rivasseau, C., S. Martins, and MC. Hennion. "Determination of some physicochemical parameters of microcystins (cyanobacterial toxins) and trace level analysis in environmental samples using liquid chromatograhy." *Journal Chromatography A.* 799 (1-2) (1998): 155-69.

Rivera-Utrilla, J., and M. Sánchez-Polo. "Ozonation of 1,3,6-naphthalenetrisulphonic acid catalysed by activated carbon in aqueous phase." *Applied Catalysis B: Environmental* 39 (2002): 319-329.

Sánchez-Polo, M., E. Salhi, J. Rivera-Utrilla, and U. von Gunten. "Combination of Ozone with Activated Carbon as an Alternative to Conventional Advanced Oxidation Processes." *Ozone: Science and Engineering* 28 (2006): 237-245.

Sing, Kenneth S. W. "Physisorption of nitrogen by porous materials." *Journal of Porous Materials* 2 (1995): 5-8.

Sivonen, K., and G. Jones. "Cyanobacterial toxins." *Toxin Cyanobacteria in Water: A guide to their Public Health Consequences, Monitoring and Management*, 1999.

Snoeyink, Vernon L., and R. Scott Summers. *Water Quality and Treatment - A handbook of community water supplies: Chapter 13 - Adsorption of organic compounds.* 5th. American Water Works Association, McGraw-Hill, Inc., 1999.

Subramanyam, B., and A. Das. "Linearized and non-linearized isotherms models comparative study on adsorption of aqueous phenol solution in soil." *International Journal Science Technology* 6 (2009): 633-640.

Summers, R. S., D. R. U. Knappe, and V. L. Snoeyink. *Chapter 14: Adsorption of organic compounds by activated carbon.* n.d.

Summers, R., and L. Cummings. "Standardized Protocol for the Evaluating of GAC." *AWWA Research Foundation and American Water Works Association*, 1992.

Sze, M. F. F., and G. McKay. "An adsorption diffusion model for removal of para-chlorophenol by activated carbon derived from bituminous coal." *Environmental Pollution* 158 (2010): 1669-1674.

Teixeira, M.R., and M.J. Rosa. "Microcystins removal by nanofiltration membranes." *Separation and Purification Technology* 46 (2005): 192-201.

Vasconcelos, V. "Eutrophication, toxic cyanobacteria and cyanotoxins: when ecosystems cry for help." *Limnetica* 25 (2006): 425-432.

Vesterkvist, P.S.M., and J.A.O. Meriluoto. "Interaction between microcystins of different hydrophobicities and lipid monolayers." *Toxicon* 41 (2003): 349-355.

Wang, S., and H. Li. "Kinetic modeling and mechanism of dye adsorption on unburned carbon." *Dyes and pigments* 72 (2007): 308-314.

WHO, World Health Organization. "Toxic Cyanobacteria in water: A guide to their public health consequences monitoring and management." *E&FN Spon, London*, 2008.

Wu, S.H., and P. Pendleton. "Adsorption of anionic surfactant by activated carbon: effect of surface chemistry, ionic strength, and hydrophobicity." *Journal of Colloid and Interface Science* 243 (2001): 306-315.

Xinhui Carbon Co., Ltd. *Technical Support: Network Technology Co., Ltd.* 2010.

Yang, X., and B. Al-Duri. "Kinetic modeling of liquid-phase adsorption of reactive dyes on activated carbon." *Journal of Colloid and Interface Science* 287 (2005): 25-34.

ANNEXES

ANNEX I. CALIBRATION CURVE FOR HPLC CALIBRATION

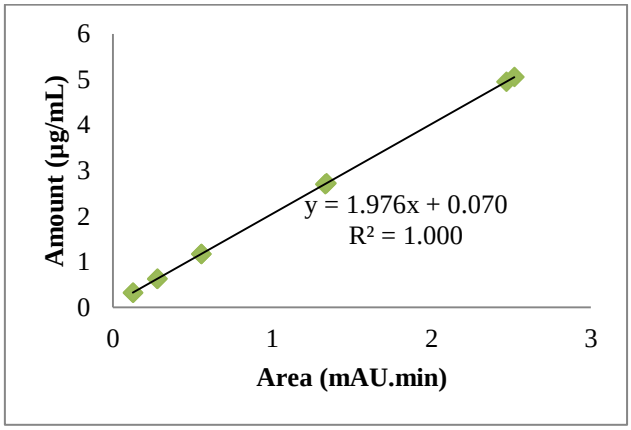

Figure AI. 1. Calibration curve between peak area and microcystin-LR concentration for HPLC calibration.

ANNEX II. QUANTIFICATION OF TANNIC ACID

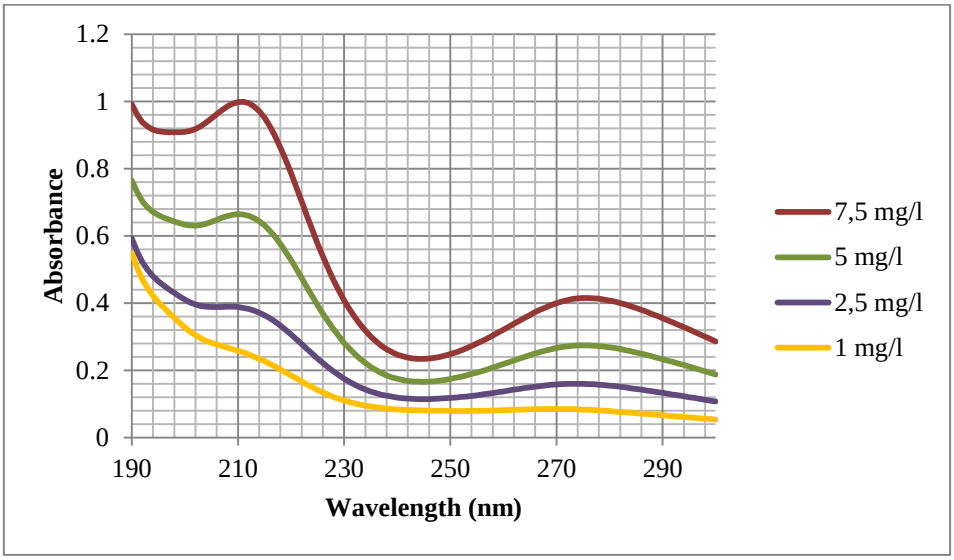

Figure AII. 1. Absorption spectra of tannic acid at 215 nm in electrolyte solution with a ionic strength of 2.5 mM.

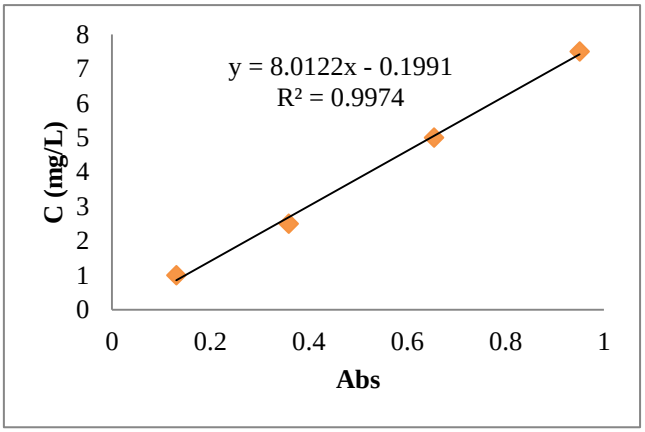

Figure AII. 2. Calibration curve between absorbance at 215 nm and tannic acid concentration for spectrophotometer calibration.

ANNEX III. PORE SIZE DISTRIBUTION OF ACTIVATED CARBONS

Porosity distribution by original Density Function Theory

Model N2 at 77 K on carbon, slit pores

Method: Non-negative regularization; No Smoothing

	NOR 125-180		
Volume in Pores	<	5.00 Å	0.00000 cm^3/g
Total volume in Pores	<=	931.26 Å	0.43021 cm^3/g
Area in Pores	>	931.26 Å	53.024 m^2/g
Total Area in Pores	>=	5.00 Å	904.371 m^2/g
	Modified NOR 125-180		
Volume in Pores	<	5.00 Å	0.00000 cm^3/g
Total volume in Pores	<=	27.34 Å	0.42836 cm^3/g
Area in Pores	>	27.34 Å	74.697 m^2/g
Total Area in Pores	>=	5.00 Å	1049.670 m^2/g
	Preloaded NOR 125-180		
Volume in Pores	<	5.00 Å	0.00000 cm^3/g
Total volume in Pores	<=	1172.33 Å	0.22036 cm^3/g
Area in Pores	>	1172.33 Å	33.956 m^2/g
Total Area in Pores	>=	5.00 Å	387.436 m^2/g

Pore size Table

NOR 125-180		**Modified NOR 125-180**		**Preloaded NOR 125-180**	
Pore Width (Å)	Incremental Pore Volume (cm^3/g)	Pore Width (Å)	Incremental Pore Volume (cm^3/g)	Pore Width (Å)	Incremental Pore Volume (cm^3/g)
5.003867552	0	5.003867552	0	5.003867552	0
5.36128664	0	5.36128664	0	5.36128664	0
5.897415219	0	5.897415219	0	5.897415219	0
6.433544011	0	6.433544011	0.102349	6.433544011	0
6.790962992	0	6.790962992	0	6.790962992	0
7.327091571	0.169387882	7.327091571	0.098469	7.327091571	0.070715
8.04192996	0.059848293	8.04192996	0.034585	8.04192996	0.019283
8.578058539	0.020322566	8.578058539	0.034461	8.578058539	0
9.292896928	0	9.292896928	0	9.292896928	0
10.00773489	0	10.00773489	0	10.00773489	0
10.90128266	0.00756421	10.90128266	0.013782	10.90128266	0
11.79483044	0.027549388	11.79483044	0.03293	11.79483044	0.026686
12.68837821	0.018230045	12.68837821	0.023835	12.68837821	0.000769
13.58192598	0.012771442	13.58192598	0.01362	13.58192598	0.0105
14.83289338	0.015204322	14.83289338	0.019201	14.83289338	0.009141
15.90515054	0.012316042	15.90515054	0.014525	15.90515054	0.005746
17.15611708	0.007096866	17.15611708	0.008619	17.15611708	0.004489
18.585793	0.005917972	18.585793	0.006723	18.585793	0.002605
20.01546978	0.003557423	20.01546978	0.005182	20.01546978	0.001393
21.6238568	0.002713214	21.6238568	0.003993	21.6238568	0.001093
23.41095234	0.00298597	23.41095234	0.004168	23.41095234	0.001616
25.19804789	0.004343335	25.19804789	0.005239	25.19804789	0.002556

27.34256221	0.005523546	27.34256221	0.006682	27.34256221	0.003554
29.48707652	0.004546279			29.48707652	0.002996
31.81030107	0.00380296			31.81030107	0.002298
34.31223586	0.003448521			34.31223586	0.002022
36.99287918	0.002076446			36.99287918	0.001439
40.03093956	0.00209902			40.03093956	0.001523
43.24771359	0.002574546			43.24771359	0.001816
46.64319445	0.002832159			46.64319445	0.002179
50.39609578	0.002722624			50.39609578	0.002191
54.32770394	0.002418896			54.32770394	0.00201
58.79544281	0.002053938			58.79544281	0.001832
63.44189191	0.001469959			63.44189191	0.001497
68.44575808	0.001269866			68.44575808	0.001419
73.98575836	0.001103459			73.98575836	0.001253
79.8831723	0.001094296			79.8831723	0.001258
86.31671354	0.001131021			86.31671354	0.001391
93.10767526	0.000817361			93.10767526	0.001136
100.6134779	0.000534778			100.6134779	0.000826
108.6554079	0.000304091			108.6554079	0.000681
117.2334651	5.34271E-05			117.2334651	0.000518
126.5263702	1.94888E-05			126.5263702	0.000497
136.7128093	0.000353411			136.7128093	0.000794
147.6140894	0.00047805			147.6140894	0.000913
159.4089173	0.000347157			159.4089173	0.000802
172.0973066	0.000407784			172.0973066	0.000788
185.8579369	0.000575049			185.8579369	0.000919
200.6908354	0.000380639			200.6908354	0.000797
216.5959748	0.000446912			216.5959748	0.00079
233.9307962	0.001006199			233.9307962	0.001288
252.5166062	0.001242078			252.5166062	0.001522
272.7107913	0.001128086			272.7107913	0.001437
294.5133516	0.000598196			294.5133516	0.00088
317.9242869	0.000325434			317.9242869	0.000576
343.3010654	0.000368871			343.3010654	0.000658
370.6436055	0.000655208			370.6436055	0.00091
400.3094025	0.001261304			400.3094025	0.001462
432.2984018	0.001371157			432.2984018	0.001495
466.7893786	0.001713355			466.7893786	0.001843
503.9609442	0.002424306			503.9609442	0.002782
544.170594	0.001732377			544.170594	0.002546
587.5969939	0.000869071			587.5969939	0.001557
634.4189191	0.000528642			634.4189191	0.00126
684.9937012	0.000293786			684.9937012	0.001431
739.6788359	0			739.6788359	0.000907
798.6529889	0			798.6529889	0.000699
862.4523218	0			862.4523218	0.00038
931.2554458	0			931.2554458	0
10000	0			1005.598686	0
				1085.660545	0
				1172.334679	0

ANNEX IV. TEXTURAL PROPERTIES OF THE ACTIVATED CARBONS

AIV.1 Volume adsorbed obtained in the t-plot report for activated carbons

NOR 125-180		Modified NOR 125-180	
P/P_0	V_{ads} (cm^3/g)	P/P_0	V_{ads} (cm^3/g)
0.000005942	20.1942	0.000005942	20.1942
0.000007601	40.3917	0.000007601	40.3917
0.000008392	60.5884	0.000008392	60.5884
0.000009862	80.7859	0.000009862	80.7859
0.000014576	100.9824	0.000014576	100.9824
0.000025865	121.1784	0.000025865	121.1784
0.000050198	141.3707	0.000050198	141.3707
0.000105004	161.5502	0.000105004	161.5502
0.000105004	181.7002	0.000246719	181.7002
0.000670459	201.7597	0.000670459	201.7597
0.001996249	221.5148	0.001996249	221.5148
0.005699602	240.4443	0.005699602	240.4443
0.014293970	257.7693	0.014293970	257.7693
0.029537125	272.4063	0.02953712	272.4063
0.050231822	283.3051	0.050231822	283.3051
0.074406731	291.4002	0.074406731	291.4002
0.103686889	298.1680	0.103686889	298.1680
0.129997255	302.8616	0.129997255	302.8616
0.157073053	306.8051	0.157073053	306.8051
0.181845568	310.2000	0.181845568	310.2002
0.205742610	313.0993	0.205742610	313.0993
0.229481009	315.8451	0.229481009	315.8451
0.253391403	318.4692	0.253391403	318.4692
0.278088403	321.0248	0.278088403	321.0248
0.302877914	323.4818	0.302877914	323.4818
0.401087964	332.2223	0.401087964	332.2223
0.499869296	340.2045	0.499869296	340.2045
0.598545679	348.3992	0.598545679	348.3992
0.699529991	357.3852	0.699529991	357.3852
0.799233024	367.4008	0.799233024	367.4008
0.859741252	374.8312	0.859741252	374.8312
0.899602408	381.4146	0.899602408	381.4146
0.924625154	387.5113	0.924625154	387.5113
0.948292009	396.6891	0.948292009	396.6891
0.971271748	412.6427		
0.986083079	431.1248		
0.888819732	397.6386		
0.800997501	386.3593		
0.696675406	377.5045		
0.606061456	370.5778		
0.502524990	362.1192		
0.405119820	333.2219		
0.296534034	323.1109		
0.200852266	312.5714		
0.104172263	298.3250		

AIV.II Determination of A_{BET}, A_{ext}, micropore volume and single point total volume for NOR 125-180

Determination of specific area using BET method

With this method, the monolayer capacity is obtained from the physical adsorption isotherm, experimentally determined. Adsorption with nitrogen at 77 K is recommended. Usually a type II or IV isotherm is obtained and the BET equation (I.1) is applied.

$$\frac{\frac{P}{P_0}}{V_{ads}\left(1-\frac{P}{P_0}\right)} = \frac{1}{n_m^a\, c} + \frac{c-1}{n_m^a\, c} \times \frac{P}{P_0} \textbf{ [I. 1]}$$

where, P and P_0 are respectively the equilibrium pressure and the pressure of saturation (at the temperature used). V_{ads} is the amount adsorbed at pressure p, n_m^a (mol/g) the amount adsorbed on the monolayer and c the is BET constant.

Plotting the BET equation, number of moles adsorbed in the monolayer (n_m^a) and the BET constant (c), through values of the slop and origin interception.

BET area (m^2/g) was determined from the following equation:

$$A_{BET} = N \times n_m^a \times a_m \textbf{ [I. 2]}$$

where N is the Avogadro number (6.02×10^{23} mol^{-1}) and a_m is the area occupied by one molecule of the absorbate (for N_2 is 16.2×10^{-20} m^2).

Determination of microporous volume (V_{micro}) and external area (A_{ext})

T-plot method was used to calculate the microporous volume and the external area of the AC, by plotting V_{ads} vs t. The intercept will give the V_{micro} and the slop the value of A_{ext}, just needing a conversion with the density factor (that for N_2 is 0.001547 = 34.7 cm^3/mol/22.4×10^3 mol.cm^3/mol).

Determination of the single point total pore volume

The total pore volume is obtained from the Gurvitsh rule as follows:

$$V_p = n_{sat}^a * V_M^t \textbf{ [I. 3]}$$

where n_{sat}^a (mol/g) is the adsorbed amount at saturation and V_M^t is the molar volume adsorbed in the liquid stage.

ANNEX V. ADSORPTION/DESORPTION ISOTHERM PLOTS

NOR 125-180

Analysis adsorptive: N2
Analysis Bath: 77.35 K

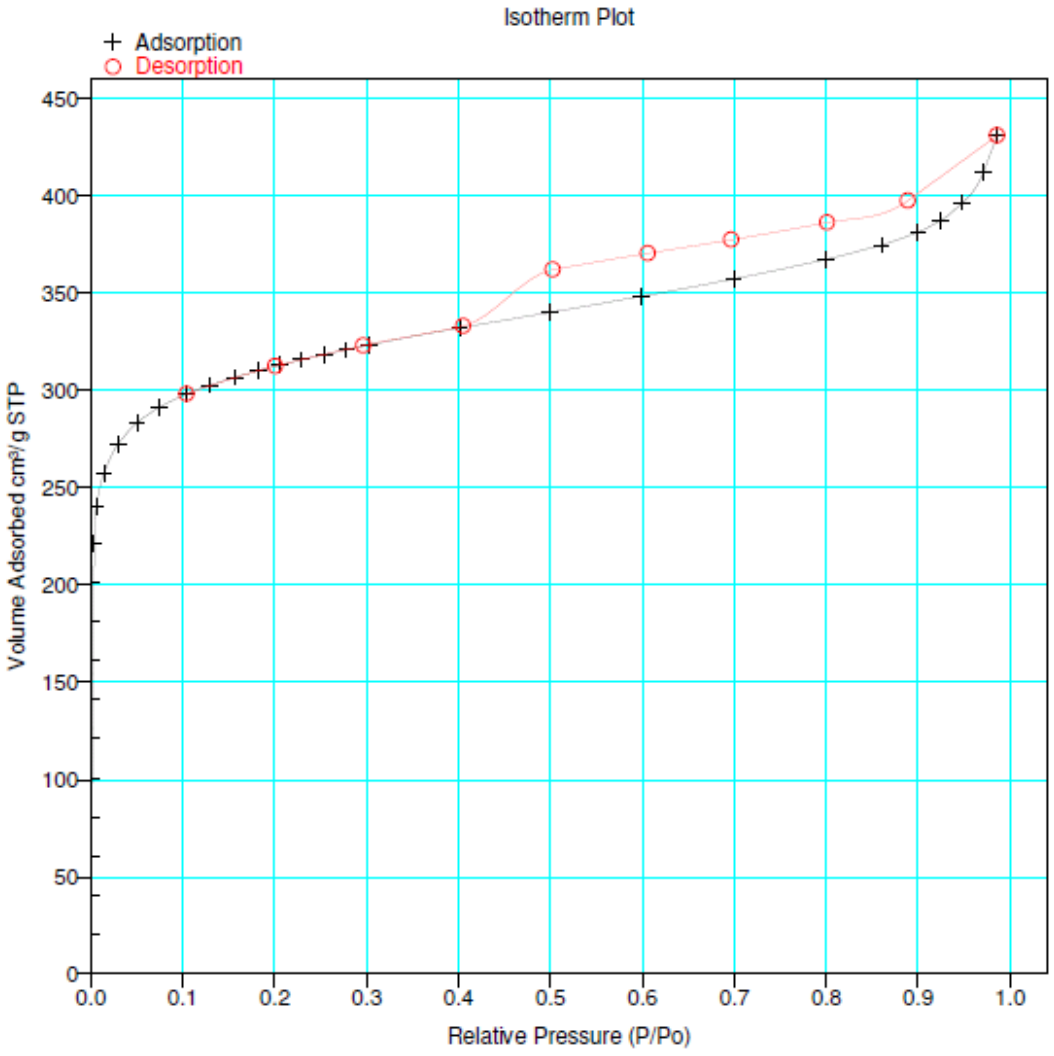

Figure AV. 1. Adsorption/desorption isotherm plots for NOR 125-180.

NOR 63-90

Analysis adsorptive: N2
Analysis Bath: 77.35 K

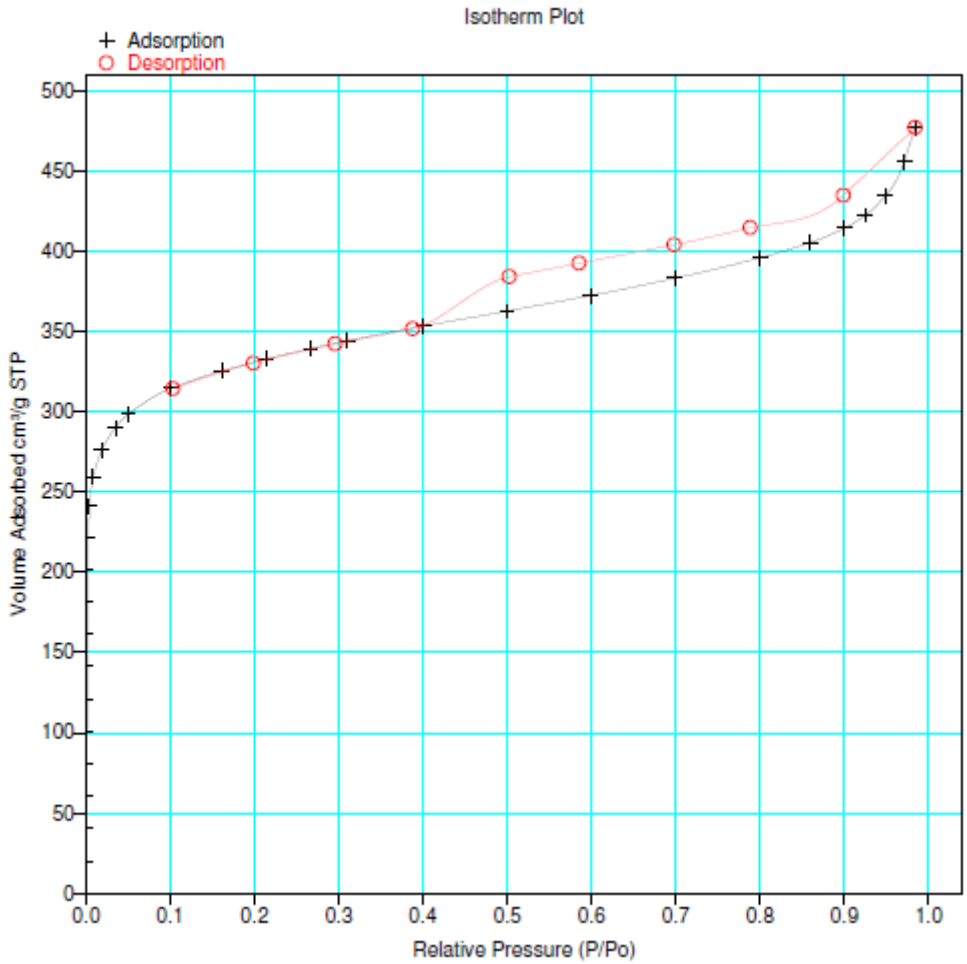

Figure AV. 2. Adsorption/desorption isotherm plots for NOR 63-90.

Modified NOR 125-180

Analysis adsorptive: N2
Analysis Bath: 77.35 K

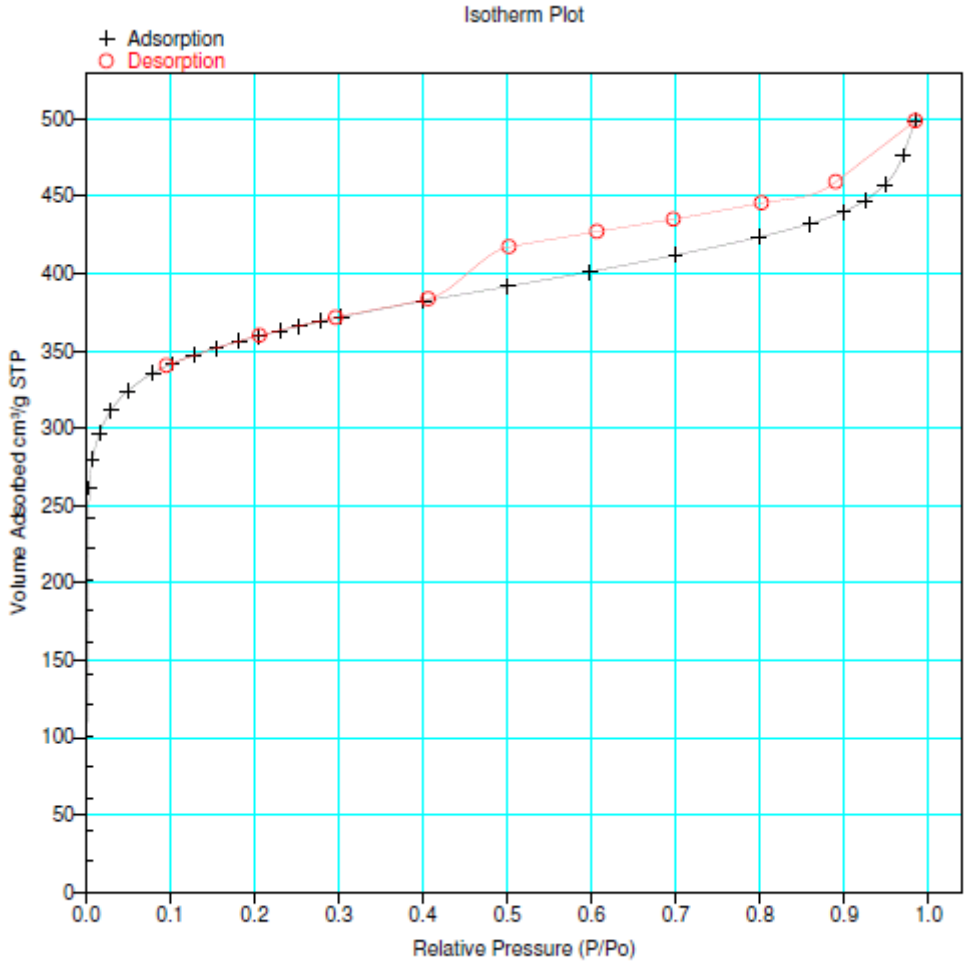

Figure AV. 3. Adsorption/desorption isotherm plots for modified NOR 125-180.

Preloaded NOR 125-180

Analysis adsorptive: N2
Analysis Bath: 77.35 K

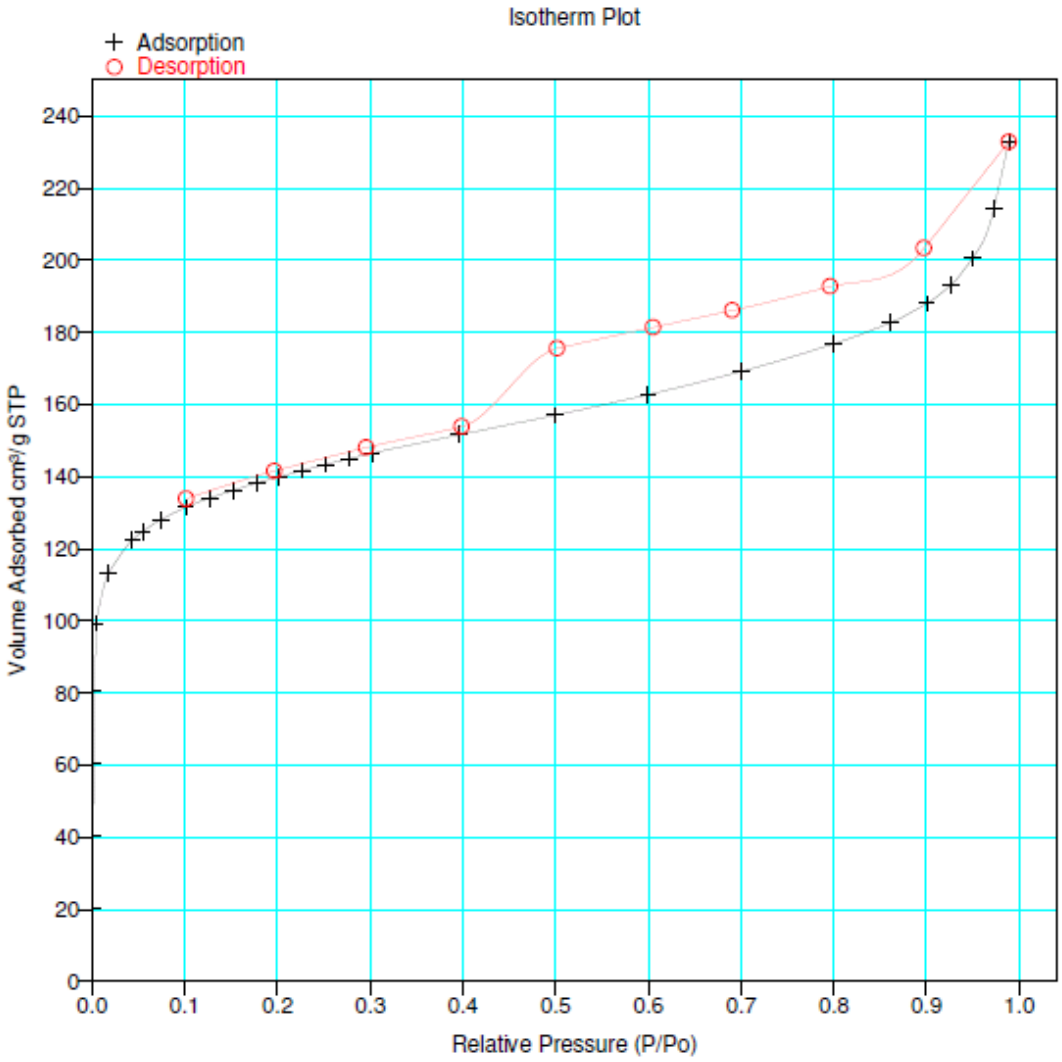

Figure AV. 4. Adsorption/desorption isotherm plots for preloaded NOR 125-180.